SOLID SAMPLING ELECTROTHERMAL VAPOURIZATION COUPLED TO INDUCTIVELY COUPLED PLASMA OPTICAL EMISSION SPECTROMETRY FOR GEOCHEMICAL EXPLORATION

by

FARHAD KAVEH

A thesis submitted to the Department of Chemistry

In conformity with the requirements for

the degree of Doctor of Philosophy

Queen's University

Kingston, Ontario, Canada

August, 2014

Abstract

The direct analysis of solid samples by electrothermal vapourization (ETV) coupled to inductively coupled plasma (ICP) optical emission spectrometry (OES) is typically reserved to niche applications. This thesis is focused on a new niche application: geochemical exploration. First, solid sampling (SS) ETV-ICP-OES was used to determine the distribution of elements in soil samples in the Flin Flon-Snow Lake terrain, Manitoba, Canada in order to locate the undercover ore deposit. Samples were first vaporized by ETV and the vapor was then introduced into the ICP.

Under optimal conditions and with a four-step ETV temperature program, the surface distribution of some pathfinder elements in soils showed obvious anomalies delineating the undercover ore. External calibration with 0–4 mg of soil reference material, together with internal standardization with an argon emission line, yielded results for Zn and P in good agreement with those obtained, following aqua regia (AR) digestion, by ICP mass spectrometry (MS).

The vertical distribution of target elements in soil samples from the same area was also determined, which revealed anomalously high concentrations toward the surface of the profile in the area above the undercover ore. Again, good agreement was obtained with results by AR-ICP-MS for those elements that could be determined by ICP-MS. Hence, SS-ETV-ICP-OES completely eliminates the need for extraction or digestion of samples prior to analysis, which significantly simplifies the analysis of soils.

Finally, in order to increase the amount of solid analyzed, the outlet of SS-ETV-ICP-OES was connected to a switching valve (for venting of pyrolysis products), itself connected to the side arm of a sheathing device whose other inlet was connected to a

nebulizer/spray chamber. The aerosol exiting the nebulizer and spray chamber was heated to 400 °C by applying infrared heating to the sheathing device and bottom of the torch while vaporized analytes produced by ETV were transferred to the ICP. This system allowed the amount of sample to be increased from 5 to 13 mg without extinguishing the plasma, resulting in a 2-10 fold improvement in sensitivity and detection limit versus conventional SS-ETV-ICP-OES, and as accurate but more precise analysis of soil .

Co-Authorship

All the work contained in this thesis was done by the author in the Department of Chemistry at Queen's University under the supervision of Dr. Diane Beauchemin.

Chapter 3 presents materials from the publication in Geochemistry: Exploration, Environment, Analysis, entitled "Solid sampling ETV-ICP-OES to study the distribution of elements in clay and soil samples for mineral exploration", by Masquelin, A., Kaveh, F., Asfaw, A., Oates, C.J and Beauchemin, D. Only the work actually done by me, pertaining to the analysis of soils, is included in this chapter. All the authors and in particular Beauchemin, D aided in revising the manuscript.

Chapter 4 presents materials from the publication in Geochemistry: Exploration, Environment, Analysis, entitled "Direct analysis of soils by ETV-ICP-OES: a powerful tool for mineral exploration", by Kaveh, F., Oates, C.J and Beauchemin, D. I generated all the data presented within the context of this chapter. All the authors and in particular Beauchemin, D aided in revising the manuscript.

Chapter 5 presents materials from the publication in Journal of Analytical Atomic Spectrometery, entitled "Improvement of the capabilities of solid sampling ETV-ICP-OES by coupling ETV to a nebulisation/pre-evaporation system", by Kaveh, F and Beauchemin, D. I generated all the data presented within the context of this chapter, while Beauchemin, D aided in revising the manuscript.

Acknowledgements

First and foremost, I would like to express my sincere thanks to my supervisor, Dr. Diane Beauchemin, for her knowledge, support and friendship during the course of this work. This allowed me to achieve my dreams. All of this became possible due to her guidance and consistent support since the beginning of my Ph.D. program.

I am also grateful to Dr. Gregory Jerkiewicz and Dr. Richard Oleschuk for serving on my supervisory committee. Dr. Chris Oates of Anglo American plc is thanked for providing his geochemical expertise and guidance with the interpretation of profiles. I would also like to thank Dr. Alemayehu Asfaw for his training on the SS-ETV-ICP-OES system as well as the relevant software. I sincerely thank everyone else in Dr. Beauchemin's group for their help.

I would also like to acknowledge the financial assistance from the Natural Sciences and Engineering Research Council of Canada (NSERC), Queen’s University School of Graduate Studies and Research, and the Department of Chemistry.

Finally, with all my heart and soul, I would like to thank my mother and brother, and my father who is no longer with us. They supported me to go to university and encouraged me when I lost confidence in myself. Without them, I would not have come so far.

Statement of Originality

I hereby certify that all of the work described within this thesis is the original work of the author. Any published (or unpublished) ideas and/or techniques from the work of others are fully acknowledged in accordance with the standard referencing practices.

(Farhad Kaveh)

(August, 2014)

Table of Contents

List of Figures

List of Tables

List of Abbreviations

AA-ED	Anglo American Exploration Division
AR	Aqua regia
BP	Boiling point
CCD	Charge coupled device
CRM	Certified reference material
DDW	Doubly de-ionized water
DSI	Direct sample insertion
EIEs	Easily ionized elements
ETV	Electrothermal vaporization
GFAAS	Graphite furnace atomic absorption spectrophotometry
HC	Heater/condenser
ICP-OES	Inductively coupled plasma optical emission spectrometry
ICP-MS	Inductively coupled plasma mass spectrometry
IR	Infrared
IRM	Internal reference material
IRZ	Initial radiation zone
LA	Laser ablation
LDA	Linear discriminant analysis
MD	Membrane desolvator
MVA	Multivariate analysis
NAA	Neutron activation analysis
NAZ	Normal analytical zone
NIST	National Institute of Standards and Technology
PCA	Principal component analysis
PCC	Pearson correlation coefficient
PET	Pre-evaporation tube
PHZ	Preheating zone
ppm	Parts per million
ppb	Parts per billion

PTFE	Polytetrafluoroethylene
R12	Dichlorodifluoromethane
R^2	Square of the correlation coefficient
RF	Radio frequency
RSD	Relative standard deviation
SS	Solid sampling
SS-ETV-ICP-OES	Solid sampling electrothermal vaporization inductively coupled plasma optical emission spectrometry
USN	Ultrasonic nebulizer
VMS	Volcanogenic massive sulfide
VT	Vaporization temperature
XRF	X-ray fluorescence

Chapter 1- Introduction

1.1. Geochemical exploration

Growing global demand for minerals and metals has driven exploration efforts towards regions of buried mineralisation, often under extensive sedimentary overburden. Geochemistry, a sub-discipline of geology that studies the chemistry of earth materials, has become the primary technique of choice in this exploration. Geochemical prospecting for minerals is defined as any method of mineral exploration based on regular measurement of chemical properties of numerous naturally occurring materials. These materials include rock, soil, glacial debris, vegetation, sediment or water, and the chemical property measured is usually the trace concentration of target or pathfinder elements. Geochemical methods for exploration mainly rely on the presence of secondary expressions in surface sampling media. The purpose of the measurements is the detection of a geochemical "anomaly" or area where the chemical pattern shows the existence of ore in the surrounding area. Geochemical anomalies are usually indicated by higher concentrations of pathfinder elements in comparison with areas free of undercover ore deposits. The regular abundance of an element in any material where the equilibrium has not been disturbed by the occurrence of a mineral deposit is normally referred to as background.

Although geochemical studies based on the analysis of samples of waters, sediments and vegetation are common ways of identifying and locating most types of mineralization, their application in areas with thick overburden cover (i.e. glacial) and for mainly discrete or small ore bodies is often limited.[1] In recent years, soil has been

used in exploration because it can retain indicator or pathfinder elements above buried deposits.[2] The monitoring of indicator elements in the soil samples is often the only useful approach of geochemical exploration in regions with thick overburden cover or for numerous types of valuable deposits. The number and type of these indicator elements is dependent on the ore deposit type. For example, topaz or $Al_2SiO_4(F,OH)_2$ is the main indicator mineral in soil samples above tin ore deposits, which can produce Al, Si and F as pathfinder elements.[3] Target or pathfinder elements are usually grouped into major, minor and trace elements based on their abundance in the geological samples. Major elements usually have concentrations of weight percentages (%), while minor and trace elements have concentrations of parts per million (ppm) and parts per billion (ppb), respectively.

In some areas, trace elements can be significantly enriched as a consequence of natural processes and form concentration anomalies in soils or sediments. The formation of secondary anomalies in the surface environment involves mobilisation, transport and deposition of pathfinder elements, and understanding of the geochemical processes in such environments allows a reduction of costs and environmental impact by avoiding superfluous drilling of barren prospects.[4] Furthermore, the detection of element sources and transport processes in the near-surface environment has a broad variety of applications in disciplines beyond mineral exploration, such as civil engineering, agriculture, and environmental sciences.

1.2. Processes for the migration of elements

Mass transport by water in suspension or solution accounts for the majority of all element transport in the subsurface environment. Solids dissolved in water may migrate as part of the water mass advection or mass diffusion. The first of these, advection, is usually more important by several orders of magnitude and happens as a result of upward flow of water and its dissolved contents. For example, the groundwater may effuse at the surface during earthquakes. This earthquake-induced surface migration of groundwater was reported in a desert area of Iran in 1903 and 1923.[5] Also, streams of warm groundwater at the surface were observed during Matsuchiro earthquake in Japan.[6] In this mechanism, fractures in the brittle upper crust generated by pre-seismic extension create pathways for groundwater transfer and storage. Stress fields usually become intense during earthquakes which can close these fractures and push the groundwater to the surface. The groundwater migration is usually very slow, as basement rocks have very low permeability. Thus, the effusion of water may take weeks following an earthquake.[7] Advective migration by deeply rooted plants is also another mechanism for the advective transfer of groundwater to the surface. For example, it has been reported that plants may root as deep as 100 m in some arid areas, resulting in a capillary that can draw groundwater to the surface.[8]

Mass diffusion usually happens as a result of chemical or electrical gradients. In chemical diffusion, vertical migration of elements from a buried deposit to the surface comprises passage through the vadose or undersaturated region. This vadose zone is usually not dry, except in hyper-arid climates. The film of water around mineral grains of the rock, which comes from precipitation remaining after evaporation and run-off, moves

downward to help recharge to groundwater. The degree to which this water film moves can be estimated by determining depth profiles of elements in the water film extracted from drill core. Chlorine (Cl) is usually used for this purpose because the Cl content of rain per volume of precipitation is quite constant over time for a given zone, but the Cl content of soil water usually increases with increased dryness, and consequently evapotranspiration, which also reduces the downward flow of moisture recharging to the groundwater. As a result, when precipitation is greater, adding more water and Cl on the surface, profiles travel slowly downwards, thus reflecting changing moisture fluxes with time. The migration of dissolved molecules is usually affected by this moisture flux. Indeed, the degree of liquid interconnection reduces as the ground becomes drier. It can make some flow paths dead ends and groundwater molecules are consequently diffused in the vapour phase across air-filled pores to the surface. This can lead to the vertical distribution of elements from under cover ore deposit.[4]

Solids dissolved in water may also migrate as a result of electrochemical gradients. Much of the previous work in exploration geochemistry on electrochemical cells involved sulphide bodies that extend close to the surface. Electrochemical cells are usually produced around most sulphide ore deposits as a result of their oxidation. A sulphide body can be pictured as a conductor immersed in an electrolyte or groundwater that causes redox differences between the more reduced deeper (anodic) part and the more oxidized upper (cathodic) section of the body. Anodic corrosion occurs at depth between the electrolyte and sulphide minerals (MS), producing electrons, metal ions and sulfur.

$$MS \longrightarrow M^{2+}_{(aq)} + S + 2e^-$$

As a result, upward migrations of electrons through the conductive sulphide body to areas where oxygen or other oxidants are present can lead to the following cathodic reduction:

$$O_2 + 4H^+ + 4e^- \longrightarrow 2\,H_2O$$

Because of the electrical potential created between the cathodic and anodic sites, a current flow is induced by ions in the groundwater. Indeed, cations travel to the cathode and anions to the anode. Cathodic reactions usually happen in the shallow area, close to the supply of oxidants by the water table. Water is needed as a source of dissolved oxidants and to allow the migration of dissolved cations and anions, which induces current.

Figure 1.1 shows that cations following the current path accumulate on either side of the sulphide body in a zone of high current density near to the water table. From these highly concentrated zones, cations move to the surface by spontaneous diffusion. Indeed, this diffusion within the water film is much quicker than the downward flow of the water film.[9]

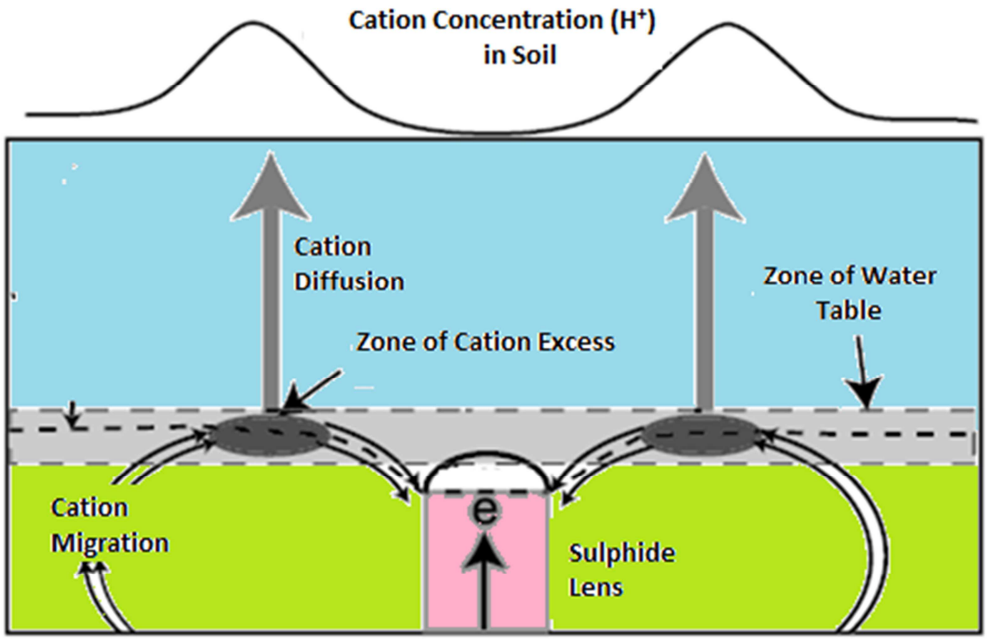

Figure 1.1. Schematic diagram of electrochemically induced upward migration of elements from a sulphide ore deposit (adapted [9]).

Finally, Hamilton *et al.* proposed a different mechanism for a sulphide body under several meters (>20m) of glacial sediments.[10,11] This model (Figure 1.2) involves migration along redox gradients, when reduction of oxidants at the sulphide/sediment interface generates a reduced environment and continued reaction requires that reduced species be removed. Redox differences between the top of the ore body and the water table close to the surface, where oxygen and groundwater are present, induce a vertical electrochemical gradient. Reduced species, such as HS^- and Fe^{2+}, move upward along this gradient until they react with oxidants moving downward, which dissipates charge away from the sulphide body. When the limited number of oxidants present between the top of the ore and the water table are consumed, a reduced 'column' may result between the

water table and the ore body. At the water table, O_2 is readily available, which enables oxidation of the reduced material, thereby reducing pH down to 2-4 and in turn increasing the dissolution of carbonate. Some elements present in a buried sulphide deposit, such as Zn and Cd, have been reported to show clear anomalies in the soils above the ore.[4]

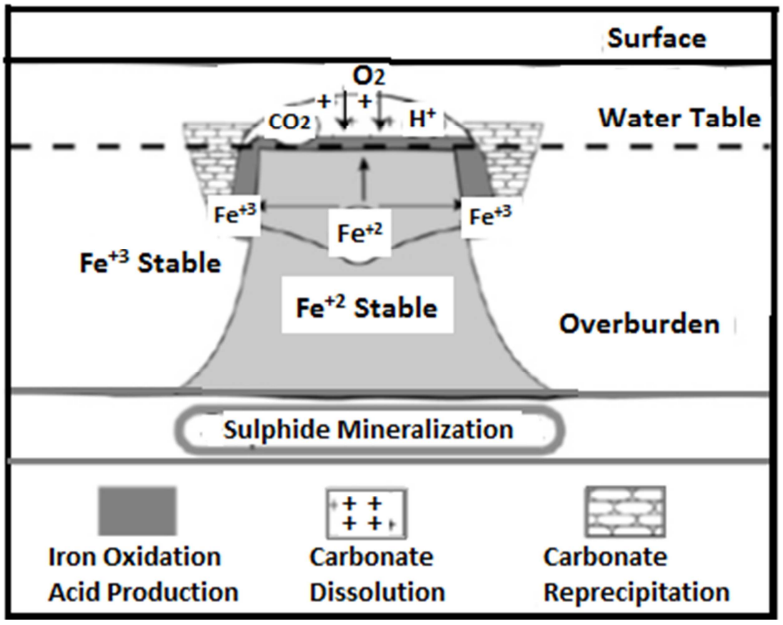

Figure 1.2. Effects of the migration of a reduced metal upwards from a sulphide ore deposit. Reaction with oxygen at and above the water table reduces pH, which induces carbonate dissolution (adapted [11]).

1.3. Geochemical exploration techniques

The preceding paragraphs showed that high-concentration elements from an ore may travel from depth and become trapped in the near surface environment where

samples can simply be collected. Media such as soils, sediments and rocks are then analyzed to look for subtle and often very low-concentration anomalies relative to their average crustal abundance, which are indicative of mineralisation below. Also, the multi-elemental analysis and, progressively, speciation analysis of a variety of environmental samples must be carried out to evaluate the impact of pollution on the environment.[12] As it was mentioned earlier, soil has indeed been used more in geochemical exploration, compared to other samples, because it can retain indicator or pathfinder elements above buried deposits.[2] It is consequently important to extract the maximum amount of information from each soil sample, which requires the development of fast, sensitive and simple techniques.

1.3.1. Electrochemical exploration

The electrochemical exploration technique is one of the primary tools for exploration of undercover ore deposits.[13-15] It involves passing a stable high-voltage direct current (DC) current for 15-20 hours between an anode and an array of special cathodes broadly spaced along a profile over a suspected sub-surface ore body. Under the influence of a potential field, the electric current causes the positively-charged metallic ions to move towards the cathodes. This system is shown in Figure 1.3, which consists of two ordinary motor generators (including one as back-up) for providing constant power to the stabilized DC supply, a 6-channel current control unit, 6 special cathode electrodes and a single anode. Motor generators are rated at 400 Hz and 2.5 kW. The alternating current provided by the motor is transformed into a very steady DC source. A switch arrangement is typically made to allow change-over to the back-up generator. This is

usually done to provide a continuous supply of power over a long period of time in case of failure of one of the components.

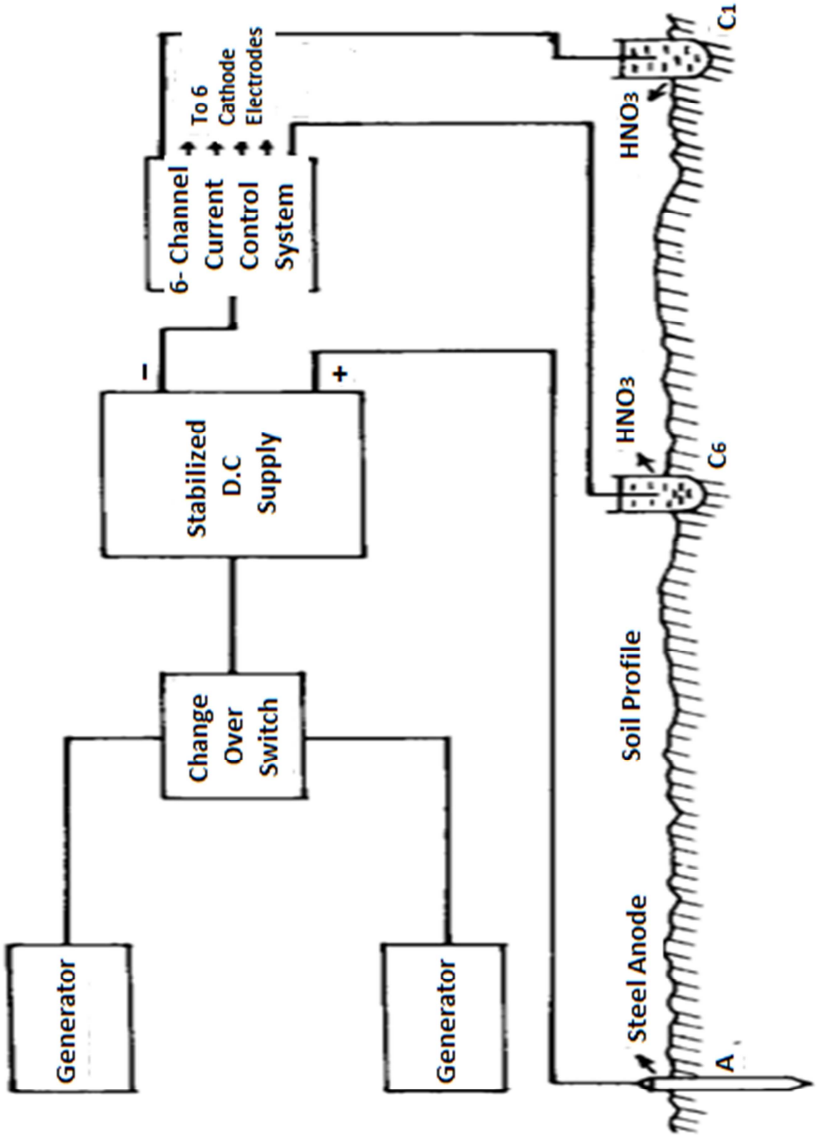

Figure 1.3. Block diagram of the electrochemical exploration technique (adapted [14]).

The 6-channel current control unit provides the same stabilized current of up to 5 A to each of 6 cathodes, each consisting of a porous ceramic pot that contains one graphite

rod initially immersed in 300 mL of electrolyte (4N nitric acid). The single anode, which consists of several robust steel electrodes, is usually placed at a distance of about 100 m from the nearest cathode. Electrolyte is added to each cathode pot from time to time to compensate the loss of electrolyte through evaporation as well as from leakage into the ground through the porous bottom of the cathode. Finally, the graphite rods and the remaining electrolytes are taken out separately for analysis. Blank samples of electrolyte and graphite rod are also used to measure the background level of contamination. All samples are then analyzed in the laboratory and, through comparison of the results for samples with those for blank samples, the probable anomalies can be detected.

However, the main drawback of electrochemical exploration is lack of resolution, particularly at depth. This is inherent to any electrical method where all of the apparatus is on the surface of the ground. For example, the instrument required to detect sulphides at a depth of 200 m should span at least 600 m across the anomalous area, which is totally unrealistic. Thus, the resolution of the technique drops considerably with depth and no amount of additional data can overcome this. Furthermore, this process is very time – consuming (15 hours), which is another disadvantage of this technique.

Various methods have been used for the analysis of soils, as shown in Table 1.1, where they are compared in terms of calibration strategy, detection limit, sample preparation and analytes.

Table 1.1 Some selected methods used to determine elements in soil samples.

Detection method	Analyte	Sample preparation	Detection limit (ppm)	Calibration strategy	Ref
NAA*	Zn, Cr, Mn and Fe	Direct solid sampling (10–50 mg) of soil sample aliquots	ND	Matrix-matched solid standards	16
NAA	Ce, Co, Cr, Cs, Eu, Fe, Hf, K, La, Na, Rb, Sc, Th, U, Yb, and Zn	Direct solid sampling (100 mg) of soil sample aliquots	ND	Matrix-matched solid standards	17
XRF**	Cr, As, Se, Cd, Hg and Pb	Pressed powder pellets (4.5 g of soil powder in an Al ring)	0.8 (Se) – 2.9 (Hg)	Matrix-matched solid standards	18
GFAAS^{+}	As, Cr, Cu and Pb	Direct solid sampling (100 mg) of soil sample aliquots	ND	Matrix-matched external calibration	19
GFAAS	Cr	Wet digestion (mixture of HF, HNO_3 and HCl)	0.0015	Matrix-matched external calibration	20
ICP-MS$^{\#}$	Cd, Cr, Co, Cu, Mn, Ni, Pb, Zn	Microwave-assisted digestion with HNO_3/HCl	0.01 (Pb, Co and Cd)- 2.3 (Zn)	Matrix-matched external calibration	21
ICP-MS	Tl	Aqua regia digestion	0.0012	Matrix-matched external calibration	22
ICP-OES$^{\&}$	Cd, Co, Cr, Cu, Mn, Ni, Pb, and Zn	Microwave-assisted digestion with HNO_3 and HF	0.2 (Cd)- 7 (Zn)	Aqueous standards	23
ICP-OES	Al, As, Ca, Cd, Co, Cr, Cu, Fe, K, Mg, Mn, Na, Ni, P, Pb, S, Sb, Zn	Microwave-assisted digestion with aqua regia	As (0.05)- Al (6.28)	Matrix-matched external calibration	24
ICP-OES	Cr, V, Ni, Cu, Co,Zn, Mn, Mg, Si, Al, Fe	Aqua regia digestion	ND	Method of standard addition	25
ICP-OES	B	Wet digestion with HNO_3, HF and $HClO_4$	ND	Matrix-matched external calibration and internal standardization	26

*Neutron activation analysis ND: Not determined
** X-Ray fluorescence
+ Graphite furnace atomic absorption spectrophotometry
$^{\#}$ Inductively coupled plasma mass spectrometry
$^{\&}$ Inductively coupled plasma atomic emission spectrometry

All the approaches in Table 1.1 have their own strengths and limitations. In NAA, the sample is placed in a nuclear reactor by a remote-handling system and a known flux of thermal neutrons is used to irradiate it. The soil sample is then removed from the reactor and the activation products are measured, typically by γ -spectrometry. This technique is able to perform multi-element analysis (up to 74 elements) on small (50–100 mg) solid samples with detection limits < 1 ppm, depending on the element and matrix. However, this technique requires special irradiation facilities and highly-trained personnel, which may limit the availability of the method to national facilities. Also, concerns over nuclear radiation and the scarcity of facilities have made the NAA technique less common.

XRF usually analyzes soils directly or with minimum sample preparation (e.g. drying and grinding). In this technique, soil samples are irradiated with primary X-rays (with typical attenuation depth of 1 to 100 μm) from a X-ray tube or radioactive source. This ejects inner electrons from atoms and an X-ray fluorescence spectrum is observed when outer electrons fall into these vacancies. The wavelengths observed are characteristic of the elements present. The main advantage of XRF for soil analysis is the availability of portable XRF instruments appropriate for high-throughput elemental testing and spectrochemical analysis of a wide range of metals and other materials in the field.[27] Also, new instruments, such as total reflection-XRF, have been developed in recent years in which the incident X-ray beam is focused at the sample surface at such an acute angle that it is reflected, thus decreasing background interference problems produced by diffusion into the bulk.[28,29] However, this technique is only able to detect elements with atomic numbers greater than about 8, which means that it cannot be used to

determine elements such as Be. Also, when compared to other methods, XRF has fairly high limits of detection (0.8-3 ppm) as well as the possibility of matrix effects.

GFAAS uses an electrically heated graphite tube, which is heated to a temperature up to 3000 °C, to produce a cloud of atoms. These free atoms will absorb light at frequencies or wavelengths characteristic of the element of interest. The amount of light absorption can be linearly correlated to the concentration of analyte present. The main advantages of GFAAS include high atom density and relatively long residence time in the tube, which improves detection limits down to the sub-ppb range. However, this technique can only measure one element at a time and would not be appropriate for routine analyses requiring the simultaneous multi-elemental analysis of a small sample. Also, because of relatively slow analysis time (3-4 minutes per element) and narrow dynamic range (10^2), the performance of this technique is still somewhat limited.

1.3.2. ICP-OES and ICP-MS

In recent years, ICP-OES and ICP-MS have become very popular and common tools for the routine analysis of soil samples because they have some distinct advantages over other existing techniques, such as great sensitivity, selectivity, wide dynamic range and simultaneous multi-element capability coupled with very low detection limits. ICP-OES is usually used for the multi-element determination of major, minor and trace elements while ICP-MS is preferred for multi-element analysis at ultratrace levels.[12,30] ICP-MS can also provide isotopic information. On the other hand, matrix effects are usually smaller in ICP-OES than ICP-MS, because ICP-OES involves the passive measurement of emitted light while, in ICP-MS, ions must be physically extracted from

the plasma. In addition, high mass resolution MS is often needed in ICP-MS to remove polyatomic spectroscopic interferences that originate from the complex matrix of solid samples. These interferences may mask the analyte signal profile, thus degrading the detection power of the technique.[31] This problem usually arises because, in ICPMS, each analyte has only one or a few isotopes, while a large number of emission lines are typically accessible in ICP-OES for each analyte, allowing the selection of one or more interference-free emission lines in each case. As a result, although ICP-OES does not offer as low a DL as ICP-MS, it is usually more appropriate for soil analysis. In fact, as will be seen in this thesis, if essentially 100% of the sample is introduced into the ICP, ICP-OES may well provide a sufficiently low DL, which will enable the analysis of samples with maximum accuracy for a relatively lower cost than possible with ICP-MS. That is why ICP-OES is widely used for analysis of soil samples. Some interesting examples of works that have been done so far to determine the elemental content of soil samples using ICP-OES are summarized in Table 1.1.

The ICP-OES technique usually requires a nebulizer and spray chamber for sample introduction of solutions into the plasma. Hence, geological samples such as soils require a dissolution step that is lengthy and may lead to contamination or analyte loss. Also, the transport efficiency that is typically obtained by using nebulizers for sample introduction into the plasma is usually less than 2-5%. In addition, the simultaneous introduction of analyte elements, matrix components and solvents into the ICP can give rise to both spectroscopic and non-spectroscopic interferences.[32] Developing improved sample introduction systems for resolving the aforementioned problems is important for plasma spectrometry.

1.4. Motivation

One approach that increases sample transport efficiency and requires a small sample size is electrothermal vaporization (ETV), which has been studied over the last 40 years as a sample introduction technique in combination with ICP-OES for the direct determination of elements in both liquid and solid samples.[33-40] Although this technique is more expensive to purchase and operate than nebulization systems and generates transient signals that require fast detection, the use of ETV for sample introduction in ICP-OES offers many advantages for numerous applications.[41-43] It allows the analysis of a small amount of solid sample, while providing a lower detection limit than solution nebulization.[41] Additionally, temperature steps can be used to isolate the analyte from intrusive elements that have different vaporization temperatures prior to the introduction of aerosol into the ICP, thereby removing spectroscopic interference in ICP-OES.[33] Furthermore, the multi-elemental capability, wide linear dynamic range and high sensitivity of ETV-ICP-OES make this technique most suitable for the direct analysis of geological samples such as soils.

Yet, only one application of solid sampling (SS) - ETV-ICP-OES to soil analysis could be found in the literature. Schron *et al.*[38] performed the multi-elemental analysis of soil by induction heating ETV-ICP-OES using standard reference materials of powdered soil for external calibration. In their work, SS-ETV-ICP-OES was used for the determination of Cr, Cu, Ni, Pb, and Zn in the trace element range (10 to 500 µg/g) and the transport efficiency of the analytes was improved by high temperature vapor halogenation. The detection limits for SS-ETV-ICP-OES using a sample weight of 3 mg were 0.7 to 6 µg/g. However, this report only focused on elemental analysis (just 5

elements) of certified reference soil samples, and did not consider real soil samples above buried deposits. Thus, the applicability of this technique was not shown in geochemical exploration.

The objective of this work was to develop a simple method using direct solid sampling ETV-ICP-OES for the analysis of a series of soil samples. Indeed, in contrast to other report focused on elemental analysis of soil samples,[38] SS-ETV-ICP-OES was used in geochemical exploration to study the distribution of elements in soil so as to find where they are anomalous (i.e. significantly above background), as this may be used to locate undercover ore deposits.

1.5. Scope of this thesis

The next chapter reviews the ICP-OES technique along with the limitations associated with conventional sample introduction techniques. Methods currently being used for improving the capabilities of ICP-OES are also discussed, in particular ETV as a direct solid sampling technique in combination with ICP-OES. The main objective of this thesis, which was using SS-ETV-ICP-OES in geochemical exploration, is also detailed at the end of Chapter 2.

Chapter 3 and 4 describe the novel application of SS-ETV-ICP-OES to study the surface and vertical distribution of elements in soil samples for mineral exploration. Chapter 5 describes the development of an improved SS-ETV-ICP-OES system to increase the amount of solid that can be introduced without extinguishing the plasma. As will be shown, this system improved the reproducibility of results for inhomogeneous

samples, such as soils. Finally, the conclusions and future work are discussed in Chapter 6.

Chapter 2- Literature review

2.1. Inductively Coupled Plasma Optical Emission Spectrometry

Nowadays, ICP-OES is a recognized technique for the multi-element determination of major, minor and trace elements in a wide range of samples (such as environmental, geological and biological).[23,44-52] The principle of the method is to use a high temperature to excite atoms and ions into higher energy levels. This excited state is not stable because of the atom's or ion's natural tendency to return to the ground state. When excited atoms or ions move back to the ground level, they typically release energy. This energy is referred to as emission radiation, and its intensity depends on the temperature, number of atoms or ions in excited states and the atom or ion type. A single element has a number of emission lines that can be used for quantitative analysis. However, the most frequently used lines depend on their sensitivity and on the presence of possible interferences.[53]

Since the first study reporting the successful development of an ICP for optical emission spectrometry by Fassel and co-workers at Iowa State University,[54] the number of publications referring to ICP-OES has grown at an explosive rate.[55] A typical ICP torch consists of three concentric quartz tubes, which are normally referred to as the "outer," "intermediate," and "inner" (also known as "carrier gas") tubes (Figure 2.1). The outer argon gas flow (10-15 L/min) is required to sustain the plasma and to prevent it from melting the quartz tube. The intermediate Ar gas flow (0-1.5 L/min) positions the plasma above the torch injector, and the inner Ar flow (0.5-1.5 L/min) carries the sample aerosol into the heart of the plasma, thereby creating a central channel.

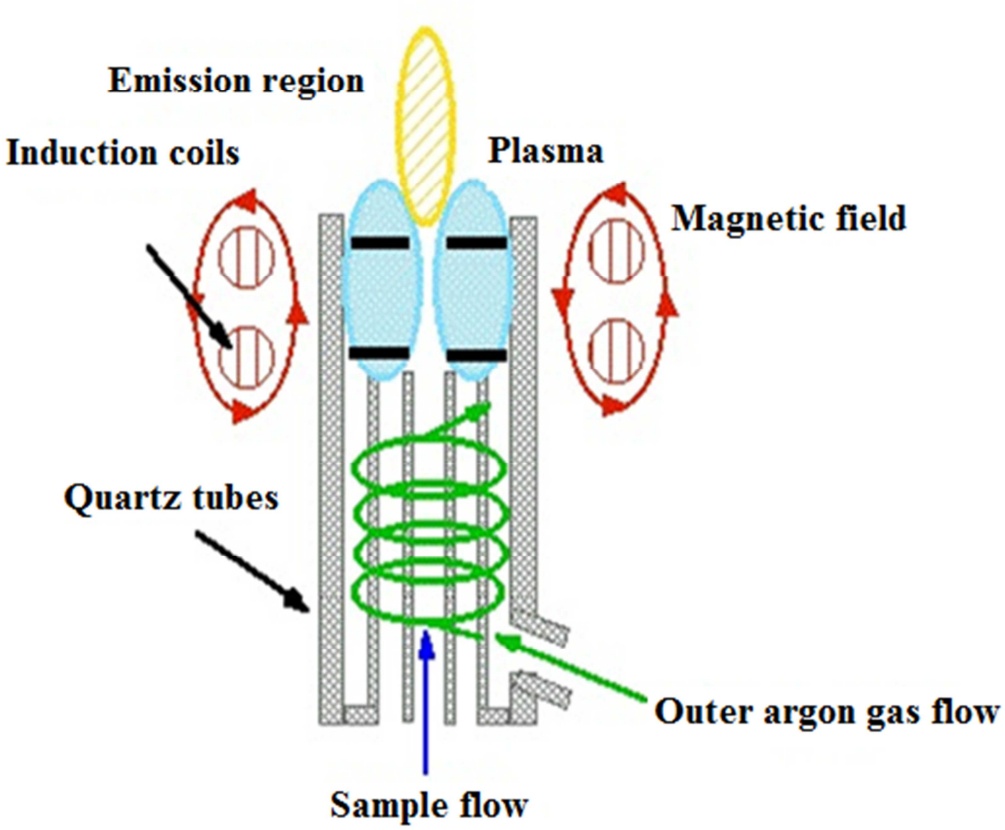

Figure 2.1. Generation of a typical ICP (adapted [56]).

A two- or three-turn copper coil, called the load coil, surrounds the top section of the torch, and is connected to a radio frequency (RF) generator that supplies power to the load coil. This creates an alternating current inside the coil at a rate corresponding to the frequency of the RF generator, which in turn induces high-frequency oscillation of magnetic fields inside the top of the torch. While argon gas flows through the torch, a spark from a Tesla causes production of electrons and ions in the argon gas surrounded by the load coil. These ions and electrons are then accelerated by the magnetic field, and collide with other argon atoms, causing further ionization. This process continues until a high-temperature plasma (7000-10000 K) is formed where, following desolvation,

vaporization and atomization, excitation and ionization of atoms occur. Adding energy to the plasma using RF-induced collision is known as inductive coupling, and accordingly the plasma is called an ICP. The ICP is sustained within the torch as long as enough RF energy is applied.

Figure 2.2 demonstrates the temperature gradient within the ICP with reference to height above the load coil. The induction region at the base of the plasma is the region where the inductive energy transfer occurs. This is also the area of maximum temperature and it is characterized by an intense continuum emission. Obviously, from the induction region upward towards to the tail plume, the temperature decreases. Between the point of sample introduction into the ICP and the point of generation of excited atoms and ions within the ICP, several processes happen as illustrated in Figure 2.3 for NaCl.

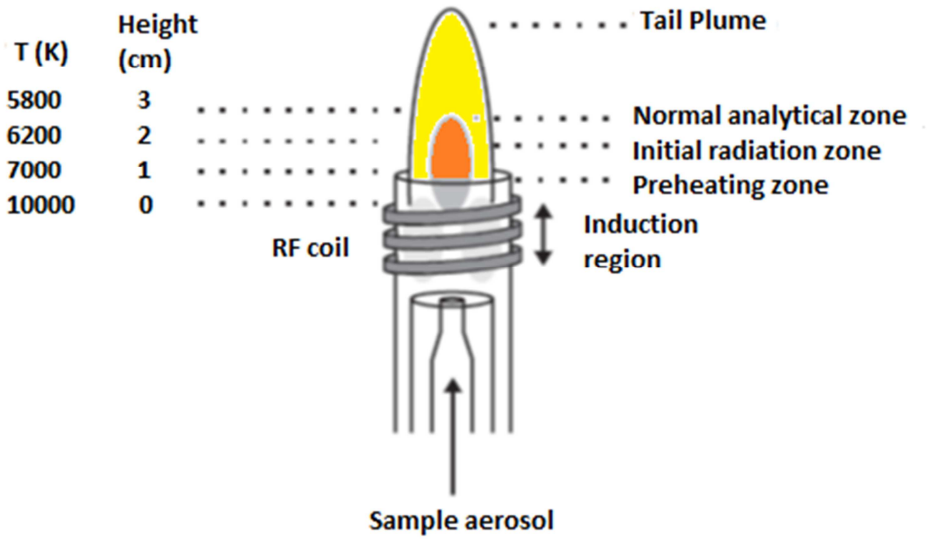

Figure 2.2. Temperature as a function of height above the load coil (adapted [55]).

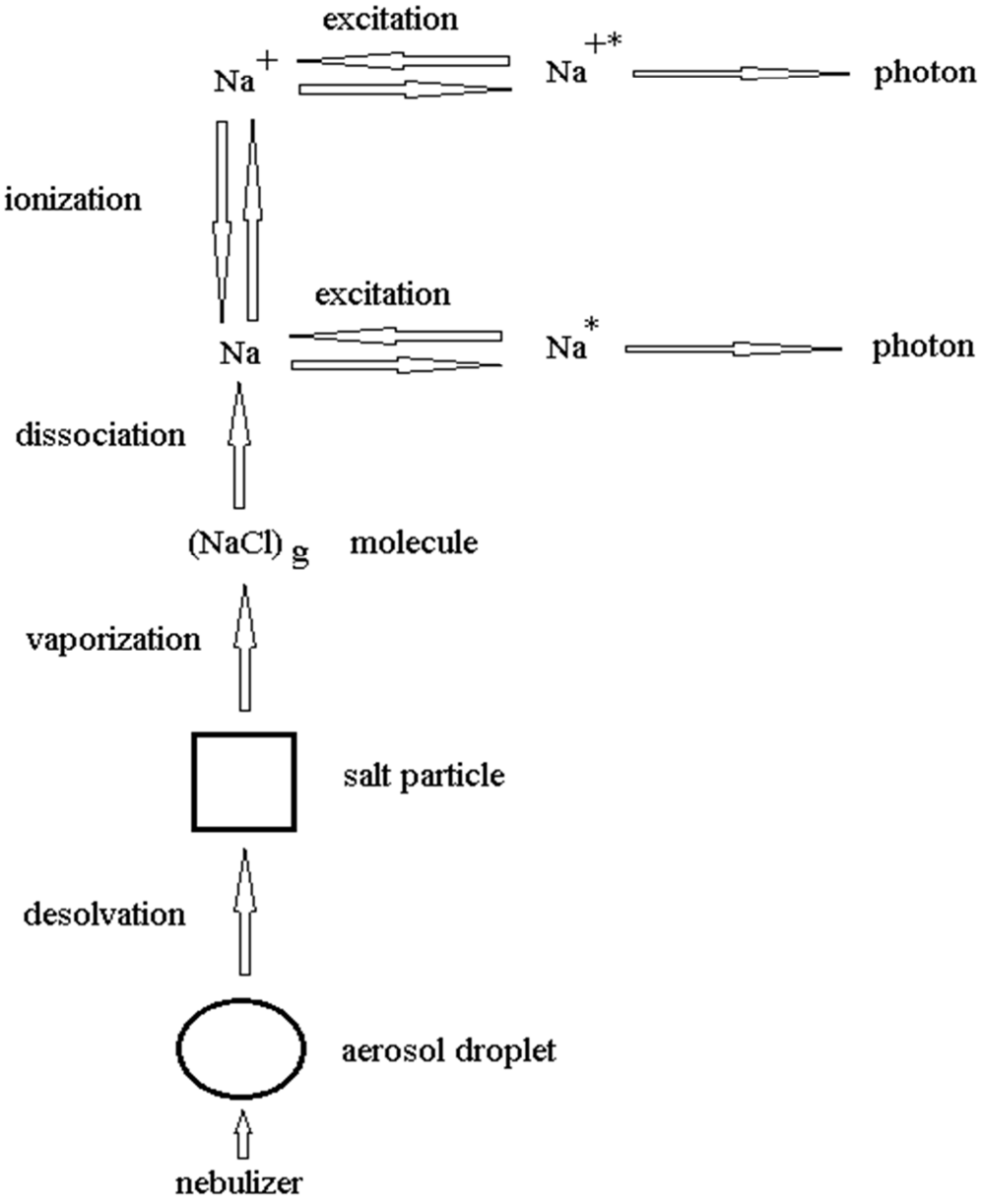

Figure 2.3. Schematic diagram demonstrating processes undergone by an aerosol droplet during transport through the ICP.

Upon entering the plasma, the sample aerosol droplets experience three separated processes. The earliest step is called desolvation, or the elimination of the solvent from

the droplets, resulting in microscopic solid particulates or a dry aerosol. The solid particles are then decomposed into gaseous state molecules during the vaporization step. The third step is atomization, or the breaking of the gaseous molecules into atoms. These steps happen mainly in the preheating zone (PHZ). The time scale for these steps to happen in the ICP is on the order of a few milliseconds.[57] Finally, excitation and ionization of the atoms happen, followed by the emission of radiation from these excited species. These steps occur predominantly in the initial radiation zone (IRZ) and the normal analytical zone (NAZ), from which the emission spectrum is typically collected.[58] The three main mechanisms for ionization of an analyte are thermal ionization, charge transfer, and Penning ionization.

Thermal ionization happens when the kinetic energy of the colliding electron is larger than the threshold energy for ionization of the analyte, M. This process is explained by

$$M + e^- \longrightarrow M^+ + 2e^-$$

In an argon plasma, ionization can also result from charge transfer between argon ions and analyte atoms as described by

$$Ar^+ + M \longrightarrow Ar + M^{+*}$$

The resulting analyte ion is usually produced in an excited electronic state (indicated by *). For this purpose, the total energy for ionization and excitation of analyte must be less than the first ionization potential of argon (15.76 eV).

Penning ionization of analyte ions usually results from the collision of metastable argon atoms, Ar_m, as is shown by

$$Ar_m + M \longrightarrow Ar + M^+ + e^-$$

This mechanism is less probable than the previous two mechanisms due to the low population of argon metastable species as compared to the population of argon ions and electrons in the ICP.[59]

The emitted electromagnetic radiation, at wavelengths characteristic of each element, is then diffracted into its spectral components in the optical system and finally is measured by ICP-OES detectors. The measured element intensities are then evaluated by the instrument's software.

Nowadays, the ICP is not only the most famous source for OES but it is also an outstanding ion source for mass spectrometry (MS).[60] ICP-MS features low detection limits (parts-per-trillion for most elements) and the ability to do isotopic analysis. On the other hand, although ICP-MS is generally preferred for multi-elemental analysis at ultra-trace levels as it is more sensitive than ICP-OES, it is subject to non-spectroscopic interferences (also called matrix effects) in addition to spectroscopic interferences.[12,61] The ICP-MS instrumentation is also more expensive to purchase and operate than ICP-OES because of all the vacuum components that require regular maintenance. In contrast, ICP-OES, which involves the passive measurement of emitted light, is less affected by matrix effects than ICP-MS, where ions must be physically extracted from the plasma. Therefore, a much larger dissolved solid amount (several % vs less than 0.2 % m/v in ICP-MS) can be introduced in ICP-OES, which can translate into less sample pre-treatment or dilution and hence a higher sample throughput. These features have made ICP-OES an appropriate technique for elemental analysis in geological, clinical and environmental systems.[62]

2.2. Conventional sample introduction for ICP-OES

ICP-OES conventionally uses a nebulizer and spray chamber for sample introduction into the plasma, which requires that samples be in solution. An aerosol, or very fine mist of liquid droplets, is usually produced from the liquid sample by a nebulizer. The most common nebulizer in use today is the pneumatic nebulizer (Figure 2.4), which was first fabricated in 1979 by Meinhard.[63] It operates by using the Venturi effect, where argon gas introduced in the side arm exits at the nozzle and causes a region of low pressure. As a result, the liquid sample is drawn up through the capillary tube (about 250 µm in diameter) and exits through the nozzle. The physical interaction of liquid sample and argon gas finally produces a coarse aerosol.

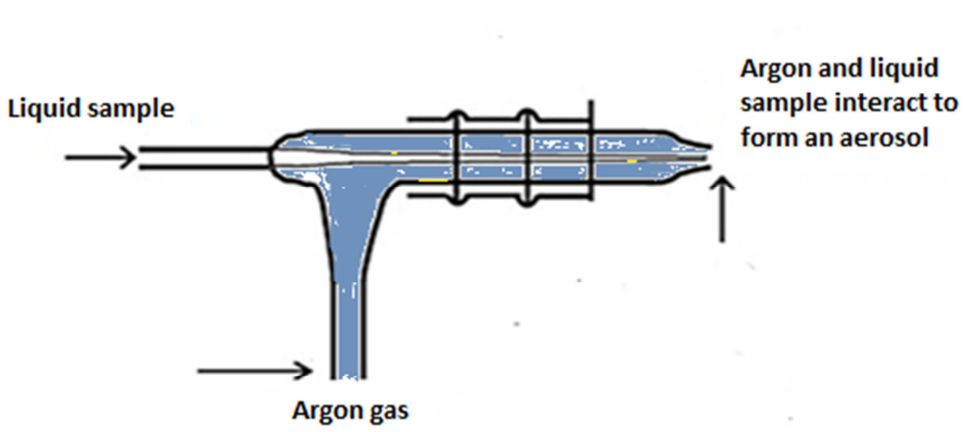

Figure 2.4. Schematic diagram of the pneumatic nebulizer (adapted [64]).

Introduction of the coarse aerosols produced by the nebulizers directly into the plasma would extinguish or induce cooling of the plasma. Also, larger droplets might

pass through the plasma without being desolvated.[65] Thus, a spray chamber is usually placed between the nebulizer and the ICP torch to remove large droplets from the aerosol.

Figure 2.5 shows a double-pass spray chamber which is comprised of two concentric tubes, an inlet for the nebulizer, an exit for the more appropriate aerosol, and a waste drain. The aerosol generated by the nebulizer is then introduced into the inner tube of the double-pass spray chamber and interacts with the internal surface of the spray chamber. As a result, smaller droplets (with a mean droplet size of about 8 µm in diameter) are produced in the system while large droplets go to drain.

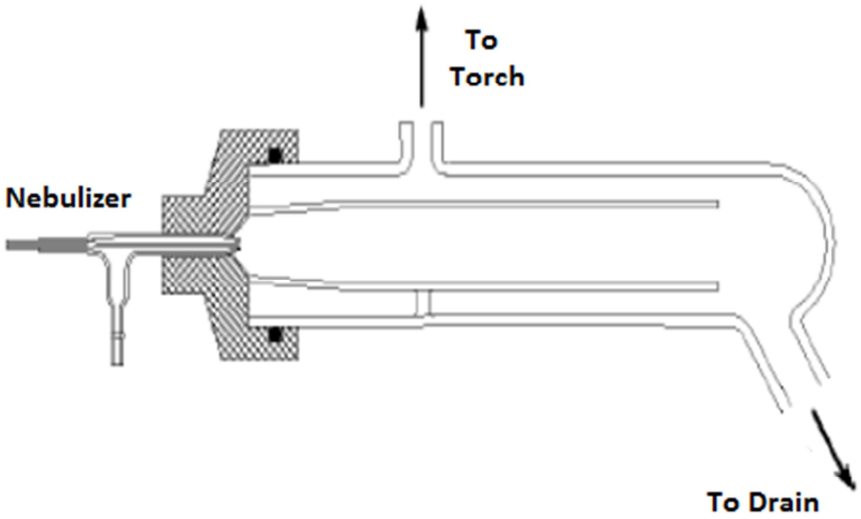

Figure 2.5. Schematic diagram of the double-pass spray chamber (adapted [30]).

2.3. Limitations associated with conventional sample introduction

The transport efficiency that is typically obtained by using a concentric nebulizer and spray chamber for sample introduction into the plasma is usually less than 2-5%,

because the majority of the sample collects on the wall of spray chamber and goes down the drain, resulting in a significant sensitivity loss. In addition, for analysis of solid samples such as soils, a dissolution step is then typically required before analysis. For example, in the hot plate digestion, 0.5 g of soil sample is weighed into a Teflon decomposition closed vessel, to which 5.0 mL each of concentrated HNO_3 and concentrated HCl are added. The mixture is then heated on a hot plate at 200 °C for 48 h and then 1 mL of HF, 3 mL of HNO_3 and 2 mL of HCl are added to the dried sample. HNO_3 is usually used to decompose the organic matrix into carbon dioxide as shown below:

$$(CH_2)_n + 2\,HNO_3 \longrightarrow CO_2 + 2\,NO + 2\,H_2O$$

HF is typically used to decompose the silicates as shown below:

$$SiO_2 + 6\,HF \longrightarrow H_2SiF_6 + 2\,H_2O$$

Also, HCl is frequently used to decompose the inorganic part of the matrix by forming soluble chlorides.[66]

The suspension is then sonicated for 10 min followed by centrifugation. Finally, the filtrate is diluted with 2% HNO_3 and stored in polyethylene bottles before analysis by ICP-OES.[67] The digestion step necessary for this working mode causes serious limitations on the performance of the analytical method. High time consumption, utilization of toxic acids under drastic conditions, precipitation of some elements and

possible sample contamination or analyte loss are disadvantageous aspects of using digestion.

Also, the simultaneous introduction of analyte elements, matrix components and solvents into the ICP can give rise to both spectroscopic and non-spectroscopic interferences.[32] There is indeed an average of 295 lines emitted by each element in ICP-OES, at over 100000 wavelengths in total. Spectroscopic overlap is one of the major problems associated with ICP-OES, which originates from sample components that emit radiation at or in the vicinity of the analytical line, giving a single line overlap or continuum background emission with the analyte line. Although this problem is not that important in the case of major elements, for trace elements, the analytical wavelength must be selected carefully. Even with the most skillful selection of lines to be employed for analysis, it is often impossible to find analytical lines without interference from other elements, which then needs to be corrected.

Other elements present in the sample matrix may also affect the analyte signal even if they do not generate spectroscopic interference. These non-spectroscopic interferences are called “matrix effects”, as matrix elements present in large concentration are generally responsible. They induce changes in analyte signal through changes in nebulization efficiency or in excitation temperature, which may be compensated using internal standardization with one to three elements.[62] For example, an analyte emission line with a low sum of excitation and ionization energy can be used to compensate for changes in sample introduction efficiency, while one with a high sum energy sum will be affected by changes in both nebulization and plasma temperature.[62]

Non-spectroscopic interferences or matrix effects are divided into physical and ionization interferences. For example, in a physical interference, a change in the acid concentration or dissolved solid content results in changes in the nebulization rate, due to variations in the viscosity, density and surface tension of the solution. These effects may influence droplet size, which can change the sensitivity of analysis. In an ionization interference, the analyte is not easily ionized while the interfering element in the matrix is ionized readily. In fact, thermal ionization, by which analyte ions are produced in the ICP is an equilibrium process on which Le Chatelier's principle may apply. Thus, if a moderately large concentration of easily ionized elements (EIEs) is present in the sample matrix, the number of electrons in the central channel of the plasma would be increased.[68] As a result, the thermal ionization equilibrium may be shifted toward the neutral atom, which results in a suppression of the ionic signal. One way to compensate for this problem is to increase the residence time of the analyte in the plasma by changing the plasma operating conditions so as to allow more time for thermal ionization to happen. In other words, the analyte is then allowed to reach a hotter region of the plasma, where there are more collisions, which can change the equilibrium back toward formation of ions and finally excited ions. Ionic emission is usually preferred because it is more sensitive than atomic emission for many elements.

Different ways are used to increase the residence time of the analyte in the plasma such as increasing the RF power, decreasing the nebulizer gas flow rate or monitoring the plasma higher above the induction coil (i.e., increase the observation height), but any of these alone or in combination will concurrently result in a sacrifice in sensitivity, as it

translates into sampling the plasma higher above the induction coil than the position that is optimal in terms of sensitivity, as shown in Figure 2.2.

Finally, as the amount of some samples, such as biological samples, is often limited, sample introduction systems that require very small sample sizes are essential. For these reasons, if solid samples can be analyzed directly with in situ separation from the sample matrix, labor cost would be reduced, contamination from chemical reagents eliminated and sample throughput increased.

2.4. Methods currently being used for improving the capabilities of ICP-OES

2.4.1. Mixed-gas plasmas

While argon is the most frequently used gas for inductively coupled plasma spectrometry, the use of mixed-gas plasmas has been reported to improve certain analytical characteristics of the ICP. Mixed-gas plasmas are those generated when argon is partially substituted by foreign gases such as N_2, O_2, H_2 and He. These gases are also introduced in the Ar ICP as additional flows. For example, an addition of O_2 is useful when introducing organic samples into the plasma to prevent soot deposition on the torch and increase electron density in the ICP.[69] As a result, the thermodynamic characteristics of the ICP are improved, in turn enhancing energy transfer and plasma robustness. Also, matrix effects may be reduced, predominantly in the case of samples whose matrix is usually complex.[69] Furthermore, some refractory materials such as coal have been analyzed using Ar–O_2 and Ar–N_2 plasmas in ICP OES,[70,71] which resulted in an improvement of precision and accuracy when compared with the standard Ar ICP. Addition of H_2 and He to the Ar ICP has also reduced the matrix effects for analysis of

ceramic powder samples in the ICP.[72] Accurate and precise results may be achieved in such plasmas, by means of calibration with aqueous standards and internal standardization. However, it has been reported that addition of a huge amount of a molecular gas such as N_2 to the outer gas flow can reduce the ionization and excitation temperatures in the plasma due to the extra energy needed to break down the nitrogen molecules.[73] Also, emission by molecular species generated in the ICP can increase the background signal. The use of mixed-gas plasmas may also reduce the lifetime of the torch. Hence, they are usually reserved to specific applications.

2.4.2. Alternative sample introduction techniques

Many methods have been designed to refine the aerosol entering the plasma for improved analytical performance of ICP-OES. These include development of new nebulizers to improve the properties of the aerosol itself and desolvation systems to remove the solvent (which affect analyte ionization and plasma robustness). For example, one way of increasing the sample transport efficiency is to use a higher efficiency nebulization system, such as an ultrasonic nebulizer (USN). Nevertheless, the larger amount of sample aerosol entering the plasma creates an increased solvent load, which cools the plasma. As a result, more plasma energy is required to desolvate the sample aerosol, leaving less for analyte excitation or ionization. This not only deteriorates analytical performance of the ICP but may also causes plasma extinction. A desolvation system, which usually involves a heater/condenser (HC) to correspondingly vaporize and condense as much solvent as possible, is thus normally used to decrease the solvent load. An additional decrease in solvent load and aerosol droplet size can also be achieved by

using a membrane desolvator (MD), which in turn simplifies aerosol desolvation and vaporization in the plasma.[74] Additionally, the method of eliminating solvent efficiently preconcentrates the analytes. However, matrix effects are exacerbated compared to those obtained using a conventional sample introduction system, because the matrix is pre-concentrated along with the analytes.[75,76] Eliminating water thus has a disadvantageous outcome as water acts as a load buffer, which minimizes (dilutes) matrix effects.[77] Water is also the main source of hydrogen in the plasma and the thermal conductivity of hydrogen accelerates energy transfer between the bulk of the plasma and the central channel, where the analyte is located.

In the next studies, the analytical performance of ICP-OES was improved by replacing the heater and condenser of a commercial USN with a pre-evaporation tube (PET) covered with heating tape (HT). While some radiative heating takes place, mostly conductive heating occurs, resulting in a temperature gradient from the tube's wall, where temperature is highest, towards its centre. In this system (Figure.2.6), the PET was placed between the spray chamber and the torch to pre-vaporize aerosol droplets without removing water and allowed the analysis of elements, such as Hg, that would otherwise be lost in the desolvation system.[78]

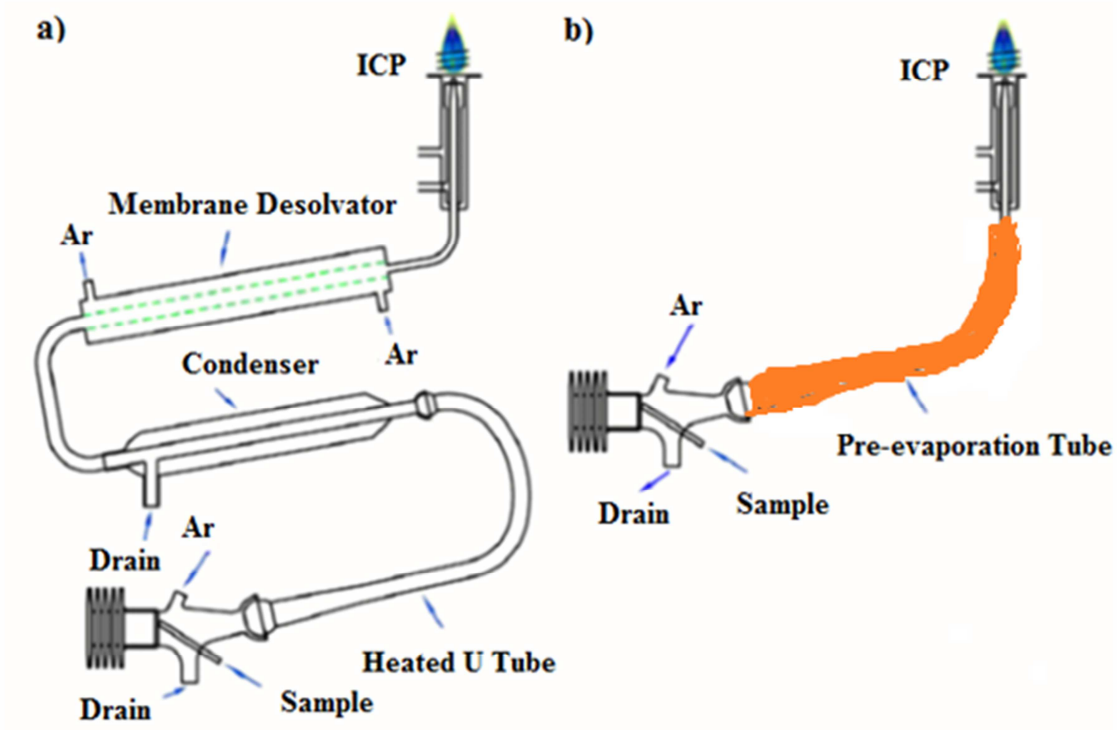

Figure 2.6. Ultrasonic nebulizer: a) with heater, condenser and membrane desolvator (USN–HC–MD); b) directly connected to ICP through long pre-evaporation tube (USN–PET). (adapted [78]).

Compared to conventional PN, the use of USN-PET(HT) in ICP-OES lead to a substantial improvement in detection limit without jeopardizing plasma robustness, i.e. the ability of the plasma to accept variations in matrix structure or solvent loading without a major change in plasma excitation characteristics.[78] However, compared to USN-HC-MD, the improvement in detection limit was not significant and the plasma extinguished when the sample uptake rate was raised above 0.3 mL min^{-1}, due to the high solvent load and non-uniform heating with heating tape.[78] In the next studies, the pre-

evaporation process was improved by using infrared (IR) heating instead of convective heating with heating tape (Figure 2.7).[79]

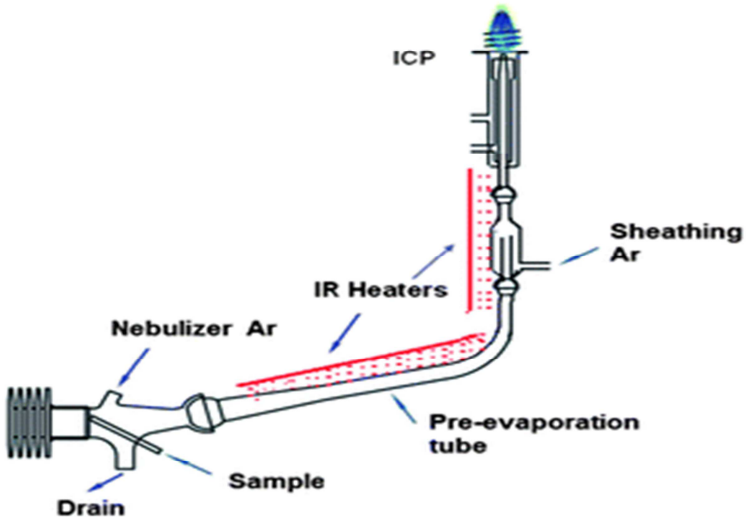

Figure 2.7. Ultrasonic nebulizer directly connected to the torch through IR-heated PET (USN-PET(IR)).[79]

Indeed, IR radiation is directly transformed into heat upon absorption by a material,[80] resulting in fast heating rate and uniform drying/heating. This design is an easy way to significantly increase the analytical performance (sensitivity, detection limit, plasma robustness and memory effects) of ICP-OES. Because IR heating is both efficient and uniform, the plasma can tolerate an increased sample uptake rate. The increased amount of water vapor then increases the plasma excitation condition and robustness so much that precise and accurate multielement analysis of samples can be done by a simple external calibration, without matrix-matching, using an Ar emission line as an internal

standard.[79] Also, this method of using USN allows the determination of elements, such as Hg and B, which would be lost in the desolvation system of USN-HC.

However, solid samples still need to be digested prior to nebulization in such system, which is very lengthy and may result in analyte loss or sample contamination. These problems coud be completely avoided using direct solid sampling introduction techniques in combination with ICP-OES.

2.4.3 Direct solid sample introduction techniques

So far, many strategies for direct solid sample analysis have been used in ICP-OES. However, almost no approach has received widespread acceptance. Most of these techniques are plagued by poor precision and difficulties in standardization.

2.4.3.1 Direct solid sample insertion

Direct sample insertion (DSI) involves placing a sample, either liquid or solid, into a sample carrying probe made of different materials, such as graphite, tantalum, or tungsten, and then inserting the probe directly into the plasma. The energy transfer from the plasma causes a fast heating of the sample probe and vaporization of the analyte species into the lCP. The advantages of the approach are high sample transport efficiency and short analysis time. Poor precision (15-20 %) in comparison to aqueous solutions and problems related to the probe, such as reactivity, deterioration and memory effects are the main limitations of this technique.[81] In addition, this technique may not be efficient for the direct analysis of some samples with complex and refractory matrices, such as geological samples.[82] For these reasons, this approach is not commercially available.

2.4.3.2. Laser ablation

In laser ablation (LA), a laser beam is used to vaporize solid materials when it is focused on a small spot (1 to 50 µm). When the laser radiation strikes the surface, it generates a high temperature vapor plume of atoms, ions and molecules, which can then be transferred by a gas stream into the ICP.

Laser ablation has the potential for fast analysis of solid samples of entirely unknown composition. The accuracy in quantitative analysis depends, to a great extent, on the availability of calibration standards and on the ability to carry out internal standardization. Powdered samples, such as soils samples, are usually pressed into a pellet with a binder prior to LA analysis, which may introduce contamination. Matrix effects and the lack of solid reference materials are other drawbacks of LA-ICP-OES, which can significantly reduce the accuracy of analysis.[83] The use of femtosecond, instead of nanosecond, LA can drastically reduce elemental fractionation effects, especially at high repetition rates. For example, a recently developed IR-femtosecond LA system uses a narrow laser beam, producing small craters (17 µm in diameter), which is moved in a series of concentric circle trajectories at high repetition rates with a galvanometric scanning beam device to produce craters of 100 µm in diameter. Particle-size fractionation was reduced by using a high repetition rate as well as a high scanner speed to dilute large particles ablated from the surface with smaller particles ablated from deeper in the crater. Furthermore, using wet plasma conditions, which provide higher robustness and larger tolerance to mass loading than dry plasma conditions, can decreaseminimized elemental fractionation inherent to the ICP. [84] However, femtosecond lasers are much more expensive than lasers operating in the nanosecond domain.

2.4.3.3. Dry powder introduction

In this technique, sample powders are introduced consistently into an ICP by a powder sampler based on linear motion of the powder container towards an uptake capillary.[85] The most important problem with this technique is that the degree of sample vaporization in the plasma is dependent on sample matrix and particle size. For example, experimental results showed that 10 µm SiO_2 partic1es were 20-25% vaporized and 5 µm partic1es were 60-70% vaporized in the plasma.[86] Even high power plasmas may not be able to completely vaporize large particles of solid samples. In a study conducted by Borgianni *et al.*[87], the behavior of CuO (boiling point (BP) 2400 °C), NiO (BP 2530 °C), TiO_2 (BP 3230 °C) and $A1_2O_3$ (BP 3240 °C) injected along the axis of an argon plasma powered by a 15 kW radio frequency generator at 4 MHz was investigated. For 60-µm particles, the decomposition percentages were 60%, 28%, 18% and 10% for the above mentioned materials, respectively. Thus, even in such a powerful plasma, the decomposition percentages were low and depended on the particle properties. This implies that incomplete vaporization of partic1es would lead to low and matrix-dependent signals. That is why this technique is not commercially available.

2.4.3.4. Electrothermal vaporization (ETV)

One approach to sample introduction that decreases matrix effects and can handle a limited sample size is electrothermal vaporization (ETV), which has been studied over the last 40 years as a sample introduction technique in combination with ICP-OES for the direct determination of elements in both liquid and solid samples. In this technique, the solid samples can be directly weighed in graphite boats, which are then placed into the

graphite furnace tube of the ETV system by an autosampler. In the ETV system, a sample is heated in steps so as to desolvate it, pyrolyze the matrix and vaporize the analytes, which are then transported directly into the ICP by an argon gas flow via a Teflon transfer tube. A second argon gas flow (the so-called bypass gas) is essential to minimize transport losses on the way from the graphite furnace to the plasma. A reactant gas is usually used to transform metallic compounds into volatile halogenated species to suppress the formation of carbides and increase transport efficiency.

In addition to an enormous ability for direct analysis of solid samples, this system has gained renewed interest from the atomic spectroscopy community owing to its exceptional characteristics compared with conventional nebulization. Firstly, the small sample mass requirement of ETV is favorable to situations where only a small amount of sample is available. Secondly, although some analytes may be lost in the transfer line between the ETV and the ICP, close to 100% sample introduction efficiency can be achieved, translating into significant improvements in sensitivity and detection limit (DL). Thirdly, the ETV steps of matrix pyrolysis and analyte vaporization are separated temporally, which is helpful for reducing interferences from the matrix and can be further enhanced with judicious usage of chemical modifiers and temperature programs. Finally, the ETV approach is straightforward, as solid powders are simply deposited in a graphite boat, which reduces the risk of sample contamination.

Thus, despite the fact that an ETV system is significantly more expensive than conventional nebulization techniques, it offers unique capabilities that are well worth the investment.[88-90] The next sections review the history of ETV development and its broad

application area for the analysis of numerous samples of various types (such as geological, biological, and environmental samples) in industrial laboratories.

2.5. The history of ETV development

The first reported study combining ETV, as a source for sample introduction, with ICP-OES was by Nixon *et al*. in 1974[91] The sample was placed onto a thick tantalum filament contained in a quartz dome. The dome was fitted with an inlet for argon at the base and an outlet port at the top connected to the plasma torch. The filament was heated by an electric current, and, finally, the vaporized analytes were transported by an argon gas flow into the ICP torch where, following atomization, excitation and ionization of atoms occurred. The reported DLs for 16 elements were in the micrograms per liter range from 100-µL samples. These results clearly showed an improvement in DLs of one to two orders of magnitude compared with those obtained using nebulisation of solutions into the ICP. The evaporation chamber that was used in their study was above 100 mL in volume, a situation that could lead to some problems such as temporal peak broadening. Kitazume *et al*.[92] used a heated filament (up to 1500°C) of primarily platinum or tungsten to vaporize 10-µL samples in a smaller quartz evaporation chamber for the introduction of vaporized analytes into the ICP torch through a transfer tube.

Although a comparison of the absolute DLs with previous study showed that in most cases a superior power of detection for elements such as B, Ge and P was obtained with this method, the most important problem with this type of ETV devices was impurities from the metal filaments, which could cause a serious increase in the blank signal and memory effects. Another problem with the metal filaments was their inherent

potential to evaporate at high temperatures, thus preventing their application as a vaporizer.

In 1978, G. F. Kirkbright *et al.*[93] studied the application of a graphite rod ETV device for the introduction of microliter liquid samples, after desolvation, into an argon ICP source. In this type of heating unit, the sample was vaporized from the surface of a graphite support and upward streaming of the vaporized product was achieved with the aid of an argon sweep gas, which carried the vaporized sample to the injector tube of the ICP source. This system was labeled as 'upward streaming' system. Using this procedure, the authors were able to determine 16 elements at the subnanogram level with sufficient accuracy and excellent DLs in small sample volumes (10-µL). However, this method was difficult to apply to routine analysis of real samples as memory effects could result from the condensation of solvent vapours in the system. A second problem was that no signals were obtainable for elements forming refractory carbides (such as Zr, Cr, W,…) on the graphite rod.[94] The formation of refractory carbides resulted in incomplete vaporization of the analyte elements and decreased their related signals.

In an attempt to prevent this problem, they introduced halocarbons into the carrier gas (CCl_4 in argon) to form volatile halides of the analytes in situ, which were then easily volatilized from the graphite rod. Linear calibration curves with respect to analyte concentration clearly showed the great ability of this proposed method for transferring these refractory compound-forming elements to the plasma.

To avoid memory effects from the condensation of solvent vapours in the system, Broekaert *et al.*[95] developed a graphite furnace ICP combination with an analyte transport

system for the analysis of biological samples. In this type of graphite furnace vaporizer, the vaporized analytes were entrained towards one of the ends of a horizontal graphite tube. This version of interfacing may be labeled an ‘end-on’ streaming system. In this ETV-ICP system (Figure 2.8), micropipettes were used to introduce sample aliquots into the furnace. Solvent vapors generated during the drying step were exhausted by two opposite argon flows introduced from both sides of the tube. After sample drying, the gas flow (1) was blocked and the remaining gas flow (2) transported the vaporized analyte into the ICP. As no moisture entered the aerosol transport system, contrary to the earlier described carbon rod or tantalum filament devices, low memory effect was observed.

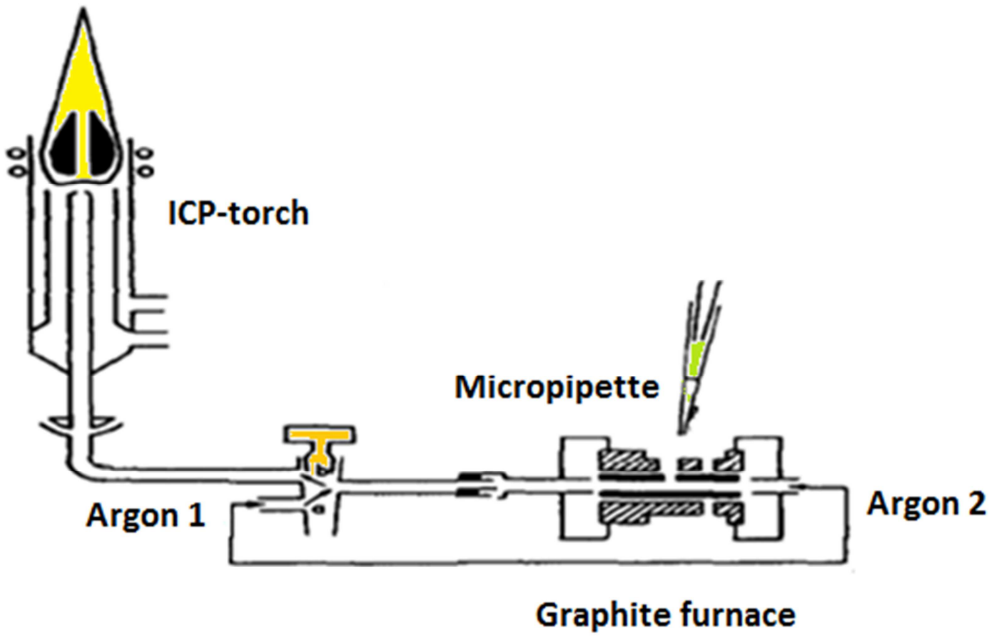

Figure 2.8. Set-up for the evaporation of samples from a graphite furnace and their introduction into an ICP. Argon gas flows: (1): gas flow for vapor elimination during sample drying, (2): carrier gas flow for the dry aerosol (adapted [95]).

However, one major problem associated with this ETV device was the condensation of analyte vapor during transportation from the graphite tube to the plasma, which resulted in poor analyte transport efficiency. An essential modification of the design of the end-on streaming system was suggested by Caruso *et al.*[96], who mixed the hot sample vapor with 'cooling argon' in close proximity to the outlet end of the graphite tube. For this purpose, an additional gas inlet was added to the graphite furnace. This design allowed the vaporized analytes to transform quickly into a dry aerosol and thus to flow in the centre of the transport line immediately after leaving the graphite tube. This device demonstrated increased analyte transport efficiency, less memory effect, lower DL, and smaller sample sizes compared to conventional nebulizers.

Because so many problems were encountered with the analysis of solid samples after wet digestion, there was a growing interest in the direct analysis of solid samples by the ETV sample introduction method. All the parameters added to the previous versions of ETV, including graphite sample holder, argon carrier gas, argon coolant gas and reaction gas (halocarbons) now could be added in one device to improve analyte transport efficiency and sensitivity. In the most modern version[97], about 1-5 mg of sample is weighed into a graphite boat, which is then introduced into the graphite tube that is part

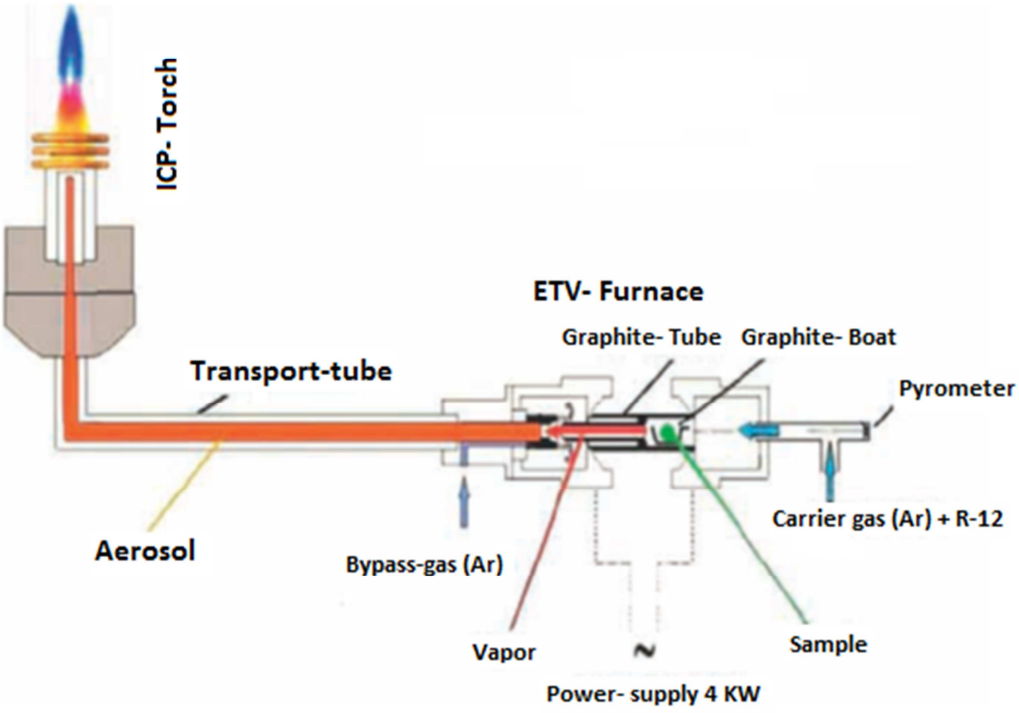

Figure 2.9. Schematic diagram of the commercially-available SS-ETV system (modified [97]).

of the ETV system (Figure 2.9) by an autosampler gripper and is then heated in the temperature-controlled graphite furnace. The vaporized analyte is then transferred into the ICP by a well-defined gas flow regime. Details of the SS-ETV-ICP-OES instrumentation are discussed in Chapter 3.

2.6. Applications of SS-ETV-ICP-OES

Nowadays, the use of ETV for sample introduction into ICP-OES has gained quite a broad application area for the analysis of numerous samples of various types (such as industrial, biological, and environmental samples). The determination of trace elements in these samples is usually restricted by the sensitivity of instruments and the

interferences caused by the complex matrix. Thus, ETV sample introduction, facilitating in situ separation of analyte and matrix in the graphite furnace using a proper temperature program, is well adapted for this analysis purpose. Because of the aforementioned problems for the analysis of solutions, many of the applications presented in analytical laboratories involved the development of direct SS strategies.

The SS-ETV-ICP-OES approach has proven to be very well suited particularly for the determination of trace impurities in high-purity ceramics and refractory materials such as alumina (Al_2O_3), boron nitride (BN), silicon carbide (SiC), titanium dioxide (TiO2) and Ta powders.[34,35,37,39,40] For example, this technique was used for the direct determination of trace amounts of impurities such as Ca, Fe, Ga, Mg, Mn, Na, Ni, V and Zn in alumina (Al_2O_3) powders without any sample pretreatment. These impurities were the cause of the common fractures in old ceramic components and SS-ETV-ICP-OES was able to detect these impurities down to the low µg/g levels.

This technique has also been employed to determine trace elements in human hair and some other biological and botanical samples as this can explain possible environmental pollution by inorganic substances.[98-103] This application offers great interest in some circumstances, such as analysis of small size plant samples, and provides a significant reduction in analysis time and costs. The main advantage of SS-ETV-ICP-OES technique for this application is the absence of matrix interferences as they are common for biological samples with conventional nebulization.

Also, this technique has been used for forensic analysis of paint and hair samples.[104,105]. For example, SS-ETV-ICP-OES method was used for discrimination of

automotive paint samples as they often constitute trace evidence at crime scenes, particularly in hit-and-run cases.[104] Two replicates of 18 automotive paint samples, collected by scraping six red-colored car wrecks from three sides (front, side and back), were analysed by SS-ETV-ICP-OES. The data matrices composed of the integrated areas of the transient signals were then analyzed by principal component analysis (PCA) and linear discriminant analysis (LDA). After classifying the major contributing variables by PCA, LDA indicated that a combination of three/four variables from Cr, Pb, Sn, and Zn properly assigned each of 18 paint samples to the correct source car. Furthermore, multi-elemental analysis of human hair has been done by SS-ETV-ICP-OES to discriminate general ethnicity and gender.[105] In this work, thirteen samples from different people with several ethnic backgrounds were analysed by SS-ETV-ICP-OES. Both PCA and LDA correctly assigned all samples for gender using Mg, S, Sr and Zn. Also, all 13 samples for general ethnicity were identified correctly by LDA. Hence, SS-ETV-ICP-OES, which only requires a very small amount of sample, shows great potential as a tool for forensic analysis of hair and paint samples.

One of the interesting applications of SS-ETV-ICP-OES is its potential to solve spectroscopic interferences in ICP-OES. In a study by Asfaw *et al.*[33], a well-known overlap that typically exists between the As and Cd lines at 228.8 nm with conventional nebulization ICP-OES was resolved by developing a selective temperature program for direct analysis of solid soil samples. In their study, As and Cd were temporally separated using a temperature program allowing selective vaporization of Cd and As at 760 and 1620 °C respectively, so that their prominent lines at 228.8 nm could be used for determination of each element by ICP-OES. The accurate results obtained for the analysis

of a solid soil certified reference material (CRM) clearly confirmed a unique feature of the method.

Finally, SS-ETV-ICP-OES has been used for the direct trace element determination in complex geological samples such as sediments, soils and rocks because dissolution of these types of samples is very time-consuming.[38] Moreover, some analytes like Cd or Hg are volatile and may be lost during traditional digestion procedures.[36] For these samples, high-grade homogeneity of the powders even at milligram levels is necessary due to the small sample weights.

Table 2.1 summarizes some interesting examples of direct solid analysis by SS-ETV-ICP-OES that have appeared in the literature during the last 10 years and evidently show the potential of SS-ETV-ICP-OES technique for analysis of different types of solid samples. In addition to the sample types, analytes of interest, related DL ranges, vaporization temperature (VT) and calibration strategies are presented as well.

Table 2.1. Examples of SS-ETV-ICP-OES applications.

Sample	Analytes / DLs (µg/g)	VT/ Calibration	Ref
Boron nitride (BN)	Al, Ca, Cr, Cu, Fe, Mg, Mn, Si, Ti 0.01 (Cu) – 0.2 (Si)	2050 °C Aqueous standards	34
Silicon carbide (SiC)	Al, Ag, As, Bi, Ca, Co, Cr, Cu Fe, Ga, K, Li, Mg, Na, Ni, Pb 0.005 (Cr) – 0.25 (K)	2200 °C Aqueous standards	37
Titanium dioxide (TiO_2)	Cr,Cu,Fe,V 0.07 (Cr) – 0.34 (Fe)	2600 °C Standard additions	39
Alumina (Al_2O_3)	Ca, Fe, Ga, Mg, Mn, Na, Ni, V, Zn 0.2 (Mg) – 100 (Na)	2300 °C Standard additions	40
Tantalum (Ta)	Ag, Al, As, Bi, Ca, Cd, Co, Cu, Fe, Ga, K, Li, Mg, Na 0.05 (Ag) – 0.25 (K)	1600 - 2700 °C Aqueous standards	35
Plant samples(1)	Al, Ca, Fe, K, Mg, Mn, Na, Zn 0.001 (Mn) – 0.08 (Ca)	1900 °C Aqueous standards	98
Plant samples(2)	P 30 (P)	2300 °C Aqueous standards	99
Botanical compounds	Pb 0.086 (pb)	2500 °C Solid standards	100
Amphipods	Ag, Cd, Co, Cu, Mn, Pb, Zn	1350 °C Aqueous standards	101
Human hair	Zn, Mn, Mg 0.3 (Mn) – 6.6 (Mg)	2200 °C Standard additions	102
Roots and leaves	Cd, Si 30 (Si)	1900 °C Aqueous standards	103
Paint	Al, B, Ba, Br, C, Ca, Cl, I, K, Li, Mg, Na, Ag, Bi, Be, Cd, Co, Cr, Cu, Fe, In, La, Mn, Mo, Ni, P, Pb, S, Sb, Se, Sn, Sr, Ti, V, W, Y, Zn and Zr ND	2200 °C ----------	104
Human hair	Ag, Ba, Be, Ca, Ce, K, Hg, Li, Mg, Mo, Na, Ni, Pb, S, Sb, Sn, Sr, Zn ND	2200 °C ----------	105
Sediments, rocks and soils	Cr, Cu, Ni, Pb, Zn 0.7 (Cu) – 6.5 (Zn)	2750 °C Solid standards	38

2.7. Calibration strategies for SS-ETV-ICP-OES

As can be seen from the table, there are several calibration strategies that may be used in direct solid analysis: calibration with multielement standard solutions, calibration by standard addition of aqueous multielement solutions and calibration with matrix-matched solid standard reference materials. Each of these procedures has its own benefits and disadvantages. For example, calibration with dry residues of aqueous standard solutions is very simple as multielement standard solutions are readily available and inexpensive, and as heterogeneity is not an issue. However, accuracy for element concentrations in SS-ETV–ICP-OES may be poor by this method. The primary reason for this poor accuracy is that the analytes in calibration standard solutions and solid samples have different transport behavior from the ETV system to the ICP. Indeed, there may be no similarity in evaporation characteristics since analytes may have different chemical forms in solid samples and aqueous standards.

The matrix-induced vaporization/transport differences between standards and samples are lessened when solid standards are used for calibration, provided that the matrix composition of the sample and the calibration standards is similar. However, these standard reference materials are not always similar to the sample matrices, possibly increasing the uncertainty of the calibration. In addition, the powder samples should always be as homogeneous as possible. Internal standards with similar excitation conditions as the analytes are usually added to standards and samples to compensate for matrix effects or variations in plasma load in ICP spectrometry. If the internal standard

truly behaves like the analyte then matrix effects are compensated, since the analyte/internal standard signal ratio should be independent of the matrix. However, it can also prolong and complicate multi-elemental analysis since the internal standards should be added to both standards and samples manually.

Finally, the standard addition calibration procedure is a possible way to circumvent most of the problems mentioned. This technique involves the addition of increasing known amounts of analytes to a number of samples so as to obtain a calibration curve whose extrapolation yields an x-intercept equal to the negative of the amount of the analyte in the sample. This method is often used for the analysis of unknown sample matrices when matrix-matching is not possible. But there is no guarantee that the added analyte will behave similarly as the analyte that is included in the sample matrix. Another drawback of the standard addition method is that every sample would require spiking with at least three different amounts of standards, so the analysis time is increased, which can lower sample throughput.

2.8. Goals of this thesis

2.8.1. Novel application of SS-ETV-ICP-OES to study the distribution of elements in soil samples for mineral exploration

This research project aims at revisiting SS-ETV-ICP-OES to further expand the range of applications of this technique, which combines the detection power of ICP-OES with all of the advantages of direct solid sampling analysis (high sample throughput, reduced risk of analyte loss and contamination, low sample mass requirement).

The primary goal of this thesis was to develop a SS-ETV-ICP-OES method allowing the direct analysis of soil samples with similar accuracy as obtained for digests by ICP-MS. Also, minimizing the analysis time for soil samples so as to maximize sample throughput. In contrast to other reports focused on elemental analysis of soil samples,[38] SS-ETV-ICP-OES was, for the first time, used in geochemical exploration to study the distribution of elements in soil so as to find where they are anomalous (i.e. significantly above background), as this may be used to locate undercover ore deposits. A geochemical orientation study executed by Anglo American Exploration Division (AA-ED) (Van Geffen 2011)[106], after identification of an anomaly east of Talbot Lake, Manitoba, Canada, provided an opportunity to test the applicability of SS-ETV-ICP-OES to geochemical exploration. After developing the SS-ETV-ICP-OES method, all the surface profile soil samples were analyzed to determine the surface distribution of pathfinder elements such as Zn, P, S and I to verify that the same or better identification of the location of undercover volcanogenic massive sulphide ore deposit could be accomplished by SS-ETV-ICP-OES as by ICP-MS following aqua regia extraction. The objectives of Chapter 4 were to further validate the SS-ETV-ICP-OES quantification method through the analysis of a soil standard reference material (SRM) and to then apply it to depth profile soil samples in order to assess the vertical distribution of elements and determine at which depth the greatest anomaly was observed. The vertical distribution of elements was also studied by qualitative analysis, an approach that proved as effective without requiring matrix-matched standards.

2.8.2. Design of an improved SS-ETV-ICP-OES system by coupling ETV to a nebulisation/pre-evaporation system for ICP-OES

The main disadvantage of the SS-ETV-ICP-OES system was that the amount of sample that the plasma could withstand without extinguishing was about 5 mg, which limited sensitivity, precision and even more so detection limits, as the latter depend on the reproducibility of the blank and on sensitivity. Finding conditions enabling the introduction of a larger amount of solid into the ICP would significantly improve these figures of merit. Hence, the final phase of the project focused on the development of a new SS-ETV-ICP-OES system to increase the amount of solid that can be introduced without extinguishing the plasma or degrading its stability so as to improve the reproducibility of results for inhomogeneous samples, such as soils.

To this end, two approaches were combined: a switching valve to vent pyrolysis products and simultaneous introduction of vapour in the ICP as this was demonstrated to increase plasma robustness.[107] After designing the new SS-ETV-ICP-OES method, the analytical performance (i.e., sensitivity, detection limit, accuracy and precision) of this system was compared to that obtained with a standard SS-ETV-ICP-OES, where the ETV system was directly connected to the torch, for the analysis of environmental samples.

Chapter 3 - Solid sampling ETV-ICP-OES to study the distribution of elements in soil samples for mineral exploration[1]

3.1. Introduction

Exploration geochemistry, which nowadays aims to locate undercover ore deposits, involves the collection, transport and analysis of numerous samples of various types (such as water, soil or sediment and rock) to map the surface and vertical distribution of elements. Soil in particular is commonly used because it can retain indicator or pathfinder elements above buried deposits.[2] However, the cost of collecting and transporting from remote sites large volumes of representative field-homogenized soil sample (2–3 kg per sample site) is significant and quickly becomes prohibitive upon an increase in sample weight or by closely spacing the sampling. It is thus important to extract the maximum amount of information from each sample, which requires the development of sensitive techniques.

Inductively coupled plasma (ICP) optical emission spectrometry (OES) is used for the multi-element determination of major, minor and trace elements.[108] For multi-element analysis at ultratrace levels, ICP mass spectrometry (MS) is preferred.[12] Both of these techniques conventionally use a nebulizer and spray chamber for sample introduction into the ICP.

However, whenever a nebulizer is used, one requirement is that the sample be in solution, which, for many geological samples, requires a dissolution step that may not

[1] A version of this chapter has been published as: Masquelin, A., **Kaveh, F**., Asfaw, A., Oates, C.J., Beauchemin, D. Solid sampling ETV-ICP-OES to study the distribution of elements in clay and soil samples for mineral exploration, *Geochemistry: Exploration, Environment, Analysis*, **2013**, 13, 11-20.

only be time-consuming but also a source of contamination or analyte loss. Methods allowing the direct analysis of solids would eliminate these shortcomings. One such sample introduction strategy is electrothermal vaporization (ETV). The sample is simply deposited in the ETV system that is resistively heated in steps, so as to desolvate the sample, pyrolyze the matrix and vaporize the analytes, which are then transported directly into the ICP. [32] It provides close to 100% sample introduction efficiency, although some analytes may be lost in the transfer line between ETV and ICP-OES. This nonetheless results in significant improvements in sensitivity. Furthermore, either liquid or solid samples can be directly processed by ETV, which is a unique feature of this sample introduction system.[32]

3.1.1. Objectives

A geochemical orientation study that was carried out by Anglo American Exploration Division (AA-ED),[106] after identification of an anomaly east of Talbot Lake, Manitoba, Canada, provided an opportunity to test the applicability of SS-ETV-ICP-OES to geochemical exploration. Indeed, as part of this geochemical orientation study, till-based soil samples collected across the Talbot line and then were digested using aqua regia and the concentrations of indicator elements were determined by ICP-MS, providing reference information for SS-ETV-ICP-OES.

The objective of this work was to develop a simple and fast method to analyze a series of soil samples by SS-ETVICP-OES, where ETV is used to vaporize solid samples and ICP-OES to determine major, minor and trace elements. This was accomplished in two ways. First, a qualitative application allowed a study of the distribution of elements

across the Talbot line. A quantification method was also developed to directly determine elements in soil samples.

3.2. Experimental

3.2.1. Samples

Along a 1000-m transect across a geophysical anomaly (i.e. the volcanogenic massive sulphide (VMS) Cu-Zn prospect that is c. 160 km SE of Flin Flon and 85 km south of Snow Lake, and was described in detail by Van Geffen *et al.*),[106] 15 sites were sampled. At each site, an area between 0.5 and 0.8 m^2 was cleared of moss, litter and roots, and one spade-depth of till was homogenized in the sample pit before 2 kg was collected. All samples were sent to Acme Analytical Laboratories in Vancouver, British Columbia, Canada, for processing. A split of the till was dried and sieved to <250 µm before analysis, a routine preparation method for soils from exploration surveys.

Table 3.1 summarizes these surface profile samples and their position along the transect line.

Table 3.1. Surface profile samples at 15 sites along the Talbot line.

Sample	Distance (m)
TALS 52161	0
TALS 52163	100
TALS 52164	200
TALS 52165	300
TALS 52166	400
TALS 52167	450
TALS 52168	500
TALS 52169	550
TALS 52171	600
TALS 52173	650
TALS 52174	700
TALS 52175	750
TALS 52176	800
TALS 52177	900
TALS 52178	1000

Thirty-gram aliquots of soil samples were analysed by ICP-MS for 53 elements following a modified aqua regia digestion at Acme Analytical Laboratories, to provide comparison values for the concentrations found by SS-ETV-ICP-OES using 4-mg aliquots. An AA-ED soil internal reference material (IRM), S5, was used for external calibration of SS-ETV-ICP-OES. This IRM was dried and sieved to <250 µm. It contained the following analyte concentrations: Zn 40.9 ± 2.41 ppm, S 0.02 ± 0.013% and P 0.053 ± 0.0028%.

3.2.2. Instrumental set-up

A SS-ETV unit (ETV 4000C, from Spectral Systems, Fürstenfeldbruck, Germany) equipped with an AD30 solid sampling autosampler for the introduction of graphite boats (shown in Figure 3.1) containing samples into the graphite tube (also shown in Figure

3.1) of the ETV system was coupled to a lateral view ICP-OES instrument (ARCOS, from SPECTRO Analytical Instruments, Kleve, Germany).

Figure 3.1. The graphite boat and tubes used for the ETV (modified[111]).

Graphite boats were 18 mm long (including a 5-mm handle) and 5 mm wide, whereas the graphite tube was 46 mm long (including a 3-mm nozzle), with a 10-mm outer diameter. A 1-metre long Teflon tube was used to connect the ETV unit to the ICP torch (a typical set-up is illustrated in Figure 3.2). ETV enables a rapid automated analysis of solid samples without need for any further sample pre-treatment.

3.2.3. Principles of operation

About 1-5 mg of solid sample is weighed into a graphite boat (Figure 3.1), which is then introduced into the graphite tube (Figure 3.1) that is part of the ETV system (Figure 3.2) by an auto-sampler gripper and is then heated in the temperature-controlled graphite furnace. The ETV temperature program is simpler than that used for the analysis of solutions and liquids, which normally consists of a minimum of four steps: drying, pyrolysis, vaporization and cleaning out. No drying step is indeed required, as there is no solvent to remove. The pyrolysis step is used to decompose the organic matrix before the

evaporation of analyte to avoid both spectroscopic and non-spectroscopic interferences.[109]

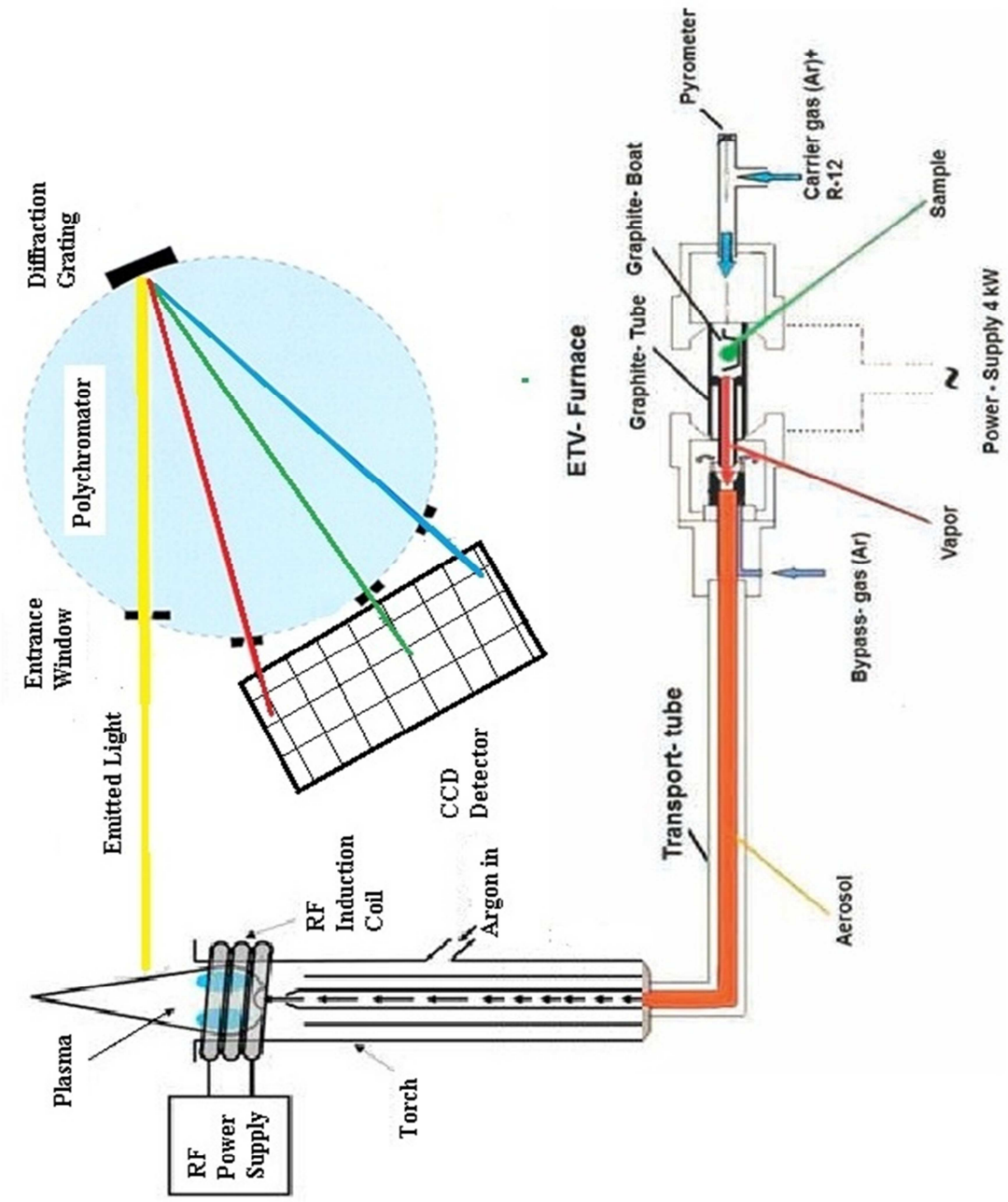

Figure 3.2. Schematic diagram of SS-ETV-ICP-OES principles of operation (modified [97,110,111]).

Thus, optimization of this temperature is a critical step for removing matrix-related interferences. During vaporization, analyte compounds are vapourised or transformed into volatile halogenated species through reaction with a halogen-containing gas, such as dichlorodifluoromethane (R12). The vaporized analytes are then transported directly into the ICP by an argon gas flow via a transfer tube. An additional cleaning step is usually required for eliminating residual materials from the graphite surface, prior to cooling. The use of halogen-containing gases or powder is most important for carbide-forming elements, and also to improve the transport efficiency of the vapours. There is no restriction in using R12 to this end because it either reacts with the analyte in the furnace or is completely atomized in the plasma. Precise temperature control, from room temperature up to 3000 °C, is achieved using a very compact pyrometer, which registers the temperature of the boat with the sample through the door on the right side. Because of the specially shaped graphite tube and precise furnace temperature control, the ETV system achieves constant and high transport efficiencies with very low memory effects.

The most important area of the system is the transition zone, where the sample vapour is becoming oversaturated and, by a well-defined gas flow regime, is transformed into a dry aerosol as illustrated in Figure 3.3. This gas flow regime arises from mixing the carrier gas stream transporting the evaporated sample with coolant gas flow (the so-called “bypass gas”). The bypass argon stream protects the surface of the cold transfer tube by forming a boundary layer. It flows from outside of the ETV unit and leads to a fast cooling of sample vapours, which is known to support the formation of nuclei in ETV-ICP procedures.[112]

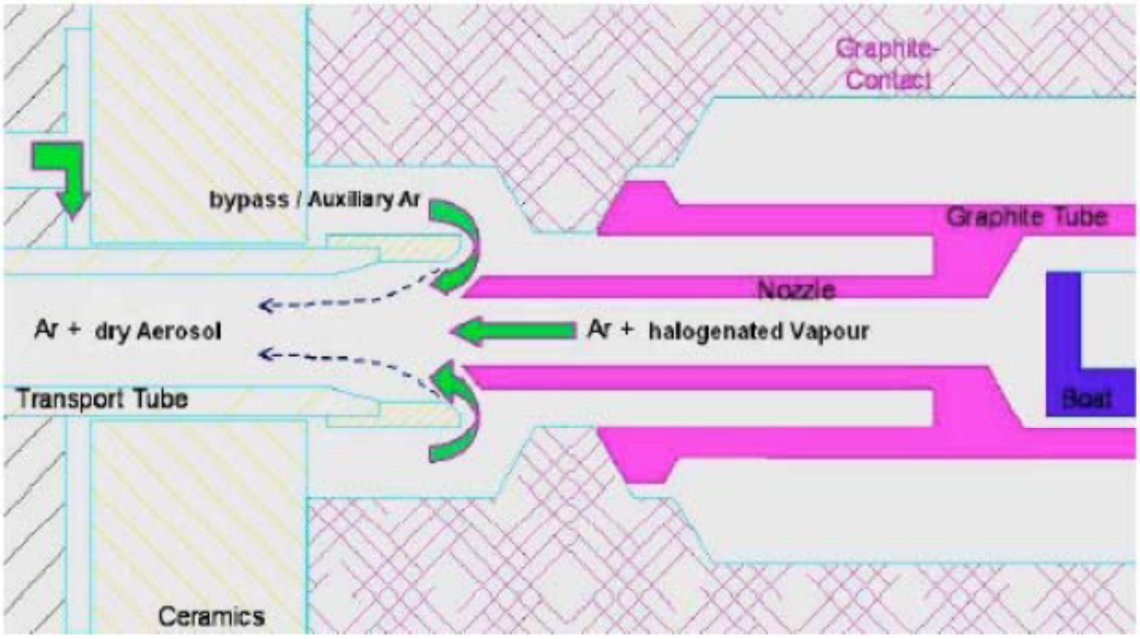

Figure 3.3. Aerosol formation in transition zone resulting from merging gas flows.[113]

The dry aerosol is then introduced via a polytetrafluoroethylene (PTFE) transport tube into the ICP where (following vapourization and atomization) excitation and ionisation of atoms occur, along with excitation of ions. The excited atoms and ions then emit element-specific radiation that is measured by a polychromator equipped with 32 linear charge coupled device (CCD) detectors for the simultaneous coverage of wavelengths between 130 and 770 nm with a resolution of 8.5 picometer. Detection in the far ultraviolet region gives access to sensitive lines for halogens and other non-metals. The polychromator of the SPECTRO ARCOS instrument is of the Paschen-Runge geometry, which uses a concave grating to disperse the emitted light over the CCD

detectors (Figure 3.2). All 32 CCD detectors are then readout and the entire spectrum is calculated in less than two seconds.

To compensate for sample loading effects, an argon emission line (Ar 763.511 nm) was used as internal standard, i.e. each analyte intensity was normalized to the Ar signal, as was done previously for the determination of elements in soil digests by nebulization using the same ICP-OES instrument.[78] Hence, the point-by-point ratio of analyte signal/Ar signal was computed to obtain the corrected transient temporal profile before the area of the peak (observed at 2200ºC) was integrated and used for quantification.

3.2.4. Method development

The good performance of SS-ETV-ICP-OES depends on its operating conditions. The carrier gas, for instance, affects the residence time of analyte in the plasma, which is important for multi-element detection. Also, an optimization of ETV gas flow rates is necessary to improve analyte transport efficiency. In this study, the temperature program, the carrier and by-pass gases (both Ar) flow rates and, finally, the dichlorodifluoromethane reactant gas (R12) flow rate were optimized using 4-mg aliquots of Talbot soil samples.

3.2.4.1. Optimization of the carrier and by-pass gases

To investigate the influence of the gas flow rates on the intensity of the analyte signals, 4-mg aliquots of soil samples were used while the carrier and bypass gas flow rates were changed from 50 to 600 mL/min, with the total gas flow rate being kept at 700 mL/min.[114] The effect of the carrier gas flow rate on the normalized peak area (i.e. area of

the peak obtained after computing the point-by-point intensity ratio of analyte over Ar 763.511 nm) of Zn and S is shown in Figure 3.4.

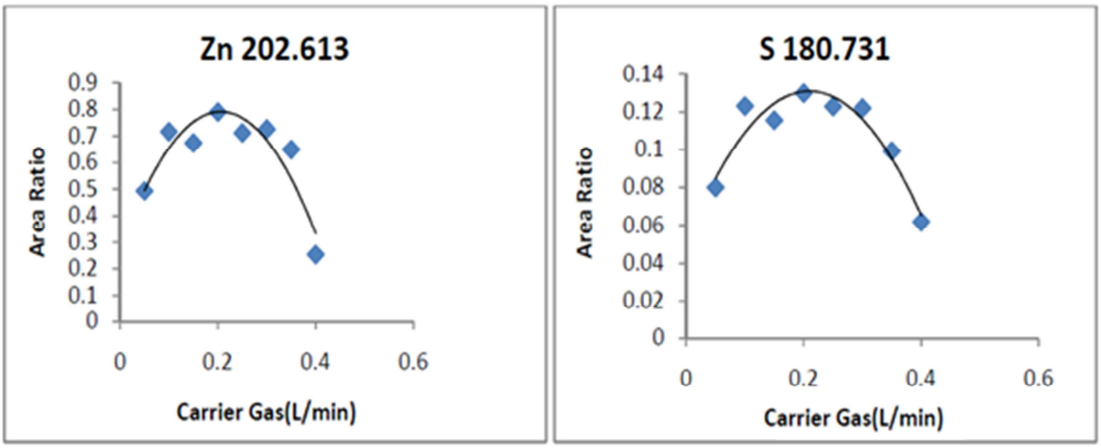

Figure 3.4. Optimization of the carrier gas flow rate for Zn and S.

The highest signal intensities for these pathfinder elements were obtained when the carrier gas flow rate was 180 mL/min, so the optimum value for bypass gas flow rate was selected as 520 mL/min.

3.2.4.2. Optimization of the reaction gas

Dichlorodifluoromethane (R-12) was used as reactant gas, since it was already reported to improve the transport efficiency and vaporization of analytes. Thus, optimization of the flow rate of this reactant gas was the next step. An addition of a small flow rate (4.1 mL/min) of R-12 reactant gas to the carrier gas was found to be most efficient for some elements, such as V and Ti, which have a tendency to form refractory carbides in the graphite furnace (Figure 3.5).

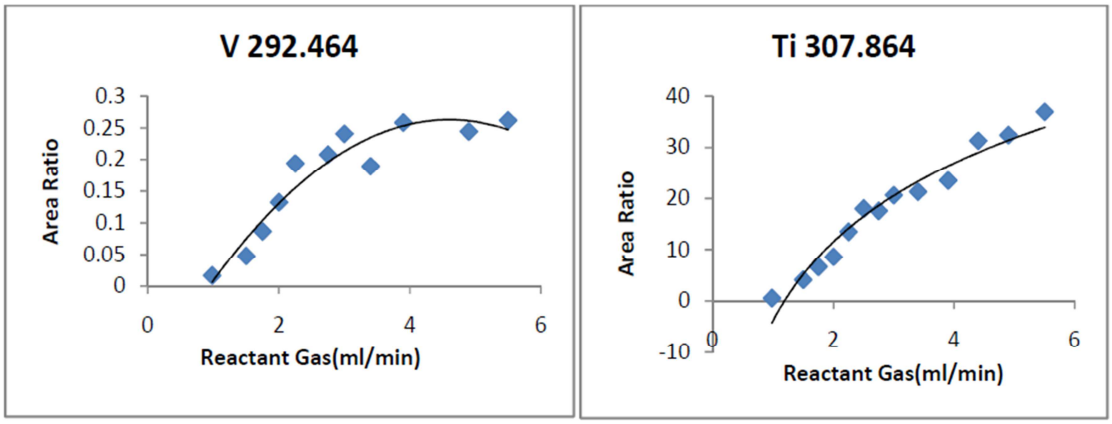

Figure 3.5. Optimization of reactant gas flow rate.

3.2.4.3. Optimization of the temperature program

For the ETV temperature program, the pyrolysis temperature was first optimized to decompose the organic matrix before evaporation of analyte to avoid spectroscopic interferences. For this purpose, the pyrolysis temperature was varied from 300 to 1200 °C. In general, with an increase of pyrolysis temperature, the resulting peak areas for target elements decreased, as shown in Figure 3.6.

In general, analyte loss (as evidenced from the appearance of a transient signal during the pyrolysis step) was observed for different elements at pyrolysis temperatures higher than 900 °C, and maximum peak areas during the vaporization step were obtained when the pyrolysis temperature was 300 °C or 400 °C. However, 400 °C was selected because an improved reproducibility of measurement was observed compared to 300 °C. The vaporization temperature was then optimized. Since different elements have various volatilities within the soil sample, compromised conditions had to be selected. As the vaporization temperature was varied from 1100 °C to 2400 °C, the peak area increased

significantly for many elements up to a temperature of 2200°C, with little gain beyond this temperature (Figure 3.6). Therefore, a temperature of 2200 °C was selected.

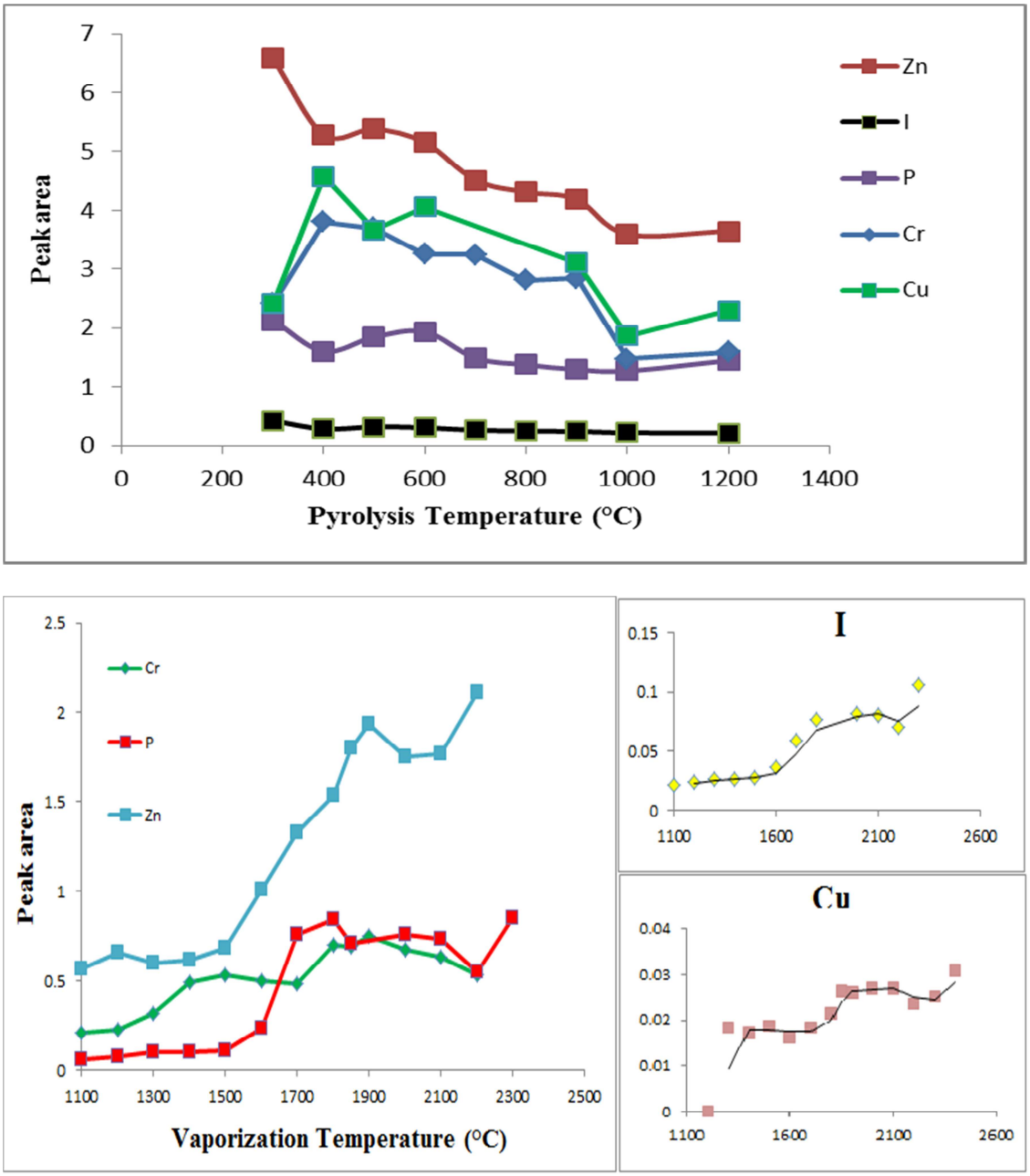

Figure 3.6. Optimization of pyrolysis and vaporization temperatures.

No clean-out step was necessary, as re-measurement of the graphite boats after the vaporization step yielded signals similar to blank samples. Also, two additional cool down steps between temperature ramps were used in the developed temperature program. The first cooling step was used in an attempt to separate the pyrolysis and vaporization steps so as to improve the resolution of the resulting peak in the vaporization step. The second cooling step after vaporization step was also used to cool down the hot graphite boats before their use for the next analysis. A temperature of 20 °C (room temperature) was used for cooling steps, as this temperature is the lowest actual temperature that can be measured by the on-line pyrometer. Figure 3.7 shows the developed temperature program used in this study.

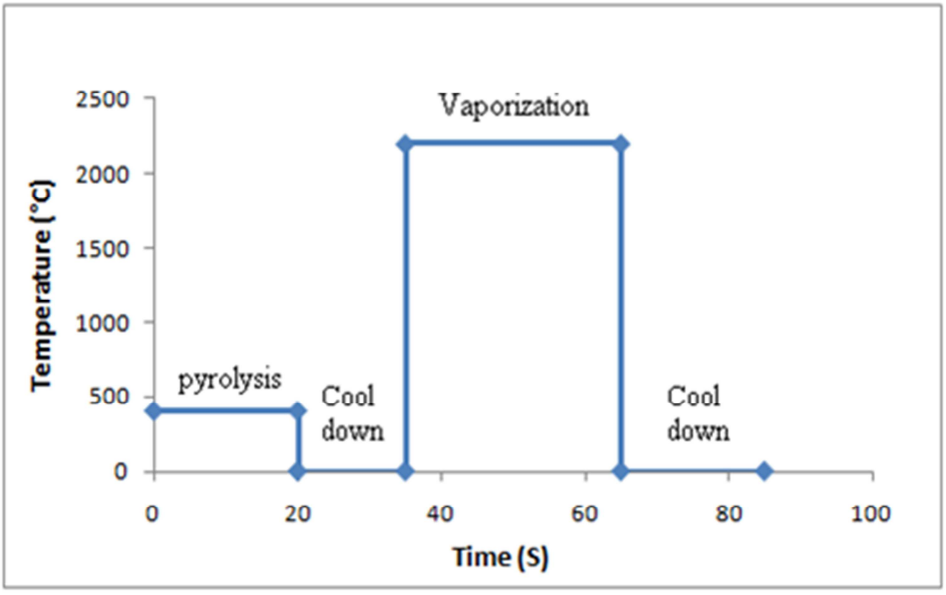

Figure 3.7. Four-step temperature program used in this study.

So, using 4 mg of sample with 4.1 mL/min of R-12, 180 mL/min Ar carrier gas and 520 mL/min Ar bypass gas, all anomalous and background soil samples from the Talbot line (15 samples in total) were analysed using the four-step temperature program. Table 3.2 summarizes the optimized conditions used for SS-ETV-ICP-OES. Data collection was accomplished by the ICP-OES software after all the measurement parameters were set to the desired values. All transient signals from soil samples were blank-subtracted after internal standardization with an argon emission line to yield the net signal.

Table 3.2. Instrumental conditions used for solid sampling ETV-ICP-OES.

ICP-OES							
Instrument	SPECTRO ARCOS lateral view						
Plasma power	1400 W						
Plasma Ar flow rate	14.00 L/min						
Auxiliary Ar flow rate	2.07 L/min						
Nebulizer Ar flow rate	0.00 L/min						
Signal scan mode	Transient						
Run time	0-100 s						
Integration time	10 ms						
ETV							
Vaporizer	ETV 4000 c						
Carrier gas (Argon 1) flow rate	180 mL/min						
Bypass gas (Argon 2) flow rate	520 mL/min						
Reactant gas (R12) flow rate	4.1 mL/min						
Four-step ETV heating program							
Steps	T (°C)	Ramp (s)	Hold (s)	Steps	T (°C)	Ramp (s)	Hold (s)
Step 1 Step 3	400 2200	0 0	20 30	Step 2 Step 4	20 20	0 0	15 20

3.3. Results

Although Ag, Al, Ar, As, Au, B, Ba, Be, Bi, Br, C, Ca, Cd, Ce, Cl, Co, Cr, Cs, Cu, Dy, Er, Eu, Fe, Ga, Gd, Ge, Hf, Hg, Ho, I, In, Ir, K, La, Li, Lu, Mg, Mn, Mo, N, Na, Nb, Ni, O, Os, P, Pb, Pr, Pt, Rb, Re, Rh, S, Sb, Sc, Se, Si, Sm, Sn, Sr, Ta, Th, Ti, Tl, Tm, U,

V, W, Y, Yb, Zn and Zr were monitored, for the purpose of investigating the repeatability of SS-ETV-ICP-OES and the suitability of this approach as a geochemical exploration tool, only selected elements, such as I, P, S and Zn, which are important pathfinder elements, are considered here.[106,115,116]

3.3.1. Internal standardisation with an argon emission line

In ICP spectrometry, internal standards with similar physical and chemical properties as the analytes must usually be added to standards and samples when performing an external calibration to compensate for matrix effects or variations in sample introduction and in plasma load,[117] which can complicate multi-element analysis. However, if a matrix-matched external calibration is carried out, then matrix-induced vapourization/transport differences between standards and samples are lessened. On the other hand, the plasma load can vary significantly between similar matrices and with sample mass, as shown in Figure 3.8 where the Ar signal is clearly increasingly suppressed as sample mass is increased whereas the Zn signal increases.

a)

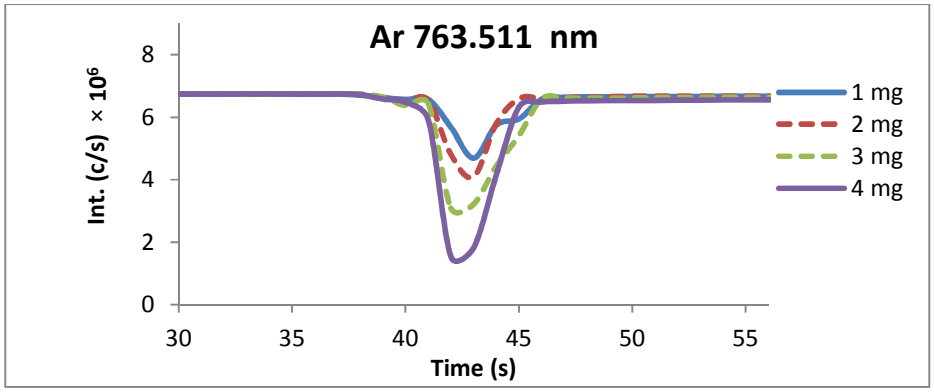
Ar 763.511 nm
Int. (c/s) × 10⁶
8
6
4
2
0
30
35
40
45
50
55
Time (s)
1 mg
2 mg
3 mg
4 mg

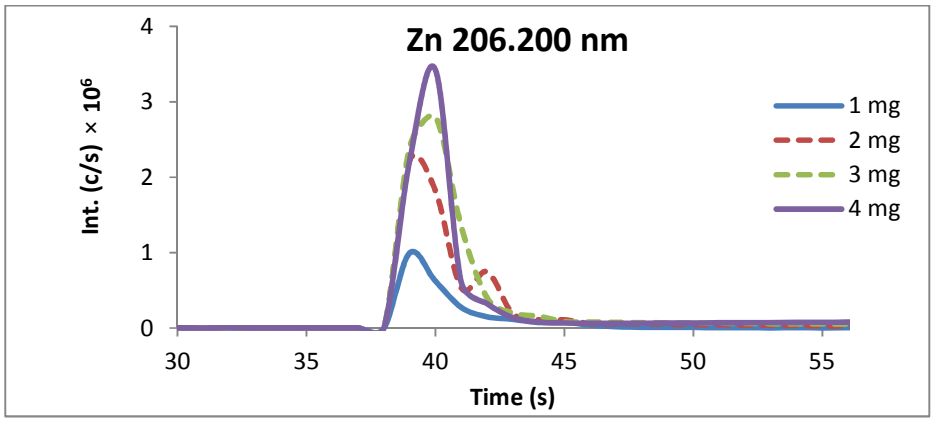
Zn 206.200 nm
Int. (c/s) × 10⁶
4
3
2
1
0
30
35
40
45
50
55
Time (s)
1 mg
2 mg
3 mg
4 mg

b)

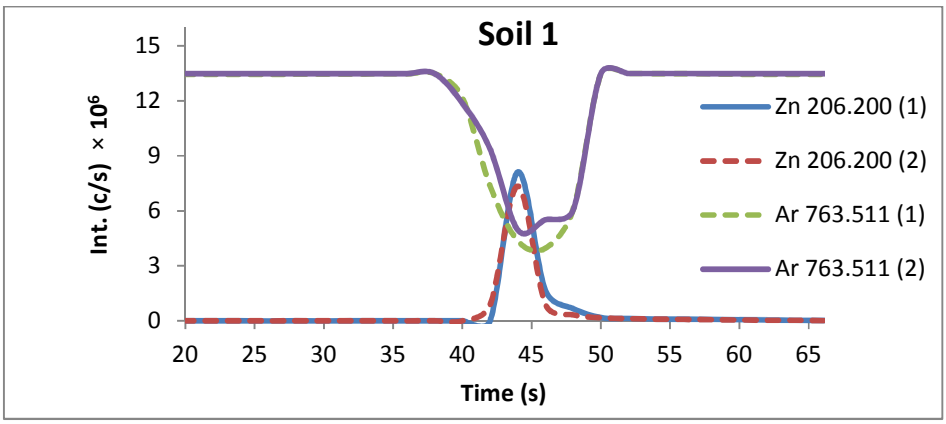
Soil 1
Int. (c/s) × 10⁶
15
12
9
6
3
0
20
25
30
35
40
45
50
55
60
65
Time (s)
Zn 206.200 (1)
Zn 206.200 (2)
Ar 763.511 (1)
Ar 763.511 (2)

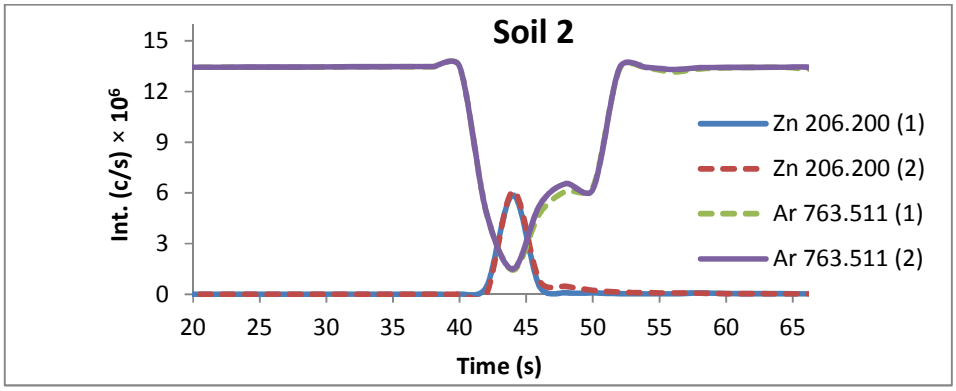

Figure 3.8. Typical Zn and Ar ETV-ICP-OES transient signals for (a) 1, 2.0, 3.0 and 4 mg of S5 IRM; (b) two 4-mg replicates of two soil samples.

Although repeatability is good for each of the two soil samples, the extent of Ar signal depression is different between the two samples, despite the fact that the same amount (4 mg) was introduced. In one case, the Ar signal drops to 3.9×10^6 c/s versus 1.4×10^6 c/s in the other case (Figure 3.8b), indicating a different effect on the plasma. Furthermore, as the amount of a given sample increases, so does the effect on the plasma (Figure 3.8a). In fact, introduction of the sample had a visible effect on the plasma. While external calibration with solid standards can be performed using different masses of a single standard, using a fixed mass of several standards or with a combination of the two approaches,[90,118-120] for the analysis using different masses of a single standard to be accurate, the matrix effect caused by the increasing mass should be compensated. Given the observations from Figure 3.8, using an Ar signal as internal standard appears indicated, as typically done in ETV-ICP-MS. Indeed, the Ar_2^+ signal is used not only to directly assess plasma loading effects but also as internal standard, to obtain accurate results,[121] correct for signal drift [122] and improve the linearity of the calibration curve

obtained by varying the mass of standard.[123] In ICP-OES, an Ar emission line can similarly be used as internal standard to compensate for matrix effect on the plasma.[67,78]

3.3.2. Detection limits

Using the optimum conditions, the detection limit was investigated; 0.5–5 mg of S5 IRM was introduced to obtain a calibration curve, and 10 empty boats were used as blanks. Table 3.3 shows the detection limits for selected elements in 4-mg samples, in comparison to those obtained from aqua regia ICP-MS (AR-ICP-MS).[106] Despite the small amount of sample used (i.e. only 4 mg), the detection limit for S was better by SS-ETV-ICP-OES than by AR-ICP-MS, while that for P was similar. Only in the case of Zn, is the DL over an order of magnitude poorer than by AR-ICP-MS.

Table 3.3. Limit of detections for selected pathfinder elements

Element	SS-ETV-ICP-OES	SS-ETV-ICP-OES (from the literature)[38]	AR-ICP-MS
P	0.003 %	Not determined	0.001%
S	0.002 %	Not determined	0.01%
Zn	2 µg/g	6.5 (µg/g)	0.1 µg/g

3.3.3. Distribution of elements in soil samples across the Talbot line

According to the AR-ICP-MS results for the soil fraction,[106] Zn and P concentrations display pronounced anomalies across the Talbot line. So, the distribution of these pathfinder elements found by SS-ETV-ICP-OES was compared with that

obtained by AR-ICP-MS. Four replicates were taken for each sample. In each case, the corrected transient signal was obtained by computing the point-by-point ratio of analyte signal/Ar signal. Then, peak area at the vaporization temperature was integrated for different soil samples across the Talbot line.

Figure 3.9 shows the distribution of Zn, P, S and I in soil samples along the Talbot line using SS-ETV-ICP-OES, with the expected anomalies evident for these elements at 400 m and 650 m.

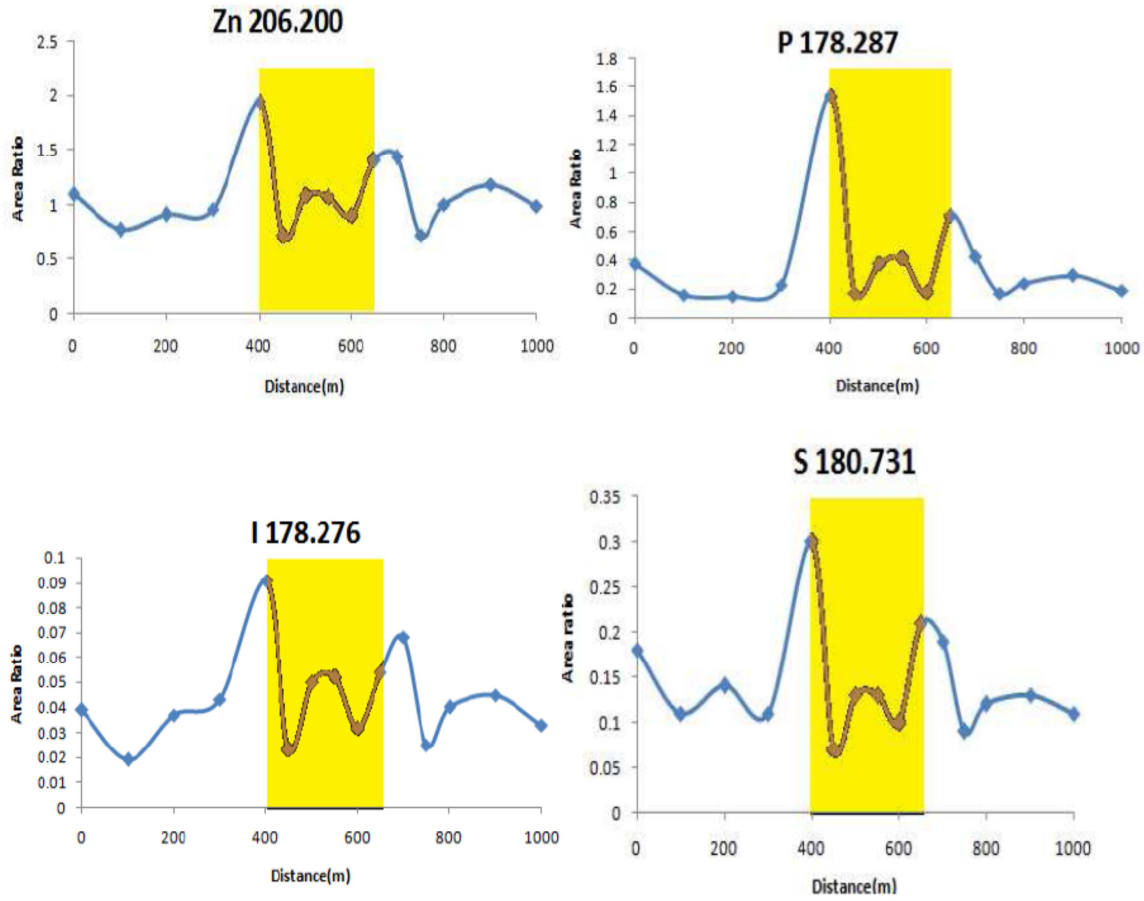

Figure 3.9. Distribution of Zn, P, S and I in Talbot soil samples along Talbot line using SS-ETV-ICP-OES. The expected anomalous area is shaded.

Moreover, the Zn and P distributions are similar to those obtained by the AR-ICP-MS method (Figure 3.10). Obviously, SS-ETV-ICP-OES leads to a significantly clearer delineation of anomalous samples from background soil samples. In any case, Figure 3.9 also shows the distribution of some elements that cannot be studied by the AR-ICP-MS method, such as S whose concentration is below the limit of detection or the halogens.

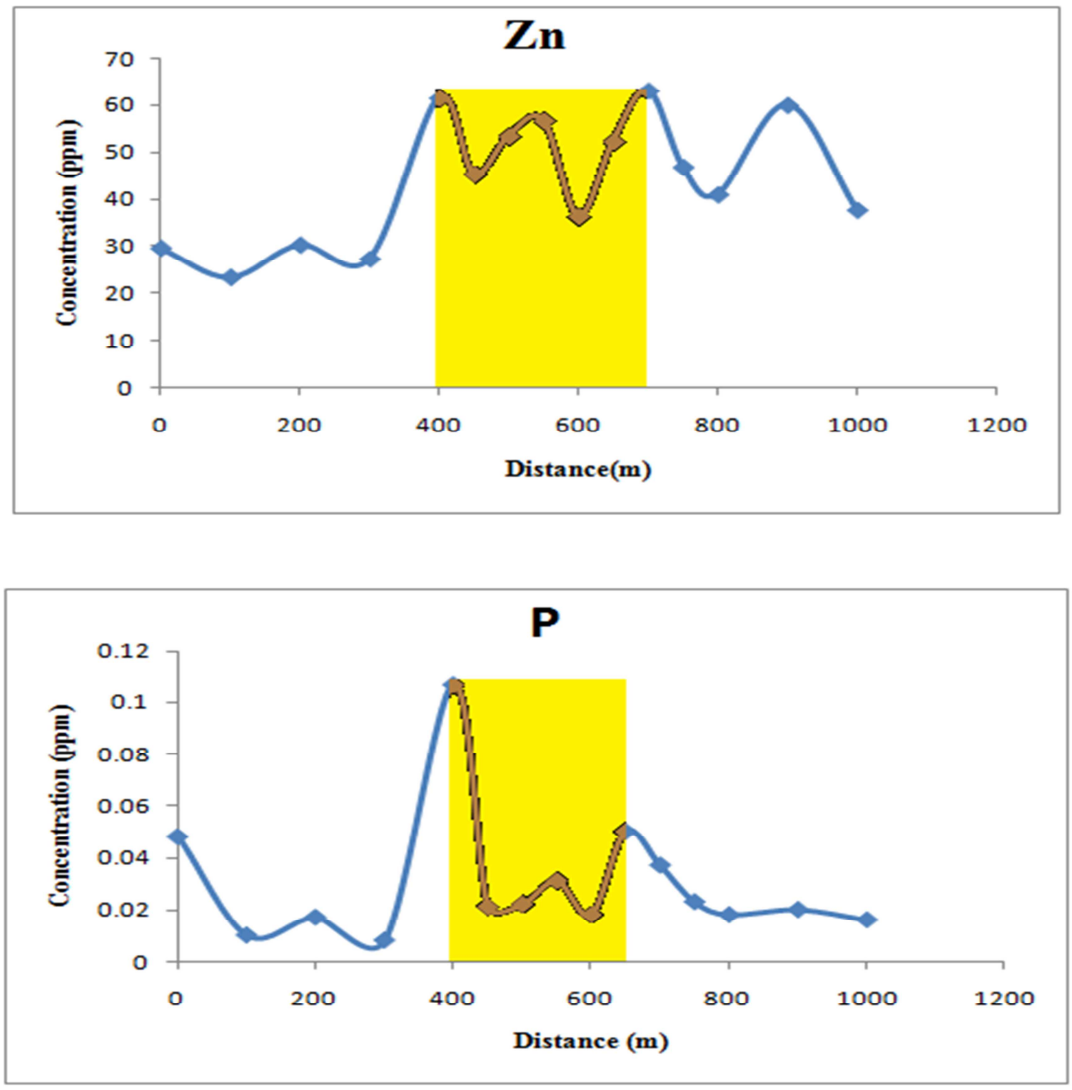

Figure 3.10. Distribution of Zn and P in soil samples along the Talbot line, using aqua-regia extraction ICP-MS analysis. The expected anomalous area is shaded.

Using SS-ETV-ICP-OES, the expected anomalies are clearly evident at 400 m and 650 m. Hence, SS-ETV-ICP-OES readily provides information that was not previously available and enables the use of S for determining the effect and depth of weathering in sulfide deposits,[116] such as, in this case, near a Palaeoproterozoic Talbot volcanogenic massive sulphide ore. Indeed, Figure 3.9 clearly shows that SS-ETV-ICP-OES readily allows the detection of higher S concentration in anomalous surface materials.

3.3.4. Quantification of elements in soils from across the Talbot line

For quantification of elements in soil samples, four replicates of 15 Talbot soil samples (Table 3.1) were analyzed with the conditions summarized in Table 2.2 to assess the possibility of using solid standards for quantification.

The AA-ED S5 soil IRM was used as a solid standard for quantification of soil samples, with internal standardisation using an Ar emission line. To make the calibration curves, the mass of S5 soil IRM was varied between 0 and 5 mg and the absolute analyte content was calculated by multiplying the weight of the sample by the certified analyte concentrations. As it is very difficult to reproducibly weigh the same amount, one replicate was used for each mass of S5. Using the optimized conditions, good correlation was obtained between peak area and the absolute concentration of analyte. Typical calibration curves using S5 as solid standard for Zn and P are shown in Figure 3.11.

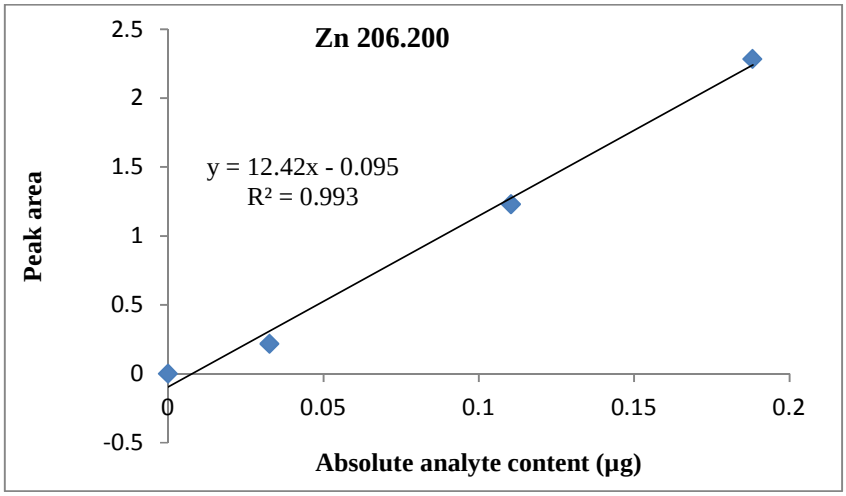

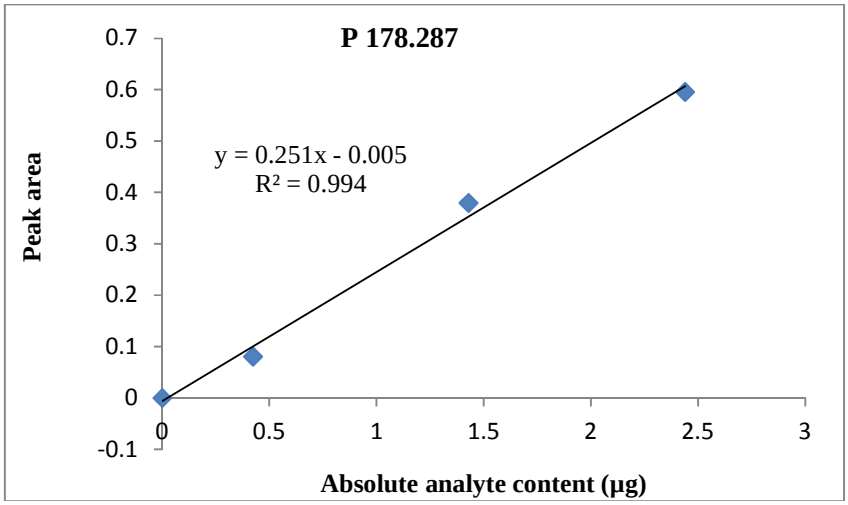

Figure 3.11. Typical calibration curves for Zn and P using 1-5 mg of S5 soil IRM.

Without internal standardisation with Ar, no linear calibration curve could be obtained. For P and Zn in soil samples, results are in agreement with the aqua regia extraction approach (Table 3.4) and S can be determined as well.

Table 3.4. Concentrations of P, S and Zn in soil samples by SS-ETV-ICP-OES (mean ± standard deviation, n=4) and AR-ICP-MS (single result from Acme Analytical Laboratories).

Sample	Distance (m)	P (%)		S (%)		Zn (ppm)	
		SS-ETV-ICP-OES	ICP-MS	SS-ETV-ICP-OES	ICP-MS	SS-ETV-ICP-OES	ICP-MS
TALS 52161	0	0.035 ± 0.029	0.048	0.020 ± 0.001	0.03	45 ± 5	29.6
TALS 52163	100	0.017 ± 0.004	0.010	0.010 ± 0.002	0.01	33 ± 9	23.4
TALS 52164	200	0.016 ± 0.004	0.017	0.010 ± 0.004	0.01	38 ± 8	30.3
TALS 52165	300	0.025 ± 0.011	0.008	0.010 ± 0.005	0.01	44 ± 8	27.3
TALS 52166	400	0.146 ± 0.029	0.107	0.030 ± 0.006	0.01	80 ± 20	61.6
TALS 52167	450	0.018 ± 0.001	0.021	0.010 ± 0.001	0.01	31 ± 6	45.4
TALS 52168	500	0.038 ± 0.011	0.022	0.010 ± 0.009	0.01	50 ± 20	53.5
TALS 52169	550	0.039 ± 0.012	0.031	0.010 ± 0.003	0.01	45 ± 8	56.8
TALS 52171	600	0.018 ± 0.003	0.018	0.011 ± 0.001	0.02	40 ± 10	36.4
TALS 52173	650	0.070 ± 0.006	0.05	0.023 ± 0.006	0.03	50 ± 20	52.4
TALS 52174	700	0.043 ± 0.018	0.037	0.020 ± 0.010	0.02	70 ± 20	63.2
TALS 52175	750	0.027 ± 0.006	0.023	0.011 ± 0.001	0.02	30 ± 10	46.9
TALS 52176	800	0.027 ± 0.006	0.018	0.011 ± 0.004	0.02	40 ± 10	41.0
TALS 52177	900	0.030 ± 0.008	0.020	0.015 ± 0.003	0.03	59 ± 6	60.1
TALS 52178	1000	0.022 ± 0.001	0.016	0.010 ± 0.001	0.03	39 ± 8	37.7

Figure 3.12 shows the similarity between the Zn and P distributions in soil samples across the Talbot line by SS-ETV-ICP-OES and AR-ICP-MS techniques. Evidently, SS-ETV-ICP-OES concentration results are slightly higher than AR-ICP-MS

technique, which confirmed that the aqua regia extraction did not dissolve the sample completely. Also, a single measurement was reported by the ICP-MS technique, so, the error bars are not shown because they are unknown.

The average relative standard deviation (RSD) for mean concentration values of Zn and P obtained by SS-ETV-ICP-OES was between 24-28%, which is commensurate with the heterogeneous nature of soil samples and the small aliquot size. This repeatability is nonetheless a satisfactory compromise in exchange for such a fast speed of analysis (i.e. 85 s per sample) by this direct solid analysis technique.[124]

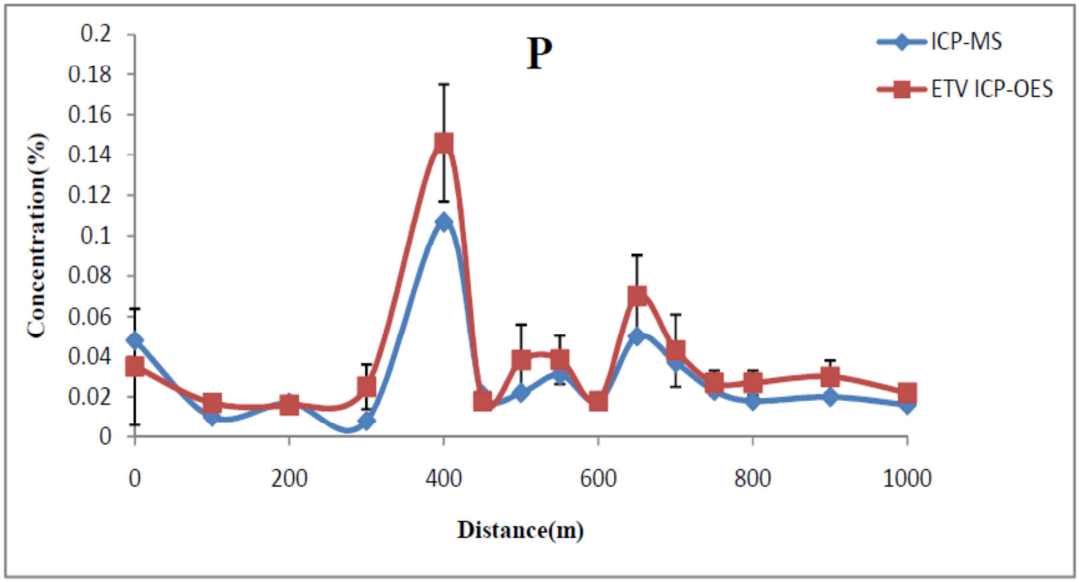

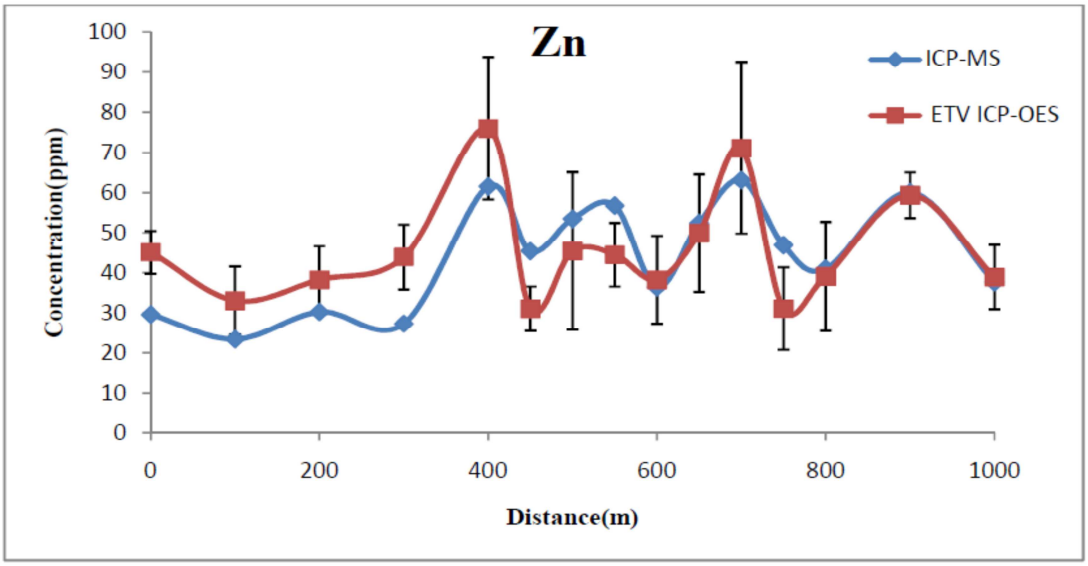

Figure 3.12. Comparison of the Zn and P distributions in soil samples obtained by SS-ETV-ICP-OES (mean ± standard deviation, *n*=4) and by AR-ICP-MS (single result from Acme Analytical Laboratories).

3.4. Discussion

The above results clearly demonstrate that SS-ETV-ICP-OES with a four-step temperature program not only enables the direct analysis of geological materials but also provides similar results to ICP-MS following aqua regia extraction, as, in the majority of cases, the AR-ICP-MS result fell within the SS-ETV-ICP-OES mean ± standard deviation. This thus demonstrates the potential of this simple approach for geochemical exploration. Although the purpose of this work was to investigate an alternative analysis technique for soils, not to assess the effect of sampling, for this technique to be accurate, the particle size must be small enough to ensure that such small aliquots are representative of the lot. Given the agreement between SS-ETV-ICP-OES (with 4-mg aliquots) and AR-ICP-MS (using several grams of sample per aliquot), sieving to <250 µm for soil samples was evidently sufficient to make, on average, 4-mg aliquots representative of the lot.

The approach is quite straightforward as the R12 reactant gas is simply added to the carrier gas. Furthermore, as the ETV temperature program only requires 85 s per sample, the approach is clearly advantageous over aqua regia extractions, which take time, require reagents and are more prone to contamination because of the multiple steps involved. Moreover, the lower sensitivity of ICP-OES compared to ICP-MS is clearly compensated by ETV sample introduction, which allows quantitative sample introduction in contrast to the 2%–5% sample introduction efficiency that is typically achieved with nebulisation.

Using internal standardisation with an Ar emission line effectively compensates for changes induced in the plasma by ETV of the sample without requiring any addition to

the sample. By simply computing the point-by-point analyte/argon intensity ratio and then integrating the area of the peak that arises at 2200ºC, the distribution of pathfinder elements in soils can readily be obtained, without the need for quantification.

If quantification is still desired, this can readily be accomplished by external calibration with different amounts of solid standard and internal standardisation with an Ar emission line, as demonstrated by the accurate determination of P, S and Zn in soils using the same four-step ETV temperature program. The introduction of different masses of one standard into the plasma is strictly equivalent to the nebulisation of different standard solutions in the plasma. Indeed, these solutions are typically prepared by dilution of different volumes of one mother solution, and, because a given volume of solution penetrates the plasma, different amounts of the mother solution are thus ultimately introduced into the plasma. In the presence of complex matrices, matrix-matching (i.e. using standards with a similar matrix as the sample) and internal standardisation may be required to account for matrix effects. However, because the analyte can be separated from the matrix in situ using a pyrolysis step prior to the vapourization step, close matrix-matching is often not necessary. For example, Detcheva et al. [120] showed that, when using SS-ETV-ICP-OES with R-12, calibration against graphite standards, dried aqueous standard solutions or various masses of a solid reference material could be used for the accurate analysis of plants materials. That is why, in this work, a soil IRM was sufficient to analyse soils, using internal standardisation with Ar to compensate for matrix effects on the plasma. Hence, because of its great simplicity and the drastically reduced sample processing that it requires, SS-ETV-ICP-OES should become an invaluable tool to assist geochemical exploration.

3.5. Conclusions

A simple and fast method was developed to directly analyse geological samples. This method allowed the analysis of all soils across the Talbot line. The distributions of Zn, P, S and I, which could be directly obtained in the soils, showed clear anomalies that could readily be quantified by external calibration with a soil standard, using an Ar emission line as internal standard to compensate for the plasma loading. The method completely eliminates the need for sample extraction or digestion.

Chapter 4 - Direct analysis of soils by ETV-ICP-OES: a powerful tool for mineral exploration[2]

4.1. Introduction

Geochemical exploration for ore deposits usually includes the measurement of some elements in numerous samples of various types (such as rock, soil, vegetation, water and sediment) in the search of a chemical pattern in the surface and vertical distribution of elements that might reveal a geochemical "anomaly" or region indicating the existence of ore in the vicinity. Soil in particular can retain indicator or pathfinder elements above buried deposits.[2]

To extract the maximum amount of information from each soil sample, fast, reliable and sensitive analytical techniques with good precision and low detection limits are necessary. Inductively coupled plasma (ICP) optical emission spectrometry (OES) is a primary method for the multi-elemental determination of major, minor and trace elements,[53,125] while ICP mass spectrometry (MS) is generally preferred for multi-elemental analysis at ultra-trace levels, as it is more sensitive than ICP-OES.[12]

Both ICP-OES and ICP-MS instruments are sold with a nebulizer and spray chamber for sample introduction into the plasma, which means that samples should be in solution. In the case of soil, this usually implies a digestion step, which takes time and uses toxic acids under drastic conditions, with the possibility of sample contamination

[2] A version of this chapter has been published as: **Kaveh, F**., Oates, C.J., Beauchemin, D. Direct analysis of soils by ETV-ICP-OES: a powerful tool for mineral exploration, *Geochemistry: Exploration, Environment, Analysis*, first published June 18, **2014**, DOI: 10.1144/geochem2013-230.

and analyte loss in the process. Furthermore, the transport efficiency with such nebulization system is usually in the range of only 2-5%. Moreover, the simultaneous introduction of analyte elements, matrix components and solvents into the ICP can give rise to both spectroscopic and non-spectroscopic interferences.[32]

Hence, an alternative sample introduction system allowing the direct analysis of solids and in situ processing of sample would clearly be advantageous, as it would eliminate the digestion step altogether, thereby drastically reducing the possibilities of contamination, and allow in situ separation of the analyte from the matrix. Such a sample introduction system is electrothermal vapourization (ETV), which has been studied over the last 40 years in combination with ICP-OES for the direct determination of elements in both liquid and solid samples.[34,35,37,39,98-103]

With a commercially-available ETV system, 1-5 mg solid samples can be directly weighed in graphite boats, which are then placed into the graphite furnace tube of the ETV system by an auto-sampler. The graphite tube is positioned between two graphite contacts, which are surrounded by argon gas so as to reduce oxidation of the graphite parts,[40] and are water-cooled for fast cool down. Each sample is then heated in steps so as to desolvate the sample, pyrolyse the matrix and vaporize the analytes, which are then transported directly into the ICP by an argon gas flow via a transfer tube. Although some analytes may be lost in this transfer line, close to 100% sample introduction efficiency can be achieved, translating into significant improvements in sensitivity and detection limits. Furthermore, because matrix pyrolysis and analyte vaporization are separated temporally, interferences from the matrix can be reduced or eliminated, a process that can

be further enhanced with judicious usage of chemical modifiers and temperature programs.[89,90,126]

The applicability of SS-ETV-ICP-OES to geochemical exploration was first demonstrated in the previous chapter, with the analysis of surface profile soil samples from 15 sites in the exploration area of an anomaly east of Talbot Lake, Manitoba, Canada, which was previously identified by a geochemical orientation study executed by AA-ED.[106] The distribution of elements, in particular Zn, P, S and I, was directly determined in soil samples by a simple external calibration, with internal standardization using an Ar emission line to compensate for sample loading effects on the plasma. Such distribution was in agreement with that obtained after digesting the same samples with aqua regia and analyzing them by ICP-MS.

4.1.1. Objectives

The objectives of this work were to further validate the previously developed SS-ETV-ICP-OES quantification method through the analysis of a soil CRM and to then apply it to soil samples in order to assess the vertical distribution of elements and determine at which depth the greatest anomaly is observed. These depth profile soil samples were taken at the same 15 sites along the Talbot line. The elimination of the digestion step also enabled a study of the distribution of halogens, which was carried out by qualitative analysis, as no reference value was available for the reference material used.

4.2. Experimental

4.2.1. Samples

A total of 68 soil samples were collected at 10-cm depth intervals between 0 to 50 cm depth at 15 sites along a 1000 m transect across a geophysical anomaly in the eastern extension of the Paleoproterozoic Flin Flon-Snow Lake terrain (1.92 – 1.88 Ga), northwestern Manitoba and northeastern Saskatchewan, about 160 km southeast of Flin Flon and 85 km south of Snow Lake, which intersects the vertical projection of mineralization. (This area is described in detail by Van Geffen *et al*. (2011)).[106] Table 4.1 summarizes the samples and their position along the transect line. The dried till was sieved and the <250-μm size fraction retained. For all quantification in the samples, an AA-ED soil IRM, dried and sieved to <250 μm, was used as a standard for external calibration. Aliquots of several grams of soil samples were also sent to Acme Analytical Laboratories for independent analysis by aqua regia extraction with ICP-MS detection.

Table 4.1. Depth profile samples down to 50 cm at 15 sites in the Talbot line.

Sample	East (m)	Depth (cm)	Sample	East (m)	Depth (cm)
45017-1	0	-10	45009-2	600	-20
45017-2	0	-20	45009-3	600	-30
45017-3	0	-30	45009-4	600	-40
45016-1	100	-10	45009-5	600	-50
45016-2	100	-20	45008-1	650	-10
45015-1	200	-10	45008-2	650	-20
45015-2	200	-20	45008-3	650	-30
45015-3	200	-30	45008-4	650	-40
45014-1	300	-10	45008-5	650	-50
45014-2	300	-20	45007-1	700	-10
45014-3	300	-30	45007-2	700	-20
45014-4	300	-40	45007-3	700	-30
45014-5	300	-50	45007-4	700	-40
45013-1	400	-10	45007-5	700	-50
45013-2	400	-20	45006-1	750	-10
45013-3	400	-30	45006-2	750	-20
45013-4	400	-40	45006-3	750	-30
45013-5	400	-50	45006-4	750	-40
45012-1	450	-10	45006-5	750	-50
45012-2	450	-20	45005-1	800	-10
45012-3	450	-30	45005-2	800	-20
45012-4	450	-40	45005-3	800	-30
45012-5	450	-50	45005-4	800	-40
45011-1	500	-10	45005-5	800	-50
45011-2	500	-20	45004-1	900	-10
45011-3	500	-30	45004-2	900	-20
45011-4	500	-40	45004-3	900	-30
45011-5	500	-50	45004-4	900	-40
45010-1	550	-10	45004-5	900	-50
45010-2	550	-20	45003-1	1000	-10
45010-3	550	-30	45003-2	1000	-20
45010-4	550	-40	45003-3	1000	-30
45010-5	550	-50	45003-4	1000	-40
45009-1	600	-10	45003-5	1000	-50

4.2.2. Instrumentation

The same instrumental set-up was used as in the previous chapter. Measurements were made using a lateral view ICP-OES instrument (ARCOS, from SPECTRO Analytical Instruments, Kleve, Germany). This polychromator is equipped with 32 linear CCD detectors in a Paschen-Runge mount assembly that delivers a resolution of 8.5 picometer in the wavelength range from 130 to 770 nm. Background-corrected signals at various emission lines were used for quantification. An ETV system (ETV 4000C, from Spectral Systems, Fürstenfeldbruck, Germany) equipped with an AD30 auto-sampler was used for introduction of graphite boats containing soil samples into the graphite tube. The outlet of the ETV unit was connected to the ICP torch by a 1-m long Teflon tube. Time synchronization between the ICP spectrometer and the ETV system was performed with the help of Smart Analyzer Vision software. This particular ETV furnace is equipped with a very compact on-line pyrometer, which provides precise temperature control from room temperature up to 3000 °C. The SS-ETV-ICP-OES experimental conditions were identical to those in Table 3.2.

4.2.3. Method

The ETV temperature program (included in Table 3.2) consisted of four steps: pyrolysis, cool down, vaporization and cool down. The pyrolysis step was used to decompose the organic matrix before vaporisation of analyte to avoid spectroscopic and non-spectroscopic interferences. An external by-pass gas was used for fast cooling of sample vapours, as this helped minimize analyte loss on the way from the furnace to the plasma. A reaction gas, R12, was also added to the carrier gas in order to transform

metallic compounds into volatile halogenated species, thereby preventing or reducing the formation of carbides and increasing transport efficiency.[38,127]

An argon emission line (763.511 nm) was used as internal standard to compensate for sample loading effects on the plasma, as was done in the previous chapter for the analysis of soil samples by SS-ETV using the same ICP-OES instrument. The corrected transient temporal profile was obtained by computing the point-by-point ratio of analyte signal/Ar signal, and the area of the peak (observed at the vaporization temperature) was then integrated. The same operating conditions were used as in the previous chapter. Four replicates of each soil sample were analysed. Calibration curves were established using 0 to 5 mg of soil IRM by plotting the analyte peak area as a function of absolute analyte content (obtained by multiplying the weight of IRM by the certified analyte concentrations). For method validation, two Montana soil CRMs were used: SRM 2710 and 2711 from the National Institute of Standards and Technology (NIST, Gaithersburg, MD, USA).

4.3. Results

4.3.1. Method Validation

As recommended for the validation of methods of analysis of soils, sediments, or other materials of a similar matrix,[128,129] the accuracy of the proposed method was first evaluated by analyzing SRM 2711, using SRM 2710 as a standard for external calibration and an Ar emission line for internal standardisation. The results are summarised in Table 4.2.

Table 4.2. Concentration (mean ± standard deviation, *n*=4) of target elements obtained by SS-ETV-ICP-OES for SRM 2711 using SRM 2710 as a standard for external calibration, as well as experimental and table values of Student's t (95% confidence level).

Element (concentration units)	Certified	Measured	$t_{experimental}$	t_{table}
Zn (µg/g)	350.4 ± 4.8	342 ± 23	0.69	3.18
P (%)	0.086 ± 0.007	0.081 ± 0.009	1.14	3.18
Cu (µg/g)	114 ± 2	128 ± 14	1.94	3.18
Al (%)	6.53 ± 0.09	6.05 ± 0.46	2.03	3.18
Ag (µg/g)	4.63 ± 0.39	4.54 ± 0.76	0.22	3.18
Ba (µg/g)	726 ± 38	690 ± 150	0.43	3.18
Pb (µg/g)	1162 ± 31	1170 ± 130	0.19	3.18
Hg (µg/g)	6.25 ± 0.19	6.1 ± 1.5	0.20	3.18
S (%)	0.042 ± 0.001	0.041 ± 0.004	0.03	3.18

They are in good agreement with the certified values, i.e. there was no significant statistical difference at the 95% confidence level according to a Student's t test. This clearly demonstrates the accuracy of the proposed method. The precision (expressed as relative standard deviation) was lower than 20 % for most of the elements, which is poorer than by nebulization and can be explained by the heterogeneous nature of soil samples and the small aliquot size (4 mg). Nonetheless, this is a satisfactory compromise in exchange for such a fast analysis speed (i.e. 85 s per sample) by this direct solid analysis technique.[124]

4.3.2. Quantification of elements in depth profile soil samples from across the Talbot line

Although numerous elements (Ag, Al, Ar, As, Au, B, Ba, Be, Bi, Br, C, Ca, Cd, Ce, Cl, Co, Cr, Cs, Cu, Dy, Er, Eu, Fe, Ga, Gd, Ge, Hf, Hg, Ho, I, In, Ir, K, La, Li, Lu, Mg, Mn, Mo, N, Na, Nb, Ni, O, Os, P, Pb, Pr, Pt, Rb, Re, Rh, S, Sb, Sc, Se, Si, Sm, Sn, Sr, Ta, Th, Ti, Tl, Tm, U, V, W, Y, Yb, Zn and Zr) were monitored, only the results for important pathfinder elements,[106] such as Zn, Cu, Pb, Al, Ba, Hg, S, P, Cl, Br and I, will be discussed.

For quantification and evaluation the vertical distribution of elements in soil samples in the Talbot profile, four replicates of 68 Talbot soil samples were analyzed with the optimized conditions summarized in Table 3.2. An AA-ED S5 soil IRM was used as a solid standard for quantification of soil samples with internal standardisation using an Ar emission line. For making the calibration curves, the mass of the S5 soil standard was varied between 0 to 5 mg and the absolute analyte content was calculated by multiplying the weight of the sample by the certified analyte concentrations. Using the optimized conditions, good correlation was obtained between peak area and the absolute concentration of analyte. Typical calibration curves using S5 as solid standard for Ag, Al, Ba, Cu, Hg, P, Pb and Zn are shown in Figure 4.1.

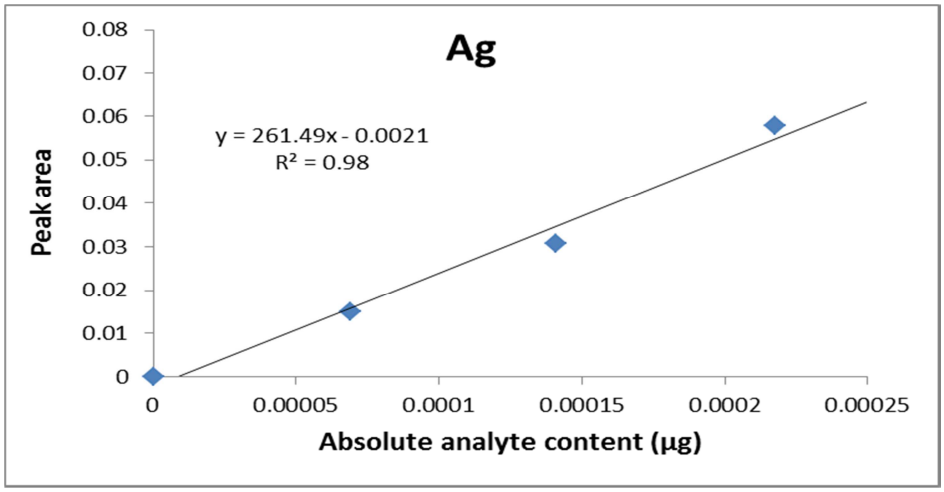
Ag
y = 261.49x - 0.0021
R² = 0.98
Peak area
0.08
0.07
0.06
0.05
0.04
0.03
0.02
0.01
0
0
0.00005
0.0001
0.00015
0.0002
0.00025
Absolute analyte content (µg)

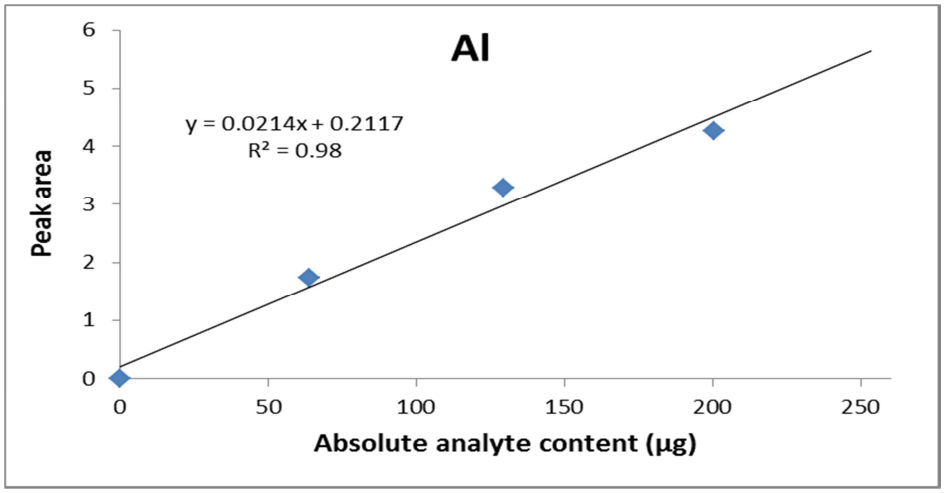
Al
y = 0.0214x + 0.2117
R² = 0.98
Peak area
6
5
4
3
2
1
0
0
50
100
150
200
250
Absolute analyte content (µg)

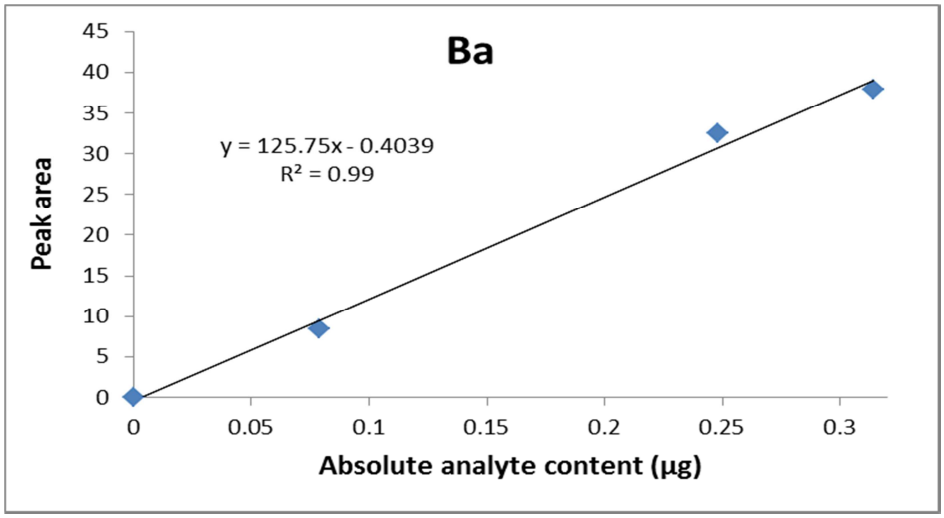
Ba
y = 125.75x - 0.4039
R² = 0.99
Peak area
45
40
35
30
25
20
15
10
5
0
0
0.05
0.1
0.15
0.2
0.25
0.3
Absolute analyte content (µg)

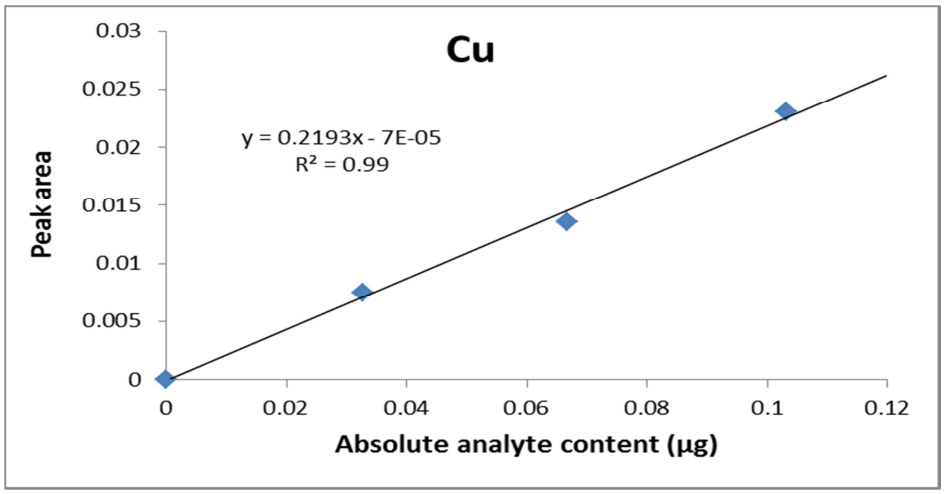
Cu
y = 0.2193x - 7E-05
R² = 0.99
Peak area
0.03
0.025
0.02
0.015
0.01
0.005
0
0
0.02
0.04
0.06
0.08
0.1
0.12
Absolute analyte content (µg)

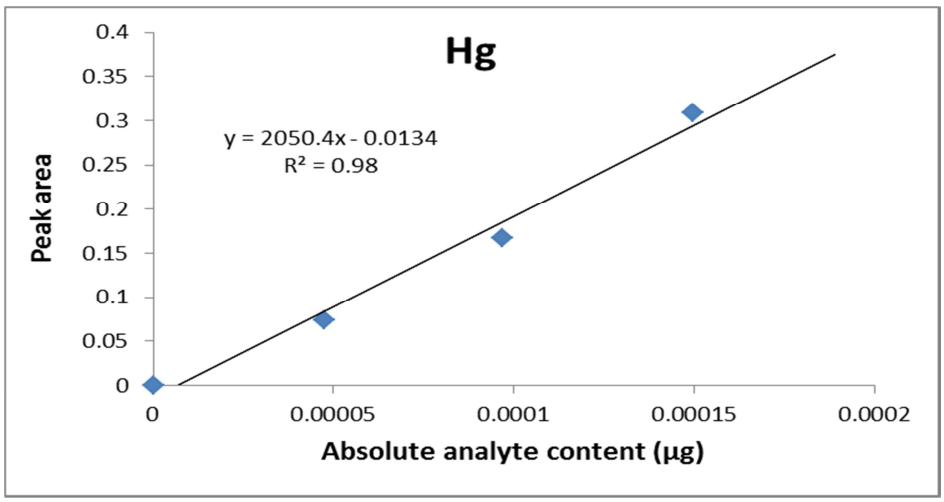
Hg
y = 2050.4x - 0.0134
R² = 0.98
Peak area
0.4
0.35
0.3
0.25
0.2
0.15
0.1
0.05
0
0
0.00005
0.0001
0.00015
0.0002
Absolute analyte content (µg)

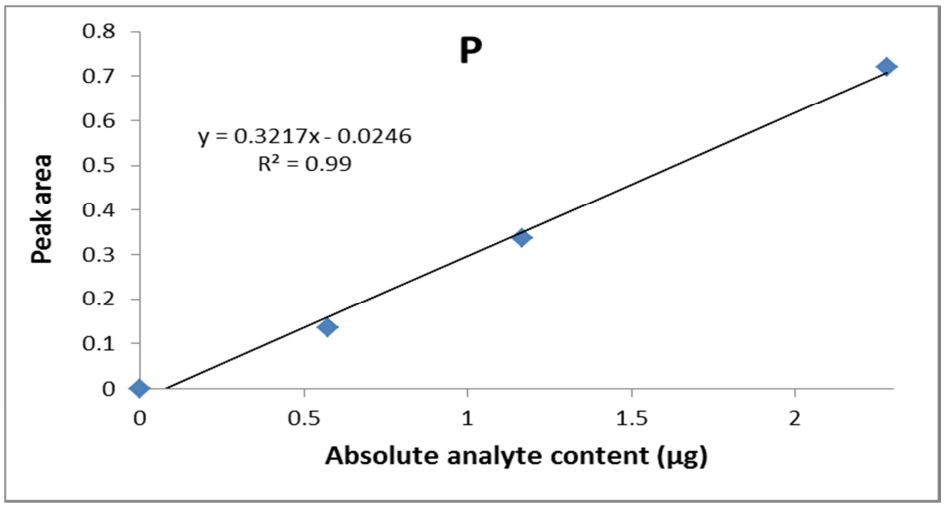
P
y = 0.3217x - 0.0246
R² = 0.99
Peak area
0.8
0.7
0.6
0.5
0.4
0.3
0.2
0.1
0
0
0.5
1
1.5
2
Absolute analyte content (µg)

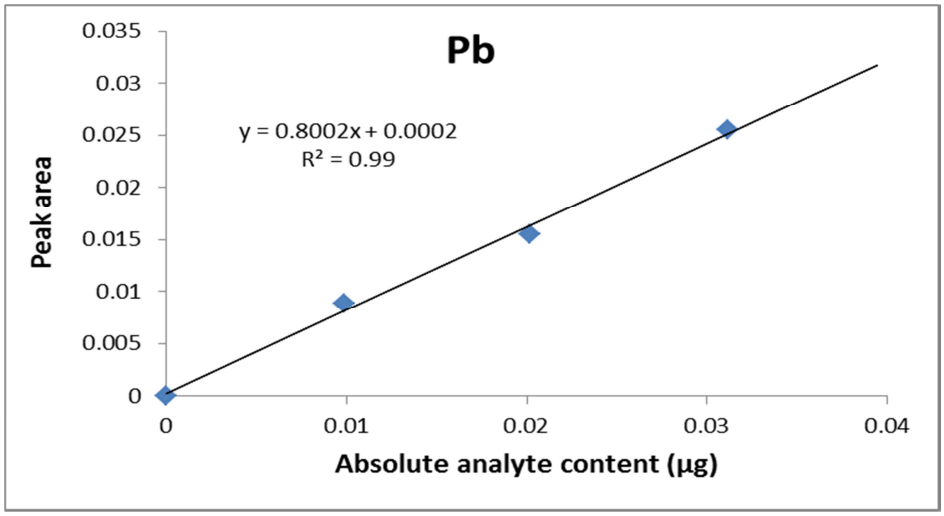

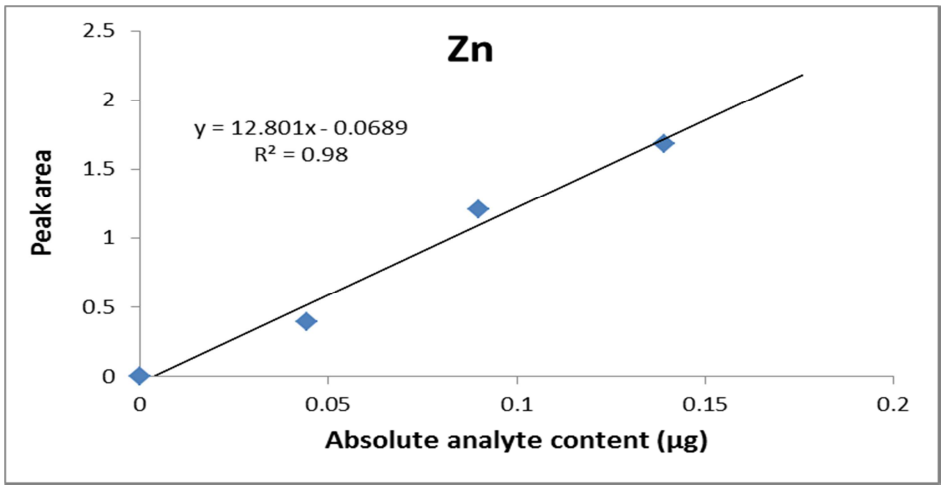

Figure 4.1. Typical calibration curves for Ag, Al, Ba, Cu, Hg, P, Pb, Zn using 1-5 mg of solid standard Anglo S5.

After quantification, the SS-ETV-ICP-OES concentration results were plotted versus depth for anomalous and background soils on the same graph to see migration pattern of the elements from the undercover ore deposit. Figure 4.2 shows Zn and S concentrations in the soil fraction of two 50-cm depth profiles in the Talbot line at 1000 and 650 m along the Talbot line. The depth distribution profile of S and Zn in background (1000 m) and anomalous samples (650 m) are completely different.

Background concentrations of Zn and S are in the same range in 1000 m, around 45 ppm and 0.015 % for Zn and S respectively and are somewhat elevated toward the depth at 1000 m. At 650 m, Zn and S concentrations are anomalously high, toward the surface of the profile. Indeed, upward migration for these elements was observed in anomalous area (650 m), while in the background area, no migration was possible. In addition, these results show that these elements exhibit the same pattern for the migration.

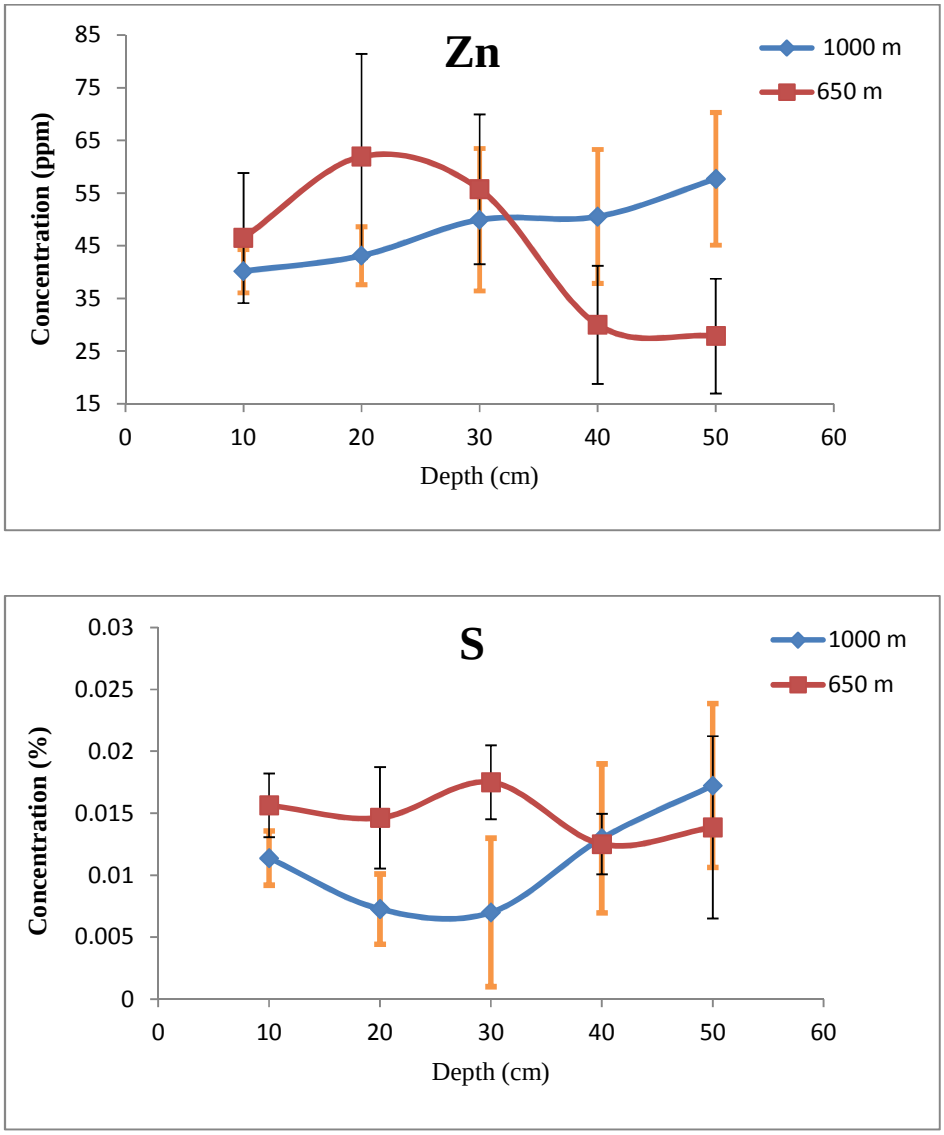

Figure 4.2. Zn and S concentrations (mean ± standard deviation, *n*=4) in the soil fraction of two 50 cm depth profiles in the Talbot line at 1000 and 650 m. At 650 m, Zn and S concentrations are anomalously high, toward the surface of the profile.

The error bars are shown in the figure for comparing the concentrations in the background and anomalous area. These trends were similar to those reported by Pim Van Geffen at Queen's university.[106]

The obtained results for target elements were also plotted versus depth on the same contour plot to see the distribution pattern of the elements above the undercover ore deposit. Figure 4.3 compares the results by SS-ETV-ICP-OES to those obtained by AR-ICP-MS for the soils at 50 cm depth.

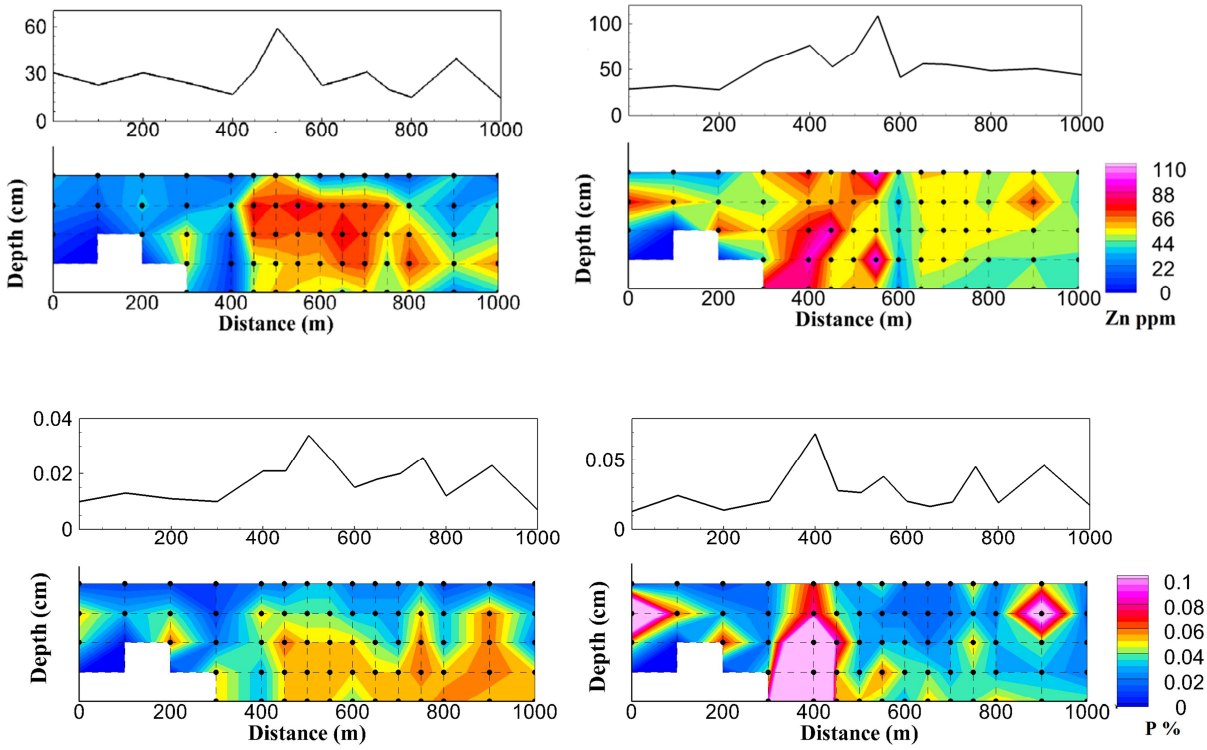

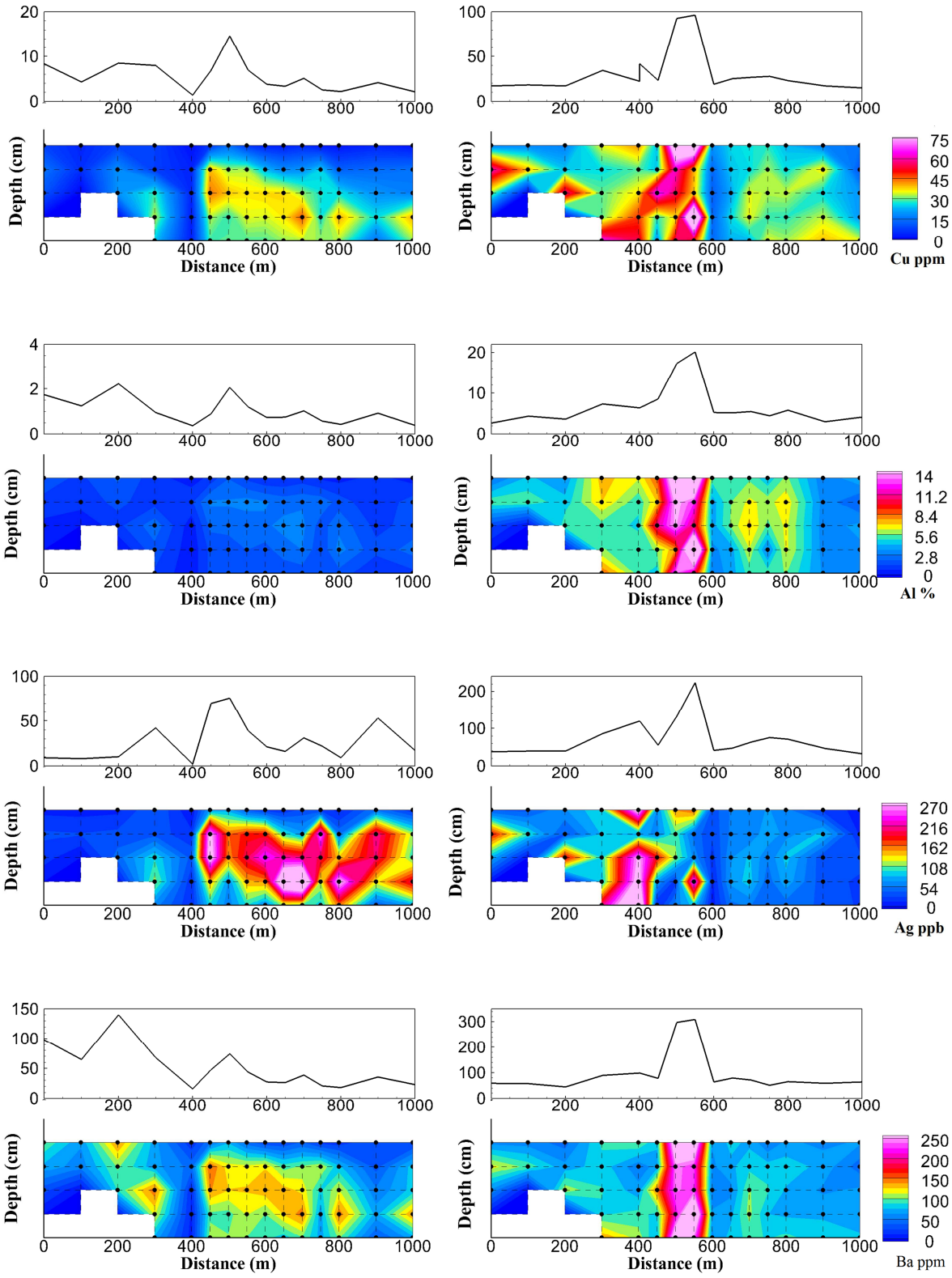
Depth (cm)
Distance (m)
Cu ppm
Al %
Ag ppb
Ba ppm

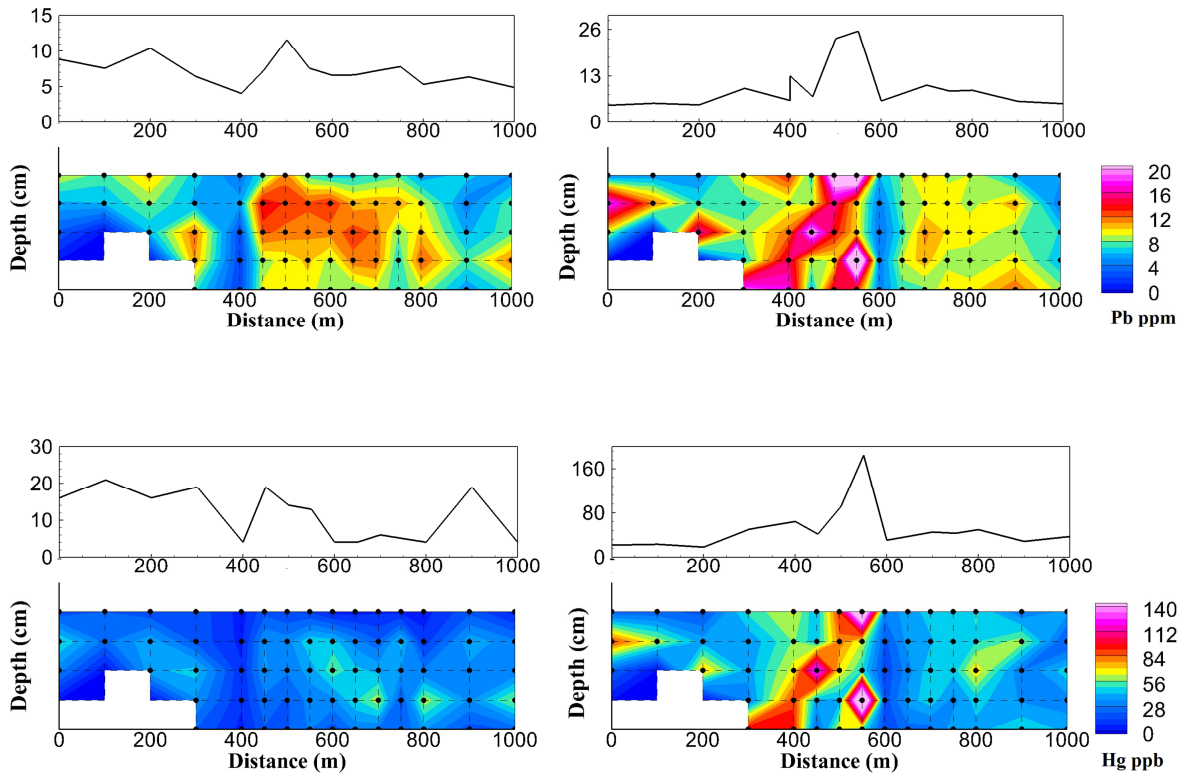

Figure 4.3. Concentrations of P, Zn, Cu, Al, Ag, Ba, Pb, Hg and Sr in the soil fraction at 50-cm depth across the transect line measured by AR-ICP-MS (left) and by SS-ETV-ICP-OES (right), with the distribution in the surface soil samples (0-10 cm) plotted on top of the contour plots.

The SS-ETV-ICP-OES results clearly reveal upward migration of these elements in the anomalous area (400-700 m), and no migration in the surrounding background area. While there is similarity between the elements distributions for 0-10 cm depth across the Talbot line by SS-ETV-ICP-OES and AR-ICP-MS, in general the concentrations determined by SS-ETV-ICP-OES are higher than by AR-ICP-MS, which indicates that the aqua regia extraction did not completely extract these elements. Furthermore, the anomalous area is clearly narrower from SS-ETV-ICP-OES results (400-700 m) than

from AR-ICP-MS results (400-900 m). This thus makes SS-ETV-ICP-OES a more useful tool for geochemical exploration.

Given that the sampling site is near a Paleoproterozoic volcanogenic massive sulphide ore and that S is useful for determining the effect and depth of weathering in sulfide deposits,[116] the S distribution pattern was examined by SS-ETV-ICP-OES and is shown in Figure 4.4, which reveals a clear anomaly at 400 m. The direct determination of S in these soil samples was readily carried out by SS-ETV-ICP-OES, whereas the S concentration in the aqua-regia extracts was too low for quantification by ICP-MS, likely because of important spectroscopic interference from $^{16}O_2^+$ on $^{32}S^+$ (the most abundant S isotope). So, despite the fact that ICP-MS offers detection limits that are orders of magnitude lower than ICP-OES, by eliminating the digestion and associated dilution steps and using a higher efficiency sample introduction system that can in addition separate the analyte from the matrix, detection by ICP-OES was not only possible but became advantageous.

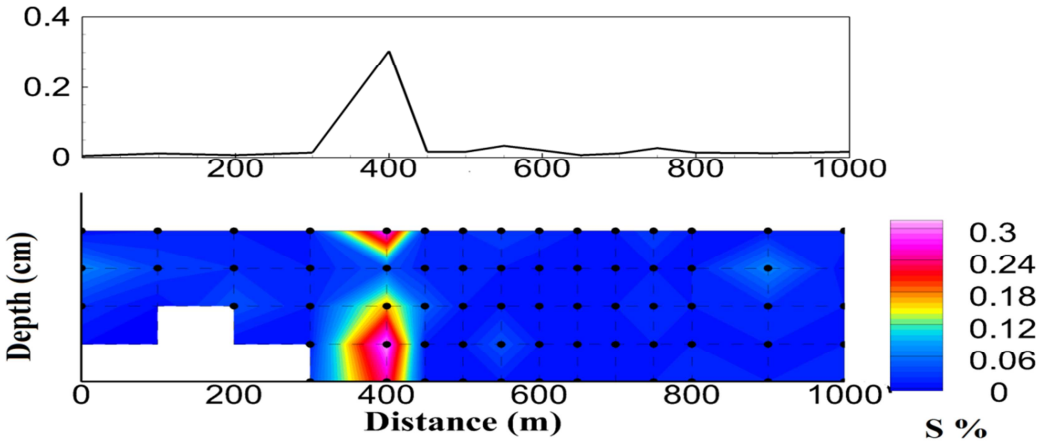

Figure 4.4. Distribution of S in depth profile soil samples along Talbot line using SS-ETV-ICP-OES. The expected anomalous area is clear at 400 m.

4.3.3. Distribution of halogens in depth profile soil samples from across the Talbot line

The distribution of halogens was also examined as these are the most important volatile elements that are not reported by the AR-ICP-MS method. As there were no certified values for halogens in the soil IRM, qualitative analysis based on peak area was used. Figure 4.5 clearly shows a high-contrast anomaly from 600 to 700 m for Cl, 400-700 m for Br and 400-600 m for I. The top 0-10 cm sample data for the halogens is also plotted as a line profile above the contour plots. This shows that a very fast qualitative analysis by SS-ETV-ICP-OES would be sufficient for geochemical exploration.

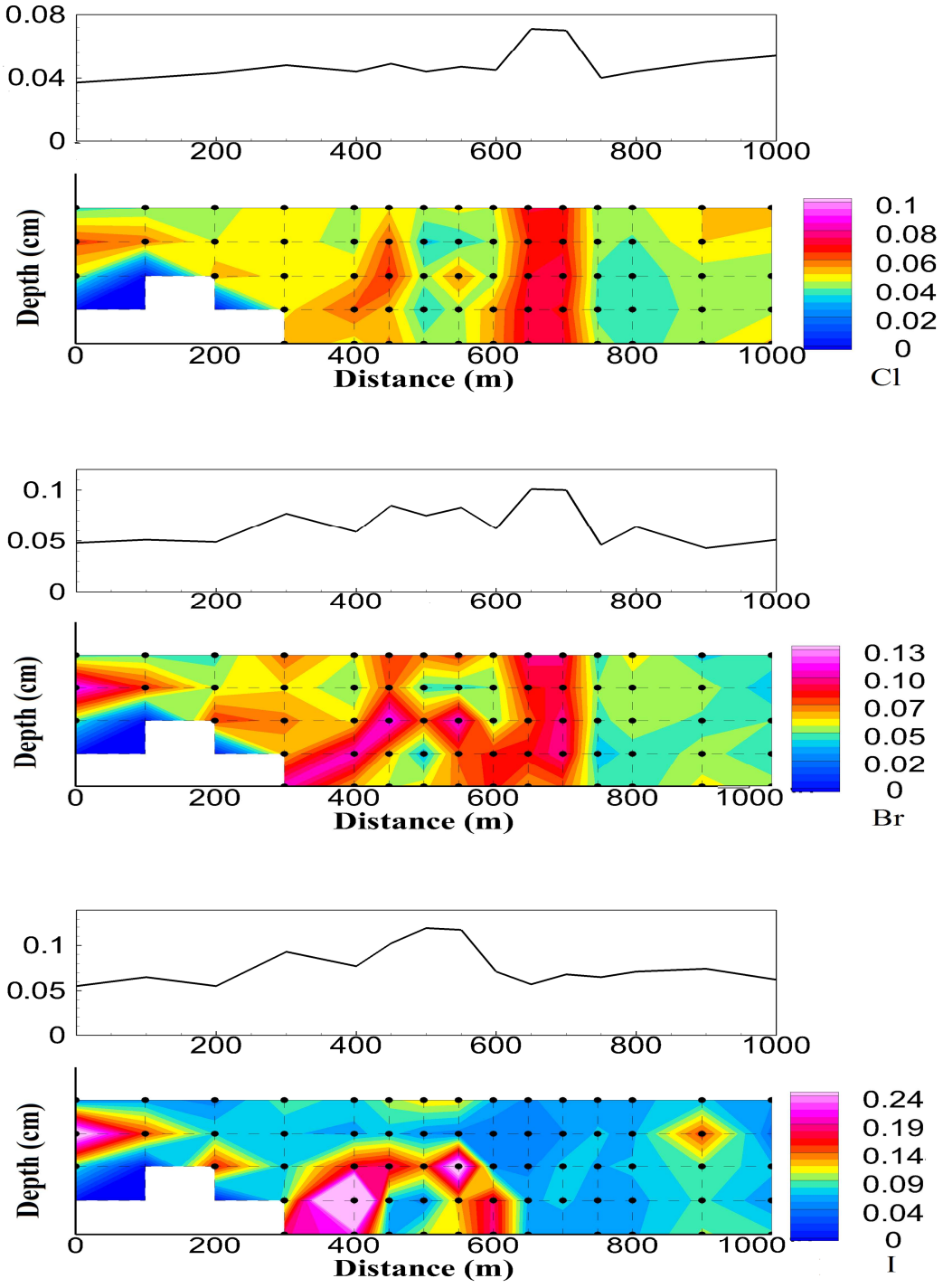

Figure 4.5. Distribution of Cl, Br and I in depth profile soil samples along Talbot line obtained using SS-ETV-ICP-OES.

4.3.4. Geochemistry and principal component analysis of the soil fraction

Principal component analysis (PCA) is a multivariate statistical method that was used to reduce data dimentionality or the number of variables by determining vectors (eigenvectors) that explain the maximum variance in all variables.[130] Principal component loadings represent the correlation of each element with three calculated factors called PC1, PC2 and PC3. The first factor, PC1, accounts for the maximum variance in multivariate (multi-element) space while PC2 describes the maximum variance uncorrelated (orthogonal) to PC1. The last factor, PC3, describes smaller vectors of maximum variance, orthogonal to both PC1 and PC2. The proportion of the total number of variables described by each factor is called eigenvalue. Thus, the Talbot soil geochemistry can be simplified from all major elements to a combination of three principal components (PC2 versus PC1 and PC3 versus PC1) to see which elements are behaving similarly in the whole profile.

PCA of the major elements in the soil indicates an Al-rich component for PC1, which correlates strongly with Ba, Cu, Pb and Zn (Table 4.3). This obviously implies that an Al-rich phase is dominant in the soil geochemistry. This is illustrated in Figure 4.6, which shows strong correlations between Al, Ba, Cu, Pb, Zn and moderate correlations between Hg, Ca and Ag as all the contour maps look very similar. Also shown in Figure 4.6 is strong correlation between Br and Cl, and moderate to weak correlations of I with Br and Cl. Pearson correlation coefficients between major elements were also determined (Table 4.4) and strongly confirm those obtained by PCA.

Table 4.3. Principal component loading of the major elements in the soil fraction from the Talbot exploration grid (*n*=68).

Element	PC1	PC2	PC3
Al	0.931	0.118	-0.055
Ba	0.916	0.074	0.018
Cu	0.832	0.056	0.488
Pb	0.794	0.133	0.534
Zn	0.755	-0.073	0.499
Ag	0.543	0.162	-0.639
Br	0.298	0.916	0.158
S	0.237	0.029	0.893
I	0.209	0.448	0.649
P	0.041	0.161	0.884
Cl	-0.131	0.904	0.035
Hg	0.806	0.06	0.532

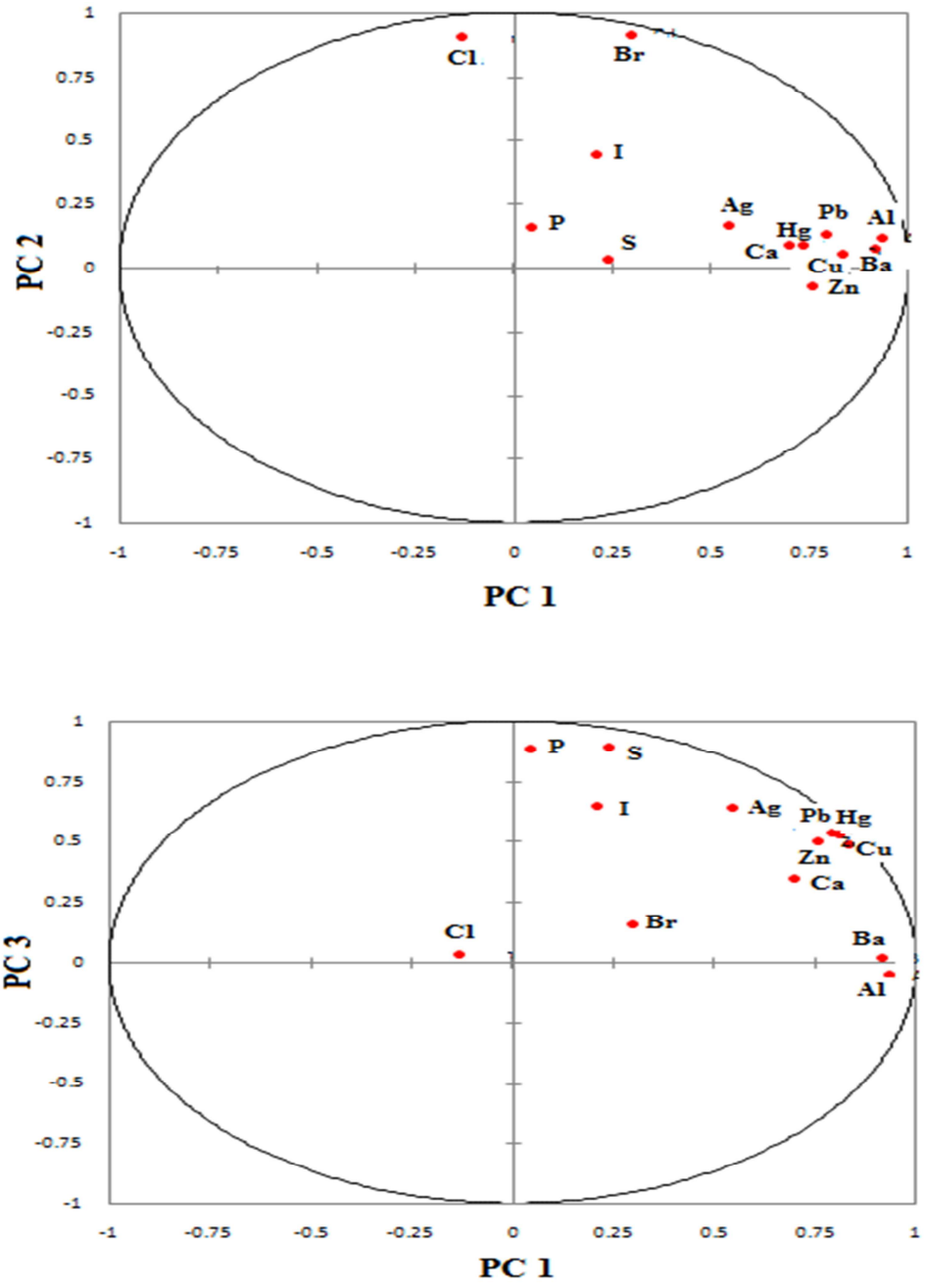

Figure 4.6. Correlations of major elements with principal components of the Talbot soil geochemistry: (a) PC2 vs PC1; (b) PC3 vs PC1.

Table 4.4. Pearson correlation coefficients between elements.

	Zn	P	Cu	Al	Ag	Ba	Pb	Hg	S	Cl	Br	I
Zn		0.42	0.84	0.70	0.76	0.61	0.86	0.90	0.62			
P	0.42		0.49	0.05	0.54	0.18	0.53	0.48	0.79			
Cu	0.84	0.49		0.72	0.77	0.81	0.98	0.91	0.60			
Al	0.70	0.05	0.72		0.52	0.86	0.69	0.73	0.24			
Ag	0.76	0.54	0.77	0.52		0.44	0.79	0.77	0.73			
Ba	0.61	0.18	0.81	0.86	0.44		0.75	0.70	0.24			
Pb	0.86	0.53	0.98	0.69	0.79	0.75		0.93	0.64			
Hg	0.90	0.48	0.91	0.73	0.77	0.70	0.93		0.68			
S	0.62	0.79	0.60	0.24	0.73	0.24	0.64	0.68				
Cl											0.77	0.24
Br										0.77		0.59
I										0.24	0.59	

Colour Coding: Very strong Δ ; Strong Δ ; Moderate Δ ; Weak Δ ; Very weak Δ

4.4. Discussion

The results of this investigation clearly show that SS-ETV-ICP-OES with a four-step temperature program is a powerful tool for mineral exploration. Not only is it able to produce similar results to ICP-MS following aqua regia extraction, but it offers some advantages versus AR-ICP-MS, as the ETV temperature program only requires 85 s per sample with no sample pretreatment. This approach is very attractive because the analytical procedure is simple, while the risk of contamination and/or analyte loss is drastically reduced compared to digestion methods. Furthermore, while internal

standards with similar excitation conditions as the analytes are usually added to standards and samples to compensate variations in sample load on the plasma, no such addition was necessary, as internal standardization using an Ar emission line was sufficient. This is another advantage of SS-ETV-ICP-OES compared to ICP-MS where the addition of at least one internal standard to all samples and standard solutions is usually necessary, which can be another source of contamination.

The depth profiles obtained by SS-ETV-ICP-OES are in general more clearly defined than those obtained by AR-ICP-MS, probably because incomplete dissolution was achieved in the latter case. The SS-ETV-ICP-OES depth profiles show that Zn, P and Ag are more concentrated at 20-50 cm depth at 400 m, whereas Cu, Al, Ba, Pb and Hg are concentrated on the surface and at 40-cm depth mostly between 500 and 600 m. Moreover, Cl, Br and I show two distributions: one at depth at 400 m and one over all depths at 600 m and over faults, suggesting that elements were deposited in the till after upward migration through structures. As the geochemical anomaly is known to lie from 400 to 600 m, all these elements could be used to locate the ore. The halogens could thus first be used to locate the general area, and confirmation of the type of ore could be obtained by looking at correlations between Pb, Cu, Zn and Hg, as the strongest correlations were observed between these four elements. The greatest anomalies occur at or below 30 cm

depth and over

Hence, quick qualitative multielement analysis by SS-ETV-ICP-OES would be sufficient to quickly determine where a massive sulfide ore deposit likely lies. This should make this technique an invaluable tool for geochemical exploration, as it permits

determination of different elements in solid soil samples without the need for labor-intensive digestion, as required for conventional analysis by ICP-based techniques.

4.5. Conclusions

The proposed SS-ETV-ICP-OES technique is a simple and fast method to directly analyse geological samples without any sample preparation. The method was validated through the accurate analysis of soil CRM. It enabled the quick analysis of all the 0 to 50 cm depth profile soil samples along the Talbot line, using external calibration with a soil standard and an Ar emission line as internal standard. In addition, the distribution of halogens was determined by qualitative analysis based on peak area and showed clear increased concentrations outlining the geochemical anomaly. Moreover, the concentrations measured by the proposed method were slightly higher than those obtained by AR-ICP-MS, showing that AR extraction did not recover all the analytes, a problem that is completely avoided by direct solid analysis. Thus, despite the fact that an ETV system is significantly more expensive than conventional nebulization techniques, it offers unique capabilities that are well worth the investment, including for geochemical exploration.

Chapter 5 - Improvement of the capabilities of SS-ETV-ICP-OES by coupling ETV to a nebulisation/pre-evaporation system[3]

5.1. Introduction

Fast and sensitive multi-elemental analysis techniques that provide accurate and precise results at low detection levels are required for the analysis of different types of samples (such as environmental, geological and biological). Inductively coupled plasma optical emission spectrometry (ICP-OES) and ICP mass spectrometry (MS) are most frequently used for simultaneous multi-elemental analysis.[44,131-133]

The latter is generally preferred for analysis at ultra-trace levels, as it is more sensitive than ICP-OES. However, ICP-MS is subject to non-spectroscopic interferences (also called matrix effects) and spectroscopic interferences;[12] whereas matrix effects are typically smaller in ICP–OES, but spectroscopic interferences due to spectrum richness, line broadening or insufficient resolving power of the spectrometer can hamper the analysis of some matrices.[134]

In both cases, a pneumatic nebulizer and spray chamber is conventionally used for sample introduction into the plasma, which requires that samples be in solution and only allows 2–5% of the sample to reach the plasma, the rest going down the drain, at a typical sample uptake rate of 1 mL/min.[135] This also means that solid samples require a dissolution step prior to analysis, which is time-consuming and may lead to analyte loss or sample contamination. Furthermore, the simultaneous introduction of analyte

[3] A version of this chapter has been published as: **Kaveh, F** and Beauchemin, D. Improvement of the capabilities of solid sampling ETV-ICP-OES by coupling ETV to a nebulisation/pre-evaporation system, *Journal of Analytical Atomic Spectrometery*, **2014**, 29, 1371-1377.

elements, matrix components and solvents into the ICP can lead to both spectroscopic and non-spectroscopic interferences.[32]

One way to both increase the sample introduction efficiency and overcome the aforementioned problems is ETV, which has been studied over the last 40 years in combination with ICP-OES and ICP-MS.[34,37,39,40,136,137] It typically involves deposition of sample on a graphite surface, which is heated in steps so as to desolvate the sample, pyrolyze the matrix and vaporize the analytes, which are then transported directly into the ICP by an argon flow via a transfer tube. This sample introduction system is very versatile, as it allows the direct analysis of liquid and slurry samples, as well as solid samples, thereby eliminating sample digestion. Furthermore, because matrix pyrolysis and analyte vaporization are separated temporally, interferences from the matrix can be reduced or eliminated, a process that can be further enhanced with judicious usage of chemical modifiers and temperature programs.[89,90,93,126]

One disadvantage of SS-ETV where all of the effluent is directed towards the ICP is that a maximum of about 5 mg of solid sample can be introduced without extinguishing the plasma, which in turn may limit sensitivity, precision and detection limit, as the latter depends on the reproducibility of the blank and on sensitivity.[138] Plasma extinction mainly arises from overloading by sample matrix during the pyrolysis step, a problem that does not occur with ETV systems allowing evacuation of the effluent during the desolvation and pyrolysis stages. However, the latter are not available with a commercially-available autosampler for the introduction of solids. The insertion of a valve at the outlet of the ETV system would enable venting of the matrix and prevent it from overloading the plasma.

Simultaneous introduction of water into the ICP via a nebulizer, while analytes are transferred from the ETV system into the ICP, may also facilitate the introduction of a larger amount of solid. Indeed, water acts as a load buffer that minimizes matrix effects and is also the main source of hydrogen in the plasma, which affects the excitation and ionization characteristics of the ICP, as it has a high thermal conductivity.[107,139]

Hence, water may facilitate energy transfer between the bulk of the plasma and the central channel, where the analyte is located. However, the polydispersity of the water aerosol typically introduced into the ICP may be an important source of noise, as bulky droplets that experience desolvation and vaporization cool the plasma in the vicinity of smaller droplets that have already reached the atomization, ionization and/or excitation step, and/or cool the plasma zones containing free atoms and atomic ions, thereby reducing the number of excited atoms or ions in OES or of ions in MS. One remedy is to pre-evaporate aerosol droplets without removing water vapour by applying infrared (IR) energy to the nebulisation system and bottom of the torch, as this resulted in significant improvements in detection limit and sensitivity for multi-elemental analysis by ICP-OES.[79]

5.1.1. Objectives

The objective of this study was to modify a SS-ETV-ICP-OES system by coupling ETV to a nebulisation/pre-evaporation system using a switching tee between the ETV system and a sheathing device connecting the nebulisation/pre-evaporation system to the ICP torch. The analytical performance (i.e., sensitivity, detection limit, accuracy and precision) of this system was then compared to that obtained with a standard SS-ETV-

ICP-OES, where the ETV system is directly connected to the torch, for the analysis of environmental samples.

5.2. Experimental

5.2.1. Instrumentation

All measurements were performed on a lateral view ARCOS ICP–OES instrument (SPECTRO Analytical Instruments, Kleve, Germany). Background-corrected signals at different emission lines were used for analysis. A SS-ETV unit (ETV 4000C, from Spectral Systems, Fürstenfeldbruck, Germany) was used along with an AD30 auto-sampler for introduction of graphite boats containing solid samples into the graphite tube. A reaction gas, CF_2Cl_2, was used to transform the elements into more volatile chlorides and fluorides so as to increase the transport efficiency,[140,141] as done in the two preceding chapters.

A PTFE switching tee (Omnifit, New York, NY) was placed at the outlet of the ETV system to enable venting of matrix products during pyrolysis and introduction of analytes into the ICP during vaporisation. It was connected to the side arm of a sheathing device whose main inlet was attached to the outlet of a Scott double-pass spray chamber. A cross-flow nebulizer continuously nebulised water, which was heated by applying IR energy to the sheathing device and bottom of the torch. The set-up is illustrated in Figure 5.1.

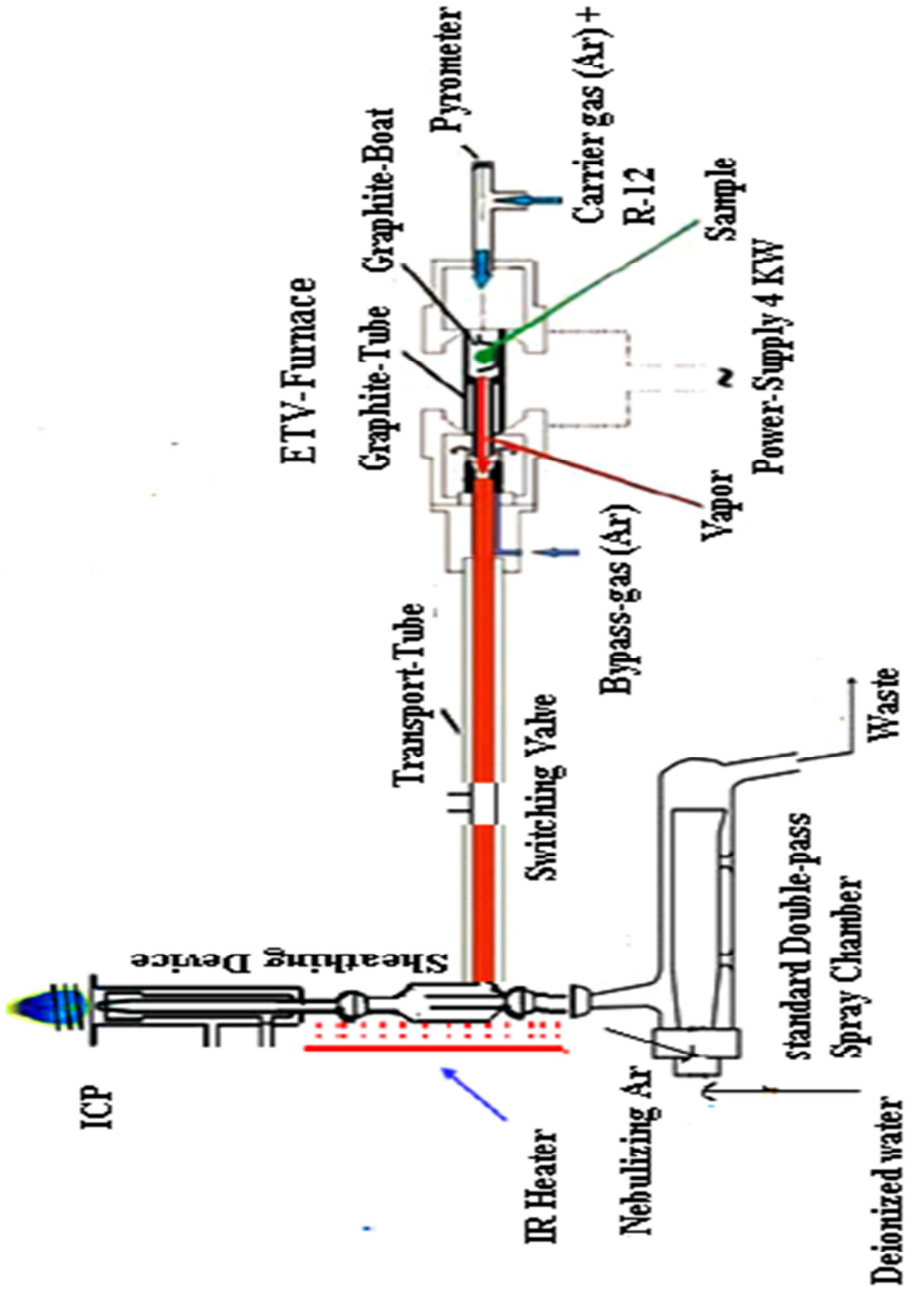

Figure 5.1. Schematic representation of the experimental set-up.

A 6-cm wide, 24.5-cm long ceramic IR 55 heater (Process Heaters Inc., Toronto, Ontario, Canada) was positioned parallel to the bottom of the torch and sheathing device

to pre-evaporate the aerosol exiting the spray chamber. Its temperature was set to 400 ^{0}C and controlled by a PL512 60 Mantle-Minder temperature controller (GLAS-COL apparatus company), which was connected to the thermocouple on the inner surface (i.e. facing the bottom of the torch and sheathing device) of the IR heater.

The Smart Analyzer Vision software was used for time synchronization between the ICP spectrometer and the ETV system. Optimized instrumental conditions for ICP-OES and the ETV heating program are summarized in Table 5.1.

5.2.2. Reagents

Doubly de-ionized water (DDW) (18.2 MΩ cm-1) (Pro UV/DI, Sartorius Stedim Biotech, Gottingen, Germany) was continuously nebulised. A 10 mg L^{-1} multi-element stock solution (Ag, As, B, Ba, Bi, Ca, Cd, Ce, Cr, Cu, Ga, Ge, Hf, Hg, In, Li, Mg, Mn, Mo, Ni, Pb, Pd, Pt, S, Sb, Se, Sr, U, W, Zn and Zr), used for background correction, was prepared through dilution of 1000 and 10000 mg/L mono-elemental plasma standard solutions (SCP Science, Baie d'Urfé, Quebec, Canada) with 2% HNO_3. The latter was prepared by dilution with DDW of reagent grade nitric acid that was purified using a DST-1000 sub-boiling distillation system (Savillex, Minnetonka, USA). A soil IRM, S5, from AA-ED, dried and sieved to <250 μm, was used for external calibration and for comparing sensitivity and detection limit between the standard and modified SS-ETV-ICP-OES. Accuracy and precision was assessed through the determination of trace and major elements in two CRMs, SS-1 and SS-2, from SCP Science (Baie d'Urfé, Quebec, Canada).

Table 5.1. Instrumental operating conditions.

ICP-OES	
Instrument	SPECTRO ARCOS lateral view
Plasma power	1450 W
Ar plasma gas flow rate	14.00 L min^{-1}
Ar auxiliary gas flow rate	2.00 L min^{-1}
Ar nebulizer gas flow rate	0.75 L min^{-1}
Sample uptake rate	1.5 mL min^{-1}
IR heater temperature	400 °C
Signal scan mode	Transient
Run time	0-85 s
Integration time	10 ms

ETV	
Vaporizer	ETV 4000 c
Ar carrier gas flow rate	180 mL min^{-1}
Ar bypass gas flow rate	520 mL min^{-1}
CF_2Cl_2 reactant gas flow rate	4.1 mL min^{-1}

ETV heating program

Step	T (°C)	Ramp (s)	Hold (s)	Step	T (°C)	Ramp (s)	Hold (s)
1	400	0	20	2	21	0	15
3	2200	0	30	4	21	0	20

5.2.3. Data treatment and calibration

To compensate for sample loading effects on the plasma, an Ar emission line (763.511 nm) was used as internal standard, i.e. each analyte signal intensity was normalized to the Ar signal, as was done in the previous two chapters. The corrected transient temporal profile was obtained by computing the point-by-point ratio of analyte signal/Ar signal before the area of the peak (observed at the vaporization temperature) was integrated. Blank correction was performed using empty boats. External calibration with 4-6 increasing amounts of CRM was performed, followed with linear regression analysis to convert peak areas into concentrations. Accuracy was verified using a Student's t-test performed at the 95% confidence level to compare the experimentally determined concentrations to certified or suggested values.

5.3. Results and Discussion

5.3.1. Coupling to nebulisation-pre-evaporation system

Just inserting the switching tee between the ETV furnace and the torch to vent pyrolysis products resulted in plasma extinction upon switching the tee back to allow passage of the ETV effluent towards the torch. While this may be due to the sudden pressure change then experienced by the plasma, no such extinction occurred when this was done with a wet plasma using the set-up shown in Figure 5.1. Moreover, up to 13 mg of soil could be introduced without extinguishing the plasma, which is significantly more than the maximum of 5 mg that could be tolerated with the conventional SS-ETV-ICP-OES system used in the previous two chapters.

5.3.2. Internal standardisation with an argon emission line

Internal standards similar in properties to the analytes are usually added to standards and samples when performing an external calibration to compensate for matrix effects or variations in sample loading in ICP spectrometry.[117] While this is relatively straightforward for solutions, as it can be done by either manually adding the internal standards to each standard and sample solution, or by merging the sample flow with the internal standard solution flow on-line, it is not as readily feasible during the direct analysis of solids. On the other hand, external calibration with matrix-matched solid standards can be performed accurately by SS-ETV-ICP spectrometry using different masses of a single standard if the loading effect caused by the increasing mass can be compensated.[90,118]

This loading effect is evident in Figure 5.2, where an increasing suppression of the Ar emission signal resulted as the amount of soil introduced was increased. Such effect is typically compensated using Ar_2^+ signal as internal standard in ETV-ICP-MS,[122,123] or using an Ar emission line (Ar 763.511 nm) in SS-ETV-ICP-OES.[104,138] The latter was thus systematically done, as it significantly improved the linearity of calibration curves.

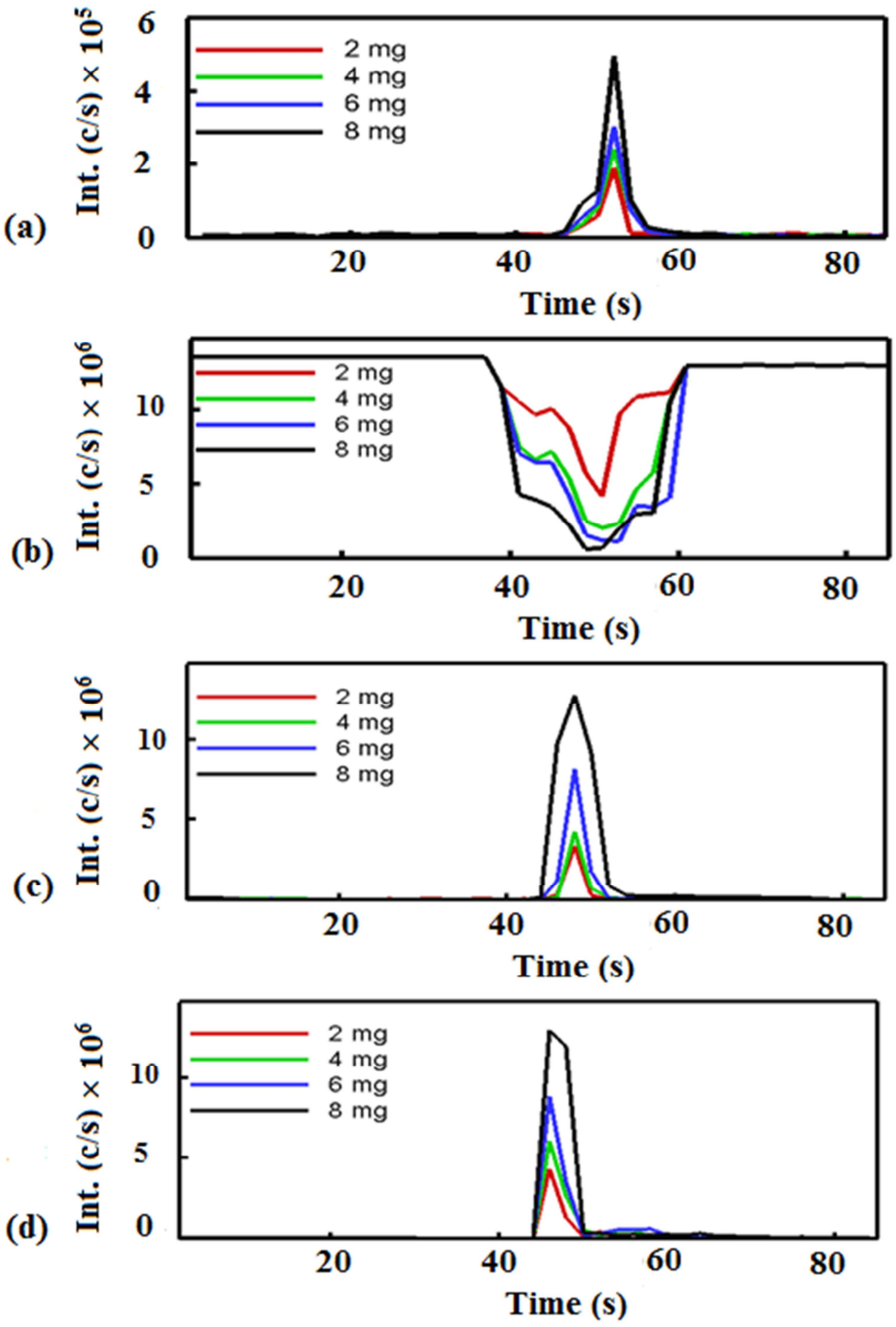

Figure 5.2. Typical In, Ar, Li and Zn transient signals observed upon introduction of 2, 4, 6 and 8 mg of S5 soil IRM in SS-ETV-ICP-OES.

5.3.3. Sensitivity and detection limit

The mass of S5 soil IRM was varied between 0 and 13 mg (at least 5 masses were used for the majority of analytes) to make calibration curves for the determination of sensitivity (i.e. the slope) and detection limit (defined as 3 times the standard deviation of the blank signal divided by sensitivity). Using the optimized conditions, good correlation was obtained between peak area and the absolute concentration of analytes. An example of typical calibration curve is shown in Figure 5.3 for Mn in S5 soil IRM.

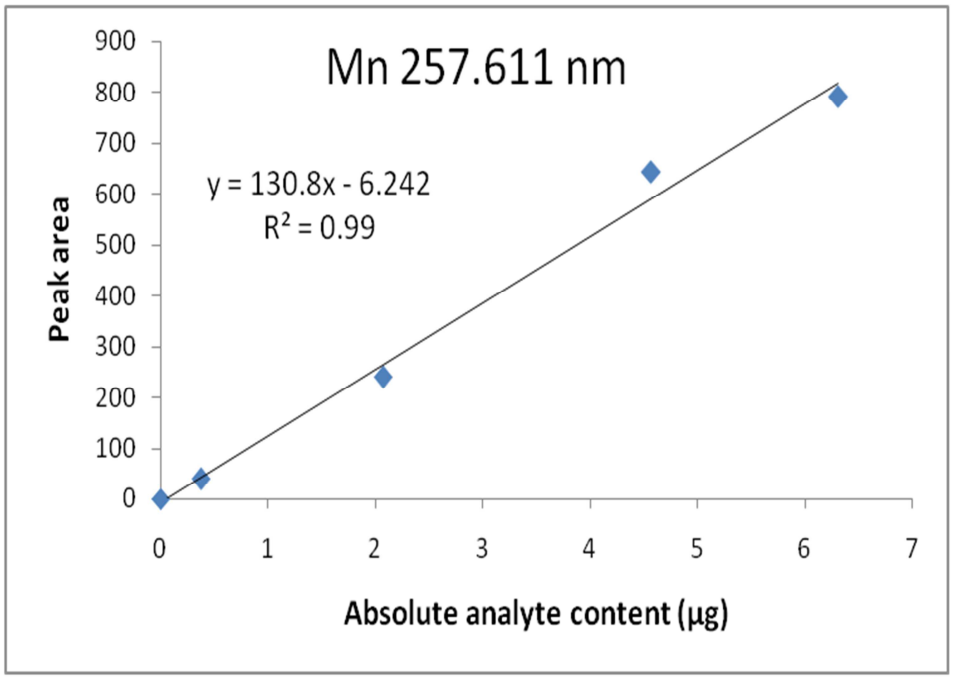

Figure 5.3. Typical calibration curve for Mn using 1-13 mg of S5 soil IRM.

Sensitivities of the modified with IR heating, modified without IR heating and conventional SS-ETV-ICP-OES systems are compared in Table 5.2, which shows that similar or improved sensitivity was obtained for all elements, with significant improvement resulting for most of the elements. The average sensitivity improvement for target analytes with the modified system with IR heating compared to the conventional one was 2.9 ± 1.2. Comparison of columns A and B also reveals that application of IR heating significantly improved sensitivity (up to 4 fold) for several elements, the average improvement being 1.4 ± 0.6 versus the same system without IR heating.

The detection limit was also calculated as the concentration of analyte yielding a signal equivalent to three times the standard deviation of the blank value (n=10) obtained using empty boats. Table 5.3 shows that the detection limits calculated based on 8-mg samples with the modified system with IR heating are better than those obtained for conventional SS-ETV-ICP-OES with 4-mg samples, the average improvement being 5.4 ± 2.7. The additional improvement beyond the 2-fold expected by simply doubling the sample size is likely a result of the very stable and robust plasma resulting from the simultaneous introduction of a pre-evaporated water aerosol.[79] This is supported by the fact that significant improvement in detection limit (up to 5 fold) was observed for several elements upon the simple application of IR heating, with an average improvement of 1.6 ± 1.0 compared to the same system without IR heating.

Table 5.2. Sensitivity (cps/µg) with three different SS-ETV-ICP-OES systems.

Analyte	λ (nm)	Modified with IR (A)	Modified without IR (B)	Conventional (C)	A/B	B/C	A/C
Ag II	224.641	2430 ± 180	801 ± 176	494 ± 27	3.0	1.6	4.9
Ag I	338.289	1635 ± 45	1947 ± 143	794 ± 35	0.8	2.5	2.0
As I	189.042	209 ± 9	161 ± 15	63 ± 6	1.3	2.6	3.3
B I	208.959	684 ± 46	396 ± 31	193 ± 19	1.7	2.1	3.5
Ba II	455.404	819 ± 66	373 ± 28	268 ± 50	2.2	1.4	3.0
Bi I	223.061	907 ± 47	819 ± 53	213 ± 12	1.1	3.8	4.2
Ca II	396.847	23 ± 3	31.0 ± 1.3	11 ± 1	0.7	2.8	2.1
Cd II	214.438	5480 ± 140	8431 ± 350	2750 ± 170	0.6	3.1	2.0
Ce II	418.660	17.0 ± 0.7	7.0 ± 1.0	7.0 ± 0.4	2.4	1.0	2.2
Cr II	205.618	39 ± 3	32 ± 3	22.0 ± 1.5	1.2	1.5	1.7
Cu II	154.796	0.80 ± 0.01	0.80 ± 0.03	0.30 ± 0.01	1.0	2.7	2.8
Cu I	165.532	0.80 ± 0.02	0.80 ± 0.05	0.40 ± 0.02	1.0	2.0	2.4
Ga II	141.444	0.80 ± 0.02	0.60 ± 0.03	0.30 ± 0.04	1.3	2.0	2.5
Ge II	164.919	188 ± 14	178 ± 7	97 ± 10	1.1	1.8	1.9
Hf II	232.247	129 ± 3	123 ± 13	52 ± 5	1.0	2.4	2.4
Hg I	184.950	7190 ± 210	6092 ± 521	4040 ± 470	1.2	1.5	1.7
Hg II	194.227	9930 ± 750	6935 ± 943	2200 ± 1800	1.4	3.2	4.5
In II	230.606	3810 ± 230	3223 ± 441	878 ± 80	1.2	3.7	4.3
In I	325.609	8790 ± 760	4252 ± 402	4230 ± 580	2.1	1.0	2.0
Li I	670.780	4170 ± 720	1960 ± 238	810 ± 130	2.1	2.4	5.1
Mg II	279.079	2.0 ± 0.2	1.6 ± 0.2	1.6 ± 0.4	1.3	1.0	1.2
Mn II	257.611	130 ± 8	78 ± 3	55 ± 2	1.7	1.4	2.3
Mo II	202.095	787 ± 50	509 ± 44	202 ± 22	1.5	2.5	3.9
Ni II	174.828	13 ± 0.9	10 ± 0.7	4.0 ± 0.4	1.3	2.5	3.4
Ni I	341.476	57 ± 4	50 ± 6	51 ± 6	1.1	1.0	1.1
Pb II	220.353	36 ± 2	36 ± 3	11 ± 1	1.0	3.4	3.1
Pd I	324.270	24200 ± 1200	16370 ± 1881	13190 ± 890	1.5	1.2	1.8
Pt II	177.708	61300 ± 5400	41218 ± 3154	14500 ± 2100	1.5	2.8	4.2
Pt I	214.423	296000 ± 16000	549995 ± 45685	127900 ± 8600	0.5	4.3	2.3
S I	182.034	2.8 ± 0.1	1.4 ± 0.1	1.2 ± 0.1	2.0	1.2	2.2
Sb I	217.581	5180 ± 240	4706 ± 313	1650 ± 140	1.1	2.9	3.1
Se I	196.090	571 ± 29	438 ± 20	147 ± 11	1.3	3.0	3.8
Sr I	394.080	930 ± 140	607 ± 44	132 ± 21	1.5	4.6	7.0
U II	409.014	466 ± 27	413 ± 25	227 ± 16	1.1	1.8	2.0
W II	207.911	4810 ± 260	4100 ± 111	1920 ± 150	1.2	2.1	2.5
Zn II	202.613	36.0 ± 1.2	34.0 ± 1.8	29 ± 1	1.1	1.2	1.2
Zn I	213.856	130 ± 5	124 ± 6	112 ± 9	1.0	1.1	1.2
Zr II	339.198	45 ± 10	12 ± 0.4	21.0 ± 2.5	3.8	0.6	2.1

Table 5.3. Detection limit (3σ, *n*=10) (µg/g) with three different SS-ETV-ICP-OES systems.

Analyte	λ (nm)	Modified with IR (A)	Modified without IR (B)	Conventional (C)	B/A	C/B	C/A
Ag II	224.641	0.001	0.002	0.007	2	3.5	7
Ag I	338.289	0.003	0.001	0.01	0.3	10	3
As I	189.042	0.02	0.03	0.1	1.5	3.3	5
B I	208.959	0.010	0.013	0.10	1.3	7.6	10
Ba II	455.404	4	6	9	1.5	1.5	2.3
Bi I	223.061	0.002	0.002	0.008	1	4	4
Ca II	396.847	300	631	700	2	1.1	2.5
Cd II	214.438	0.001	0.001	0.005	1	5	5
Ce II	418.660	3	1	20	0.3	20	7
Cr II	205.618	0.2	1	0.5	5	0.5	2.5
Cu II	154.796	2.0	2.2	4.0	1.1	1.8	2
Cu I	165.532	2	1	4	0.5	4	2
Ga II	141.444	1	2	5	2	2.5	5
Ge II	164.919	0.008	0.009	0.01	1.2	1.1	1.2
Hf II	232.247	0.02	0.02	0.1	1	5	5
Hg I	184.950	0.001	0.001	0.003	1	3	3
Hg II	194.227	0.0004	0.0006	0.004	1.5	6.6	10
In II	230.606	0.001	0.001	0.006	1	6	6
In I	325.609	0.0002	0.0005	0.001	2.5	2	5
Li I	670.780	0.01	0.02	0.1	2	5	10
Mg II	279.079	30	41	70	1.4	1.7	2.5
Mn II	257.611	0.5	1.6	2.0	3.2	1.2	4
Mo II	202.095	0.005	0.004	0.04	0.8	10	8
Ni II	174.828	0.1	0.3	0.8	3	2.6	8
Ni I	341.476	1	2	3	2	1.5	3
Pb II	220.353	0.07	0.07	0.7	1	10	10
Pd I	324.270	0.0010	0.0014	0.0040	1.4	2.8	4
Pt II	177.708	0.00003	0.00004	0.0002	1.3	5	6.7
Pt I	214.423	0.00001	0.00001	0.00005	1	5	5
S I	182.034	6	22	39	3.6	1.7	6.5
Sb I	217.581	0.0004	0.0006	0.004	1.5	6.6	10
Se I	196.090	0.005	0.006	0.04	1.2	6.6	8
Sr I	394.080	0.07	0.07	0.6	1	8.5	8.5

To demonstrate the effect of emission line type on sensitivity and detection limit, results for both types of emission lines were included for selected analytes in Tables 5.2 and 5.3. In general, the improvement was indeed higher for ionic than atomic lines, as was previously reported for ICP-OES with a nebulisation system including pre-evaporation.[79] For example, the improvement in sensitivity with the modified SS-ETV-ICP-OES compared to the conventional SS-ETV-ICP-OES when using ionic lines for Ag, Cu, Hg, In, Ni, Pt and Zn was 3.6 ± 1.3 whereas it was 1.85 ± 0.53 for atomic lines. The difference can most likely be attributed to the improved plasma excitation conditions that result from pre-evaporation of the water aerosol, [79] which increase the population of higher energy states (such as ionic lines). This is supported by the greater improvement in sensitivity upon application of IR heating for ionic lines, with an average of 1.5 ± 0.7 with/without heating, than for atomic lines, where the average with/without IR heating was 1.1 ± 0.5.

5.3.4. Application to the analysis of soil

Accuracy and precision were evaluated by analyzing a contaminated soil CRM (SS-1), using another contaminated soil CRM (SS-2) as a standard for external calibration (along with internal standardisation using Ar 763.511 nm). The results are summarised in Table 5.4. They show a good agreement between the measured and certified values for both the modified and conventional SS-ETV-OCP-OES techniques, i.e. there was no significant statistical difference at the 95% confidence level according to a Student's t test.

Table 5.4. Concentration of analytes in µg/g (mean ± standard deviation, *n*=4) in SS1 with modified and conventional SS-ETV-ICP-OES using SS2 for external calibration, as well as experimental and table values of Student's t (95% confidence level).

		Modified (8-mg aliquots)		Conventional (4-mg aliquots)	
Analyte	Certified	Measured	t_{exp}*	Measured	t_{exp}*
Ag	0.88 ± 0.03	1.0 ± 0.1	2.4	1.16 ± 0.20	2.6
As	20.7 ± 1.0	18 ± 2	2.1	21.8 ± 3.2	0.7
Ba	464 ± 16	403 ± 56	2.1	410 ± 140	0.7
Ca	50265 ± 1213	54300 ± 7200	1.1	53000 ± 14000	0.4
Cd	3.20 ± 0.25	2.8 ± 0.3	2.6	2.5 ± 0.4	3.15
Ce	40.1	40 ± 3	0.04	38.8 ± 8.2	0.3
Cr	103.0 ± 5.5	124 ± 18	2.3	132 ± 25	2.2
Cu	403 ± 10	432 ± 37	1.5	398 ± 42	0.2
Hg	0.4 ± 0.02	0.40 ± 0.04	1.5	0.38 ± 0.07	0.8
Li	14.3 ± 1.4	14 ± 2	0.3	15.8 ± 4.9	0.6
Mg	9690 ± 230	10480 ± 970	1.6	8500 ± 1700	1.4
Mn	737 ± 19	730 ± 110	0.04	740 ± 150	0.02
Mo	6.8 ± 0.35	8.4 ± 1.3	2.6	8.2 ± 1.5	1.8
Ni	59.2 ± 1.3	67 ± 7	2.1	64.4 ± 9.7	1.0
Pb	764 ± 15	691 ± 69	2.0	650 ± 100	2.1
S	1916 ± 140	1840 ± 240	0.6	1870 ± 420	0.2
Sb	5.5 ± 1.1	4.3 ± 0.8	3.12	4.61 ± 0.74	2.4
Se	0.78 ± 0.14	0.70 ± 0.08	2.0	0.69 ± 0.15	1.2
Sr	114.0 ± 1.5	113 ± 18	0.04	121 ± 37	0.3
U	0.76	0.80 ± 0.15	1.2	1.06 ± 0.29	0.5
Zn	1114 ± 36	1016 ± 92	2.1	1100 ± 170	0.15

* Table value = 3.18

However, the average relative standard deviation was 13 ± 3% with the modified approach versus 21 ± 6% with the conventional one. This significant improvement can largely be explained by the larger aliquot size with the modified approach compared to the conventional one (8 vs 4 mg), which improved the reproducibility of transient signals for samples with such a heterogeneous nature as soil. For example, Figure 5.4 shows typical repeatability of the transient signals for some selected elements such as Pb and Li using 8 mg (left) and 4 mg (right) of SS-1 soil sample, obtained by modified and conventional SS-ETV-ICP-OES approaches respectively.

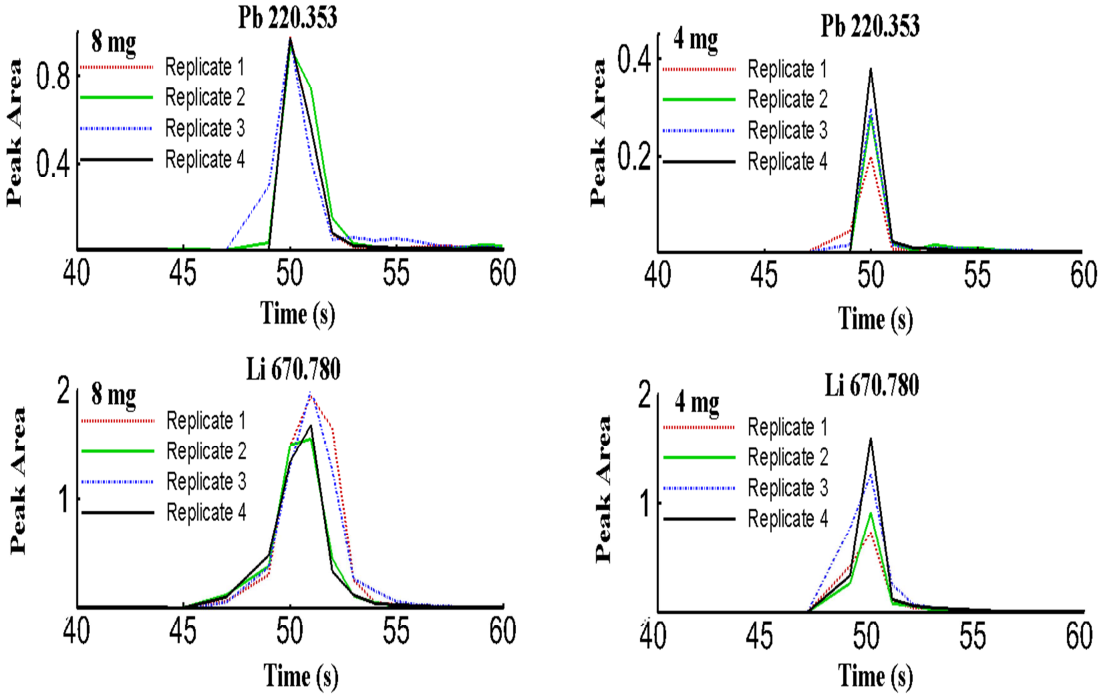

Figure 5.4. Typical transient signals for Pb and Li in 8 and 4 mg of SS-1 soil sample by modified (left) and conventional SS-ETV-ICP-OES (right).

In all cases, the peaks appear at the same time and it is also possible to see the reproducibility of the signals. The % RSD of transient signals for Pb and Li in the modified approach was 8 % and 16 % while it was 18% and 30% in the conventional SS-ETV-ICP-OES approach. This clearly shows that the transient signals are more reproducible in the modified SS-ETV-ICP-OES method as the larger amount of sample (8 mg) was introduced.

Finally, the precision for the same amount of SS1 sample (4 mg) was compared by both conventional and modified methods to see the effect of water vapour on the reproducibility of transient signals, measured as % RSD in Table 5.5. The average % RSD of transient signals for different elements with the modified approach was 15 ± 5% while it was 19 ± 7% in the conventional SS-ETV-ICP-OES approach. The average RSD improvement for target analytes with the modified system with IR heating compared to the conventional one was 1.4 ± 0.7. This clearly shows that water vapour has also a positive effect on the reproducibility of transient signals.

Table 5.5. Repeatability (expressed as % relative standard deviation, *n*=4) for selected elements in 4 mg of SS1 with modified and conventional SS-ETV-ICP-OES.

Analyte	Modified A	Conventional B	B/A
Ag	22	17	0.8
As	12	18	1.5
Ba	9	14	1.6
Ca	13	9	0.7
Cd	16	18	1.1
Ce	24	19	0.8
Cr	6	21	3.5
Cu	10	11	1.1
Hg	9	14	1.6
Li	21	35	1.7
Mg	14	26	1.9
Mn	11	20	1.8
Mo	16	16	1.0
Ni	26	20	0.8
Pb	14	16	1.1
S	13	13	1.0
Sb	17	13	0.8
Se	15	19	1.3
Sr	16	38	2.4
U	13	22	1.7
Zn	11	13	1.2

5.4. Conclusions

Installing a switching valve at the output of a commercially-available SS-ETV system and then connecting it to the side arm of a sheathing device whose main inlet is connected to a nebulizer/spray chamber is an effective way to increase the amount of solid sample that can be analysed by SS-ETV-ICP-OES. The application of uniform and efficient IR heating to the nebulization system and bottom of the torch increased plasma robustness and stability. As a result of these changes, the amount of sample aliquot that could be tolerated without extinguishing the plasma almost tripled compared to what can be introduced with conventional SS-ETV-ICP-OES. Furthermore, it also significantly improved sensitivity and detection limit, while providing similar accuracy as the conventional system, but with significantly improved precision for the analysis of soil. This new SS-ETV-ICP-OES technique enables the fast yet accurate multi-elemental analysis of soil samples by a simple external calibration with a matrix-matched soil CRM, using an Ar emission line as internal standard. Although the precision is not as good as when analysing digests, this is an acceptable compromise in exchange for the fast analysis speed (i.e. 85 s per sample) afforded by such a direct solid analysis technique.[124]

Future work will explore to which extent matrix-matching is required for accurate analysis. While experiments (not shown) have revealed that standard solutions would not be suitable for calibration, as the soil matrix modifies the vaporization characteristics of the analytes, different solid CRMs (other than soils) may be suitable as calibration standards for the analysis of soils.

Chapter 6 - Summary and Future Work

6.1. Summary of chapters

The aim of this research was to develop new methods using ETV sample introduction system in combination with ICP-OES to further expand the range of applications of this technique.

In Chapter 3, we developed a simple and fast method using SS-ETV-ICP-OES to determine the distribution of elements in soil samples from across the Talbot Lake VMS Cu-Zn prospect, in the Flin Flon-Snow Lake terrane, Manitoba, Canada in order to locate the undercover ore deposit, which is buried under Palaeozoic dolomites and Quaternary till. In the development of the method, the mass of sample, the flow rate of reactant gas (R12), the carrier and bypass gas flow rates and the temperature program were optimised. Under optimal conditions and with a four-step ETV temperature program, the distribution of the pathfinder elements (Zn, P, S and I) in soils showed clear anomalies at 400 and 650 m. The results for Zn and P were in very good agreement with results obtained, following AR digestion, by ICP-MS by AA-ED.

Moreover, the distributions of S and I could be precisely determined (these elements were not reported in the AA-ED study). Using 0–4 mg of AA-ED S5 standard mixed with 4.1 ml/min R12 as reactant gas, and using internal standardization with an argon emission line, calibration curves were obtained that, when applied to Talbot soil samples, yielded Zn, S and P concentrations in agreement with AR-ICP-MS results previously obtained by AA-ED. Hence, SS-ETV-ICP-OES completely eliminates the need for extraction or digestion of samples prior to analysis, which significantly simplifies the analysis of geochemical exploration samples.

Chapter 4 described the validation of the previously developed ETV-ICP-OES system through the accurate analysis of a soil CRM using another soil CRM as calibration standard and an Ar emission line as internal standard to compensate for sample loading effects on the plasma. Good agreement was obtained between the measured concentrations and certified values according to a paired Student's t-test. The validated method was then applied to the determination of the distribution of elements in depth profile soil samples from across the Talbot Lake VMS Cu-Zn prospect, in the Flin Flon-Snow Lake terrane, Manitoba, Canada. The concentration of target elements (Zn, P, S Cu, Al, Ag, Ba, Pb and Hg) in those soils was determined using 0-4 mg of soil internal reference material as a calibration standard, with an Ar emission line as internal standard. The depth profiles revealed anomalously high concentrations toward the surface of the profile in the anomalous area 400-700 m. Good agreement was obtained with results by AR-ICP-MS, for those elements that could be determined by ICP-MS. In fact, not only is sample dissolution unnecessary, but no quantification is required, as qualitative analysis by SS-ETV-ICP-OES is sufficient to obtain depth profiles, including for elements like Cl, which cannot be determined by ICP-MS because of the use of AR for digestion.

Chapter 5 was focused on modifying the sample introduction system to enable an increase in the amount of solid sample that can be introduced without extinguishing the plasma. To this end, the outlet of the SS-ETV system was coupled to ICP-OES through a switching tee, which was itself connected to the side arm of a sheathing device inserted between a nebulizer/spray chamber system and the ICP torch. The valve was used to evacuate the pyrolysis products during the pyrolysis step and to direct analytes towards

the ICP during the vaporisation step, so that they would merge with pre-evaporated aerosol.

The aerosol exiting the spray chamber was indeed heated by infrared heating to 400 °C the sheathing device and bottom of the torch. This system allowed the introduction of more than twice the amount of solid sample (i.e. 13 mg instead of 5 mg) without extinguishing the plasma, as only the analyte portion actually reached the ICP. Under optimum conditions and compared to conventional SS-ETV-ICP-OES (where the ETV outlet is directly connected to the torch), improvement in sensitivity by up to 5-fold and detection limit by up to 20-fold was obtained for a range of elements, the improvement being in general larger for ionic emission lines than atomic ones. This system also allowed as accurate but more precise (by about 2-fold on average) analysis of a soil CRM using another soil CRM for external calibration and an Ar emission line for internal standardization than conventional SS-ETV-ICP-OES.

6.2. General conclusions

So far, the direct SS-ETV-ICP-OES approach was optimized to determine the distribution of elements in soil samples across the Talbot line in order to locate the undercover ore deposit. The above results clearly demonstrate that ETV-ICP-OES with a four-step temperature program not only can be used for the direct analysis of geological materials but also is able to produce similar results to ICP-MS following aqua regia extraction. As the ETV temperature program only requires 85 s per sample, this approach is superior to aqua regia extractions, which is time-consuming, requires reagents and is more susceptible to contamination because of the multiple steps involved. Furthermore,

the lower sensitivity of ICP-OES compared to ICP-MS is compensated by ETV sample introduction, which provides excellent transport efficiency in contrast to the 2-5% sample introduction efficiency that is usually achieved by conventional nebulizers.

The changes induced in the plasma by ETV of the sample are compensated by selection of an Ar emission line without requiring any addition to the sample, which is an advantage to ICP-MS where the addition of at least one internal standard to all samples and standard solutions is usually necessary. By simply computing the point-by-point analyte/argon intensity ratio and then integrating the area of the peak that arises at 2200ºC, the distribution of pathfinder elements in soils can easily be obtained, without the need for quantification.

If needed, quantification can readily be achieved by external calibration with different amounts of solid standard, as showed by the accurate determination of different pathfinder elements in soils using the four-step ETV temperature program. Therefore, due to its great simplicity and the significantly reduced sample processing that it requires, SS-ETV-ICP-OES should become a valuable tool to support geochemical exploration.

Finally, in order to increase the amount of solid analyzed, the SS-ETV-ICP-OES system was modified by coupling ETV to a nebulisation/pre-evaporation systembecause the application of uniform and efficient IR heating to the nebulization system and bottom of the torch increased plasma robustness and stability. The amount of solid sample that could be tolerated without extinguishing the plasma almost tripled compared to what can be introduced with conventional SS-ETV-ICP-OES. Furthermore, this new system considerably improved sensitivity and detection limit, while providing similar accuracy as the conventional system, but with significantly improved precision for the analysis of

soil. Thus, this new ETV system can be used for accurate and precise multi-elemental analysis of soil samples.

6.3. Future work

The quick analysis of soil is both one area where SS-ETV-ICP-OES is very useful. Reviewing all the SS-ETV-ICP-OES applications presented in the literature revealed that no work has been done on the direct analysis of solid food samples. As food is a primary source of essential elements (i.e. such as Se, Cu and Zn) and an important means of exposure to toxic elements (i.e. such as Pb, Cd and Hg) for humans, it is indeed important that the levels of these elements be monitored in food both to implement regulatory and harmonized standards and to evaluate long-term exposure. For example, the permissible concentration of arsenic in salt is 0.5 mg/kg.[142] All these regulatory and harmonized standards for food are established by national governments and supranational organizations such as the European Union to facilitate world trade and improve the health of citizens of all nations. Most regulatory standards are recognized only after analytical procedures have been validated through inter-laboratory trials or have been shown to meet specified analytical criteria.

The analytical procedures used for these activities are required to determine low levels of these elements in the shortest time with maximum precision as nowadays both the types and sheer number of different foods that need to be analyzed increase. This is typically done by ICP-MS, following digestion of the sample prior to its nebulisation into the ICP.[132] This sample treatment step may lead to loss for volatile elements such as As and Cd while the potential for contamination throughout the procedure is serious due to

the relatively large amount of sample manipulation that is required. Direct solid sampling analysis of different types of food and dairy samples (i.e. rice, bean, fish, bread, sugar, meat, milk powder, wheat, and coffee) would eliminate such sample preparation, thereby increasing sample throughput.

Furthermore, the high concentration of organic matrix often induces non-spectroscopic interferences, which result in analyte signal enhancement or depression compared to that observed with matrix-free equiconcentrated solution in ICP-MS.[143] Spectroscopic interferences from polyatomic ions, which may also arise from the sample matrix, are usually avoided by selecting a less-abundant alternative isotope, in turn leading to a lowering in sensitivity, which is especially critical for those elements in low concentrations. On the other hand, matrix effects are usually smaller in ICP-OES than ICP-MS and ETV sample introduction can considerably reduce these matrix effects. Thus, SS-ETV-ICP-OES clearly seems to be more appropriate for this application. Hence, a completely different application could focus on the direct analysis of different solid food samples.

Another aspect that needs attention is the fact that, for all solid sampling techniques, including SS-ETV-ICP-OES, accurate calibration using aqueous standard solutions is often not possible because analytes in solid samples and calibration standard solutions have different transport behavior from the ETV system to the ICP. Actually, there may be no similarity in evaporation characteristics, as analytes may have different chemical forms in solid samples and liquid standards. Hence, external calibration with a CRM possessing a matrix as similar as possible to that of the sample is usually done, such as using AA-ED S5 soil standard for quantification of soil samples in this study.

However, appropriate reference materials are not always available for analysis of all sample types.[144] There is thus a need for an approach that would allow accurate quantitative analysis of solid samples using standard solutions for external calibration. One that is worth exploring is that developed in Chapter 5, where the insertion of a valve at the outlet of the ETV system enabled complete venting of the matrix and prevented it from overloading the plasma. It may be possible to use homogenous, inexpensive and widely available aqueous standard solutions for calibration with this improved ETV system to obtain similar results as with matrix-matched solid standards. For this purpose, we can introduce aqueous standard solutions either in the ETV or by simultaneous nebulization in the plasma. In the latter case, there have been some publications using nebulization (without pre-evaporation) for calibration in LA-ICP-MS, which was successful for precise in situ multielement analysis of minerals and geological samples.[145,146] Thus, we can try this procedure (with pre-evaporation) with this improved ETV-ICP-OES method. If successful, this would obviate the need for expensive CRMs.

References

1- Gent, M., Menendez, M., Toraño, J and Torno, S. A review of indicator minerals and sample processing methods for geochemical exploration. *Journal of Geochemical Exploration*, **2011**, 110, 47-60.

2- Rose, A. W., Hawkes, H.E and Webb, J.S. Geochemistry in mineral exploration. *Academic Press*, London.**1979**.

3- McClenaghan, M. B. Indicator mineral methods in mineral exploration. *Geochemistry: Exploration, Environment, Analysis*, **2005**, 5, 233-245.

4- Cameron, E. M., Hamilton, S. M., Leybourne, M. I., Hall, G. E. M and McClenaghan, M. B. Finding deeply buried deposits using geochemistry. *Geochemistry: Exploration, Environment, Analysis*, **2004**, 4, 7-32.

5- Tchalenko, J. S. The Kashmar (Turshiz) 1903 and Torbat-e Heidariyeh (South) 1923 earthquakes in Central Khorassan (Iran). *Annali di Geofisica*, **1973**, 26, 29-40.

6- Nur, A. Matsushiro, Japan, Earthquake Swarm: Confirmation of the Dilatancy-Fluid Diffusion Model. *Geology*, **1974**, 2, 217-221.

7- Sibson, R. H., Moore, J. M. M and Rankin, A. H. Seismic pumping- a hydrothermal fluid transport mechanism. *Journal of the Geological Society*, **1975**, 131, 653-659.

8- Cannon, H. L. S. Botanical Prospecting For Uranium On La Ventura Mesa Sandoval County New Mexico. Sandoval County, New Mexico. *United States Geological Survey Bulletin*, **1956**, 1009M, 391-407.

9- Govett, G. J. S., Dunlop, A. C and Atherden, P. R. Electrogeochemical techniques in deeply weathered terrain in Australia. *Journal of Geochemical Exploration*, **1984**, 21, 311-331.

10- Hamilton, S. M. Electrochemical mass-transport in overburden: a new model to account for the formation of selective leach geochemical anomalies in glacial terrain. *Journal of Geochemical Exploration*, **1998**, 63, 155-172.

11- Hamilton, S. M. Summary of Fieldwork and Other Activities, Open File Report. *Ontario Geological Survey*, Ontario, **1999**, 421–426.

12- Beauchemin, D. Environmental analysis by inductively coupled plasma mass spectrometry. *Mass Spectrometry Reviews*, **2010**, 29, 560-592.

13- Shmakin, B. M. The method of partial extraction of metals in a constant current electrical field for geochemical exploration. *Journal of Geochemical Exploration*, **1985**, 23, 27-33.

14- Talapatra, A. K.,Talukdar, R. C and De, P. K. Electrochemical technique for exploration of base metal sulphides. *Journal of Geochemical Exploration*, **1986**, 25, 389-396.

15- Wu, J., Lu, X., Xu, H and Nakagoshi, N. Geoelectrochemical-extraction Measurement Method to Look for Hidden Lead-zinc Ore Deposit and Prospecting Effect. *Advanced Materials Research*, **2013**, 95-99.

16- Ogiyama, S., Sakamoto, K.,Suzuki, H., Ushio, S., Anzai, T and Inubushi, K. Measurement of concentrations of trace metals in arable soils with animal manure application using instrumental neutron activation analysis and the concentrated acid digestion method. *Soil Science and Plant Nutrition*, **2006**, 52, 114-121.

17- Nunes, K. P., Munita, C. S., Vasconcellos, M. B. A., Oliveira, P. M. S., Croci, C. A and Faleiros, F. M. Characterization of soil samples according to their metal content. *Journal of Radioanalytical and Nuclear Chemistry*, **2009**, 281, 359-363.

18- Shibata, Y., Suyama, J., Kitano, M and Nakamura, T. X-ray fluorescence analysis of Cr, As, Se, Cd, Hg, and Pb in soil using pressed powder pellet and loose powder methods. *X-Ray Spectrometry*, **2009**, 38, 410-416.

19- Vollkopf, U., Grobenski, Z., Tamm, R and Welz, B. Solid sampling in graphite furnace atomic-absorption spectrometry using the cup-in-tube technique. *Analyst*, **1985**, 110, 573-577.

20- Figueiredo, E., Soares, M. E., Baptista, P., Castro, M and Bastos, M. L. Validation of an Electrothermal Atomization Atomic Absorption Spectrometry Method for Quantification of Total Chromium and Chromium(VI) in Wild Mushrooms and Underlying Soils. *Journal of Agricultural and Food Chemistry*, **2007**, 55, 7192-7198.

21- Melaku, S., Dams, R and Moens, L. Determination of trace elements in agricultural soil samples by inductively coupled plasma-mass spectrometry: Microwave acid digestion versus aqua regia extraction. *Analytica Chimica Acta*, **2005**, 543, 117-123.

22- Zbiral, J., Medek, P., Kubán, V., Čižmárová, E and Němec, P. Analytical methods and quality assurance. *Communications in Soil Science and Plant Analysis*, **2000**, 31, 2045-2051.

23- Bettinelli, M., Beone, G. M., Spezia, S and Baffi, C. Determination of heavy metals in soils and sediments by microwave-assisted digestion and inductively coupled plasma optical emission spectrometry analysis. *Analytica Chimica Acta*, **2000**, 424, 289-296.

24- Tighe, M., Lockwood, P., Wilson, S and Lisle, L. Comparison of Digestion Methods for ICP-OES Analysis of a Wide Range of Analytes in Heavy Metal Contaminated Soil Samples with Specific Reference to Arsenic and Antimony. *Communications in Soil Science and Plant Analysis*, **2004**, 35, 1369-1385.

25- Ure, A. Trace elements in soil: Their determination and speciation. *Fresenius' Journal of Analytical Chemistry*, **1990**, 337, 577-581.

26- Sah, R and Brown, P. Techniques for boron determination and their application to the analysis of plant and soil samples. *Plant and Soil*, **1997**, 193, 15-33.

27- Kalnicky, D. J and Singhvi, R. Field portable XRF analysis of environmental samples. *Journal of Hazardous Materials*, **2001**, 83, 93-122.

28- West, M., Ellis, A. T., Potts, P. J., Streli, C., Vanhoof, C., Wegrzynek, D and Wobrauschek, P. Atomic spectrometry update. X-Ray fluorescence spectrometry. *Journal of Analytical Atomic Spectrometry*, **2009**, 24, 1289-1326.

29- Wobrauschek, P. Total reflection x-ray fluorescence analysis—a review. *X-Ray Spectrometry*, **2007**, 36, 289-300.

30- Ghosh, S, P. V., Sowjanya. B., Srivani.P., Alagaraja. M and Banji.D. Inductively Coupled Plasma –Optical Emission Spectroscopy: A Review. *Asian Journal of Pharmaceutical Analysis*, **2013**, 3, 24-33.

31- Deconinck, I., Latkoczy, C., Günther, D., Govaert, F and Vanhaecke, F. Capabilities of laser ablation—inductively coupled plasma mass spectrometry for (trace) element analysis of car paints for forensic purposes. *Journal of analytical atomic spectrometry*, **2006**, 21, 279-287.

32- *ICP Mass Spectrometry Handbook*, ed. Nelms. S, Blackwell Publishing, Oxford, **2005**, 215-227.

33- Asfaw, A and Wibetoe, G. Potential of Solid Sampling Electrothermal Vaporization for solving spectral interference in Inductively Coupled Plasma Optical Emission Spectrometry. *Spectrochimica Acta Part B: Atomic Spectroscopy*, **2009**, 64, 363-368.

34- Barth, P., Hassler, J., Kudrik, I and Krivan, V. Determination of trace impurities in boron nitride by graphite furnace atomic absorption spectrometry and electrothermal vaporization inductively coupled plasma optical emission spectrometry using solid sampling. *Spectrochimica Acta Part B: Atomic Spectroscopy*, **2007**, 62, 924-932.

35- Friese, K. C and Krivan, V. Direct analysis of tantalum powders by electrothermal vaporization inductively coupled plasma atomic emission spectrometry. *Fresenius' Journal of Analytical Chemistry*, **1999**, 364, 72-78.

36- Resano, M., Vanhaecke, F and de Loos-Vollebregt, M. T. C. Electrothermal vaporization for sample introduction in atomic absorption, atomic emission and plasma mass spectrometry-a critical review with focus on solid sampling and slurry analysis. *Journal of Analytical Atomic Spectrometry*, **2008**, 23, 1450-1475.

37- Schäffer, U and Krivan, V. Multielement Analysis of Graphite and Silicon Carbide by Inductively Coupled Plasma Atomic Emission Spectrometry Using Solid Sampling and Electrothermal Vaporization. *Analytical Chemistry*, **1999**, 71, 849-854.

38- Schrön, W., Liebmann, A and Nimmerfall, G. Direct solid sample analysis of sediments, soils, rocks and advanced ceramics by ETV-ICP-AES and GF-AAS. *Fresenius' Journal of Analytical Chemistry*, **2000**, 366, 79-88.

39- Tianyou, P., Pingwu, D., Bin, H and Zucheng, J. Direct analysis of titanium dioxide solid powder by fluorination assisted electrothermal vaporization inductively coupled plasma atomic emission spectrometry. *Analytica Chimica Acta*, **2000**, 421, 75-81.

40- Wende, M. C and Broekaert, J. A. C. Direct solid sampling electrothermal vaporization of alumina for analysis by inductively coupled plasma optical emission spectrometry. *Spectrochimica Acta Part B: Atomic Spectroscopy*, **2002**, 57, 1897-1904.

41- Kántor, T. Electrothermal vaporization and laser ablation sample introduction for flame and plasma spectrometric analysis of solid and solution samples. *Spectrochimica Acta Part B: Atomic Spectroscopy,* **2001**, 56, 1523-1563.

42- Pan, L., Qin, Y.-c., Hu, B and Jiang, Z.-c. Determination of Nickel and Palladium in Environmental Samples by Low Temperature ETV-ICP-OES Coupled with Liquid-liquid Extraction with Dimethylglyoxime as Both Extractant and Chemical Modifier. *Chemical Research in Chinese Universities*, **2007**, 23, 399-403.

43- Nickel, H and Zadgorska, Z. A new electrothermal vaporization device for direct sampling of ceramic powders for inductively coupled plasma optical emission spectrometry. *Spectrochimica Acta Part B: Atomic Spectroscopy*, **1995**, 50, 527-535.

44- Chaves, E. S., de Loos-Vollebregt, M. T. C., Curtius, A. J and Vanhaecke, F. Determination of trace elements in biodiesel and vegetable oil by inductively coupled plasma optical emission spectrometry following alcohol dilution. *Spectrochimica Acta Part B: Atomic Spectroscopy*, **2011**, 66, 733-739.

45- Depoi, F. S., Oliveira, T.C., Moraes, D.P and Pozebon, D. Preconcentration and determination of As, Cd, Pb and Bi using different sample introduction systems, cloud point extraction and inductively coupled plasma optical emission spectrometry. *Analytical Methods*, **2012**, 4, 89-95.

46- Lara, R., Cerutti, S., Salonia, J. A., Olsina, R. A and Martinez, L. D. Trace element determination of Argentine wines using ETAAS and USN-ICP-OES. *Food and Chemical Toxicology*, **2005**, 43, 293-297.

47- Tavakoli, L., Yamini, Y., Ebrahimzadeh, H., Nezhadali, A., Shariati, S and Nourmohammadian, F. Development of cloud point extraction for simultaneous

extraction and determination of gold and palladium using ICP-OES. *Journal of Hazardous Materials*, **2008**, 152, 737-743.

48- Gomez, M. R., Cerutti, S., Sombra, L. L., Silva, M. F and Martínez, L. D. Determination of heavy metals for the quality control in argentinian herbal medicines by ETAAS and ICP-OES. *Food and Chemical Toxicology*, **2007**, 45, 1060-1064.

49- Thiel, G and Danzer, K. Direct analysis of mineral components in wine by inductively coupled plasma optical emission spectrometry (ICP-OES). *Fresenius' Journal of Analytical Chemistry*, **1997**, 357, 553-557.

50- Mikuła, B and Puzio, B. Determination of trace metals by ICP-OES in plant materials after preconcentration of 1,10-phenanthroline complexes on activated carbon. *Talanta*, **2007**, 71, 136-140.

51- Zhu, X., Chang, X., Cui, Y., Zou, X., Yang, D and Hu, Z. Solid-phase extraction of trace Cu(II) Fe(III) and Zn(II) with silica gel modified with curcumin from biological and natural water samples by ICP-OES. *Microchemical Journal*, **2007**, 86, 189-194.

52- Ribeiro, A. S., Moretto, A. L., Arruda, M. A. Z and Cadore, S. Analysis of Powdered Coffee and Milk by ICP OES after Sample Treatment with Tetramethylammonium Hydroxide. *Microchimica Acta*, **2003**, 141, 149-155.

53- El-Ghawi, U., Pátzay, G., Vajda, N and Dódizs, D. Analysis of selected fertilizers imported to Libya for major, minor, trace and toxic elements using ICP-OES and INAA. *Journal of Radioanalytical and Nuclear Chemistry*, **1999**, 242, 693-701.

54- Fassel.V.A and Wendt. R. H. Induction-coupled Plasma Spectrometric Excitation Source. *Analytical Chemistry*, **1965**, 37, 920-922.

55- Hou, X and Jones, B. T. Inductively Coupled Plasma-Optical Emission Spectrometry. *In Encyclopedia of Analytical Chemistry; John Wiley & Sons, Ltd*, **2000**, 9468–9485.

56- Introduction to ICP Instrumentation. Retrieved July 2014, from http://web.nmsu.edu/~kburke/Instrumentation/NMSU_Optima2100.html.

57- Houk, R. S. Mass spectrometry of inductively coupled plasmas. *Analytical Chemistry*, **1986**, 58, 97A-105A.

58- Boss, C.B and Fredeen, K. J. Concept, Instrumentation and Techniques in Inductively Coupled Plasma Optical Emission Spectrometry, Second Edition, *Perkin Elmer*, 1997, 36-71.

59- Haraguchi, H., Hasegaw, T and Abdullah, M. Inductively coupled plasmas in analytical atomic spectrometry: excitation mechanisms and analytical feasibilities. *Pure & Application Chemistry*, **1988**, 60, 685-696.

60- Fassel, V. Analytical inductively coupled plasma spectroscopies — past, present, and future. Z. *Analytical Chemistry*, **1986**, 324, 511-518.

61- Beauchemin, D. Inductively Coupled Plasma Mass Spectrometry. *Mass Spectrometry Reviews*, **2008**, 80, 4455-4486.

62- Beauchemin, D.,Yves Le Blanc, J. C., Peters, G. R and Persaud, A. T. Plasma Emission Spectrometry. *Analytical Chemistry*, **1994**, 66, 462R- 499R.

63- Meinhard, J. E. Pneumatic nebulizers, present and future, *in applications of Plasma Emission Spectrochemistry,* Barnes, R.M (Ed), Heyden & Son, Inc., Philadelphia, PA, USA, **1979**, 1-14.

64- Dean, J. R. Atomic Absorption and Plasma Spectroscopy. *Analytical Chemistry by Open Learning*, John Wiley & Son Ltd, Chichester, **1997**.

65- Olesik, J. W and Fister Iii, J. C. Incompletely desolvated droplets in argon inductively coupled plasmas: their number, original size and effect on emission intensities. *Spectrochimica Acta Part B: Atomic Spectroscopy*, **1991**, 46, 851-868.

66- Retrieved August 2014, from: http://s3-ap-southeast-2.amazonaws.com/jigsydney/general/PDF/188315~MW_Theorie_Probenvorbereitung_PT_en.pdf.

67- Asfaw, A and Beauchemin, D. Combination of a multimode sample introduction system with a pre-evaporation tube to improve multi-element analysis by ICP-OES. *Journal of Analytical Atomic Spectrometry*, **2012**, 27, 80-91.

68- Hanselman, D. S., Sesi, N. N., Huang, M and Hieftje, G. M. The effect of sample matrix on electron density, electron temperature and gas temperature in the argon inductively coupled plasma examined by Thomson and Rayleigh scattering. *Spectrochimica Acta Part B: Atomic Spectroscopy*, **1994**, 49, 495-526.

69- Edlund, M., Visser, H and Heitland, P. Analysis of biodiesel by argon-oxygen mixed-gas inductively coupled plasma optical emission spectrometry. *Journal of Analytical Atomic Spectrometry*, **2002**, 17, 232-235.

70- Verbeek, A. A and Brenner, I. B. Slurry nebulisation of geological materials into argon, argon-nitrogen and argon-oxygen inductively coupled plasmas. *Journal of Analytical Atomic Spectrometry*, **1989**, 4, 23-26.

71- Long, G. L and Brenner, I. B. Analysis of ceramic, geological and related refractory materials by slurry injection mixed gas inductively coupled plasma atomic emission spectrometry. *Journal of Analytical Atomic Spectrometry*, **1990**, 5, 495-499.

72- Heitland, P and Broekaert, J. A. C. Addition of Small Amounts of Helium and Hydrogen to the Working Gases in Slurry Nebulization Inductively Coupled Plasma Atomic Emission Spectrometry for the Analysis of Ceramic Powders. *Journal of Analytical Atomic Spectrometry*, **1997**, 12, 981-986.

73- Lam, J. W. H and Horlick, G. A comparison of argon and mixed gas plasmas for inductively coupled plasma-mass spectrometry. *Spectrochimica Acta Part B: Atomic Spectroscopy*, **1990**, 45, 1313-1325.

74- Botto, R. I and Zhu, J. J. Use of an ultrasonic nebulizer with membrane desolvation for analysis of volatile solvents by inductively coupled plasma atomic emission spectrometry. *Journal of Analytical Atomic Spectrometry*, **1994**, 9, 905-912.

75- Todoli, J. L., Gras, L., Hernandis, V and Mora, J. Elemental matrix effects in ICP-AES. *Journal of Analytical Atomic Spectrometry*, **2002**, 17, 142-169.

76- Sun, Y., Wu, S and Lee, C. Investigation of non-spectroscopic interference and internal standardization method in axially and radially viewed inductively coupled plasma optical emission spectrometry using cross-flow and ultrasonic nebulization. *Journal of Analytical Atomic Spectrometry*, **2003**, 18, 1163-1170.

77- Novotny, I., Farinas, J. C., Jia-liang, W., Poussel, E and Mermet, J. M. Effect of power and carrier gas flow rate on the tolerance to water loading in inductively coupled plasma atomic emission spectrometry. *Spectrochimica Acta Part B: Atomic Spectroscopy*, **1996**, 51, 1517-1526.

78- Asfaw, A and Beauchemin, D. Improvement of the capabilities of inductively coupled plasma optical emission spectrometry by replacing the desolvation system of an

ultrasonic nebulization system with a pre-evaporation tube. *Spectrochimica Acta Part B: Atomic Spectroscopy*, **2010**, 65, 376-384.

79- Asfaw, A., MacFarlane, W and Beauchemin, D. Ultrasonic nebulization with an infrared heated pre-evaporation tube for sample introduction in ICP-OES: application to geological and environmental samples. *Journal of Analytical Atomic Spectrometry*, **2012**, 27, 1254-1263.

80- Belhamra, A., Diabi, R and Moussaoui, A. Technology and Applications of Infrared Heating in Industrial Area, *Journal of Engineering and Applied Sciences*, **2007**, 2, 1183–1187.

81- Salin, E. D and Horlick, G. Direct sample insertion device for inductively coupled plasma emission spectrometry. *Analytical Chemistry*, **1979**, 51, 2284-2286.

82- Brenner, I. B., Lorber, A and Goldbart, Z. Trace element analysis of geological materials by direct solids insertion of a graphite cup into an inductively coupled plasma. *Spectrochimica Acta Part B: Atomic Spectroscopy*, **1987**, 42, 219-225.

83- Darke, S. A., Long, S. E., Pickford, C. J and Tyson, J. F. A study of laser ablation and slurry nebulisation sample introduction for the analysis of geochemical materials by inductively coupled plasma spectrometry. *Fresenius' Journal of Analytical Chemistry*, **1990**, 337, 284-289.

84- Claverie, F., Fernández, B., Pécheyran, C., Alexis, J. and Donard, O.F.X. Elemental fractionation effects in high repetition rate IR femtosecond laser ablation ICP-MS analysis of glasses. *Journal of Analytical Atomic Spectrometry*, **2009**, 24, 891-902.

85- Guevremont, R and De Silva, K. N. Direct powder introduction ICP-AES with a photodiode array spectrometer: a powder sampler based on linear motion of the powder

towards an uptake capillary. *Spectrochimica Acta Part B: Atomic Spectroscopy*, **1992**, 47, 371-385.

86- Ebdon, L., Foulkes, M. E and Hill, S. Direct atomic spectrometric analysis by slurry atomisation. Part 9. Fundamental studies of refractory samples. *Journal of Analytical Atomic Spectrometry*, **1990**, 5, 67-73.

87- Borgianni, C., Capitelli, M., Cramarossa, F.,Triolo, L and Molinari, E. The behaviour of metal oxides injected into an argon induction plasma. *Combustion and Flame*, **1969**, 13, 181-194.

88- Belarra, M. A., Resano, M., Vanhaecke, F and Moens, L. Direct solid sampling with electrothermal vaporization/atomization: what for and how? *Trends in Analytical Chemistry*, **2002**, 21, 828-839.

89- Hu, B., Li, S., Xiang, G., He, M and Jiang, Z. Recent Progress in Electrothermal Vaporization–Inductively Coupled Plasma Atomic Emission Spectrometry and Inductively Coupled Plasma Mass Spectrometry. *Applied Spectroscopy Reviews*, **2007**, 42, 203-234.

90- Verrept, P., Dams, R and Kurfürst, U. Electrothermal vaporization inductively coupled plasma atomic emission spectrometry for the analysis of solid samples: contribution to instrumentation and methodology. *Fresenius' Journal of Analytical Chemistry*, **1993**, 346, 1035-1041.

91- Nixon, D. E., Fassel, V. A and Kniseley, R. N. Inductively coupled plasma-optical emission analytical spectroscopy. Tantalum filament vaporization of microliter samples. *Analytical Chemistry*, **1974**, 46, 210-213.

92- Kitazume, E. Thermal vaporization for one-drop sample introduction into the inductively coupled plasma. *Analytical Chemistry*, **1983**, 55, 802-805.

93- Gunn, A. M., Millard, D. L and Kirkbright, G. F. Optical emission spectrometry with an inductively coupled radiofrequency argon plasma source. *Analyst*, **1978**, 103, 1066-1073.

94- Kirkbright, G. F and Snook, R. D. Volatilization of Refractory Compound Forming Elements from a Graphite Electrothermal Atomization Device for Sample Introduction into an Inductively Coupled Argon Plasma. *Analytical Chemistry*, **1979**, 51, 1938-1941.

95- Aziz, A., Broekaert, J. A. C and Leis, F. Analysis of microamounts of biological samples by evaporation in a graphite furnace and inductively coupled plasma atomic emission spectroscopy. *Spectrochimica Acta Part B: Atomic Spectroscopy*, **1982**, 37, 369-379.

96- Shen.W., Caruso, J., Fricke. F. L and Satzger. R. D. Electrothermal vaporization interface for sample introduction in inductively coupled plasma mass spectrometry. *Journal of analytical atomic spectrometry*, **1990**, 5, 451-455.

97- Hassler, J., Barth, P., Richter, S and Matschat, R. Determination of trace elements in high-purity copper by ETV-ICP OES using halocarbons as chemical modifiers. *Journal of Analytical Atomic Spectrometry*, **2011**, 26, 2404-2418.

98- Masson, P. Direct determination of major elements in solid plant materials by electrothermal vaporization inductively coupled plasma atomic emission spectrometry. *Talanta*, **2007**, 71, 1399-1404.

99- Masson, P. Direct phosphorus determination on solid plant samples by Electrothermal vaporization-inductively coupled plasma atomic emission spectrometry. *Journal of analytical atomic spectrometry*, **2011**, 26, 1290-1293.

100- Okamoto, Y. Electrothermal vaporization system using furnace-fusion technique for the determination of lead in botanical samples by inductively coupled plasma atomic emission spectrometry. *Fresenius' Journal of Analytical Chemistry*, **2000**, 367, 295-299.

101- Óvári, M., Záray, G and Hassler, J. Solid sampling electrothermal vaporization inductively coupled plasma atomic emission spectrometric method for analysis of amphipods (Dikerogammarus villosus) samples. *Microchemical Journal*, **2002**, 73, 125-130.

102- Plantikow-Voβgätter, F and Denkhaus, E. Application of an ETV-ICP system for the determination of elements in human hair. *Spectrochimica Acta Part B: Atomic Spectroscopy*, **1996**, 51, 261-270.

103- Masson, P., Dauthieu, M., Trolard, F and Denaix, L. Application of direct solid analysis of plant samples by electrothermal vaporization-inductively coupled plasma atomic emission spectrometry: Determination of Cd and Si for environmental purposes. *Spectrochimica Acta Part B: Atomic Spectroscopy*, **2007**, 62, 224-230.

104- Asfaw, A., Wibetoe, G and Beauchemin, D. Solid sampling electrothermal vaporization inductively coupled plasma optical emission spectrometry for discrimination of automotive paint samples in forensic analysis. *Journal of Analytical Atomic Spectrometry*, **2012**, 27, 1928-1934.

105- Huang, L and Beauchemin, D. Ethnic background and gender identification using electrothermal vaporization coupled to inductively coupled plasma optical emission

spectrometry for forensic analysis of human hair. *Journal of Analytical Atomic Spectrometry*, **2014**, 29, 1228-1232.

106- Van geffen, P. W. G. Geochemical indicators of buried sulphide mineraralisation under sedimentary cover near Talbot lake, Manitoba. PhD thesis, Queen's University, Kingston, Canada. **2011**.

107- Long, S. E and Browner, R. F. Influence of water on conditions in the inductively coupled argon plasma. *Spectrochimica Acta Part B: Atomic Spect*roscopy, **1988**, 43, 1461-1471.

108- Winefordner, J.D., Gornushkin, I. B., Correll, T., Gibb, E., Smith, B, W and Omenetto, N. Comparing several atomic spectrometric methods to the super stars: special emphasis on laser induced breakdown spectrometry, LIBS, a future super star. *Journal of analytical atomic spectrometry*, **2004**, 19, 1061-1083.

109- Wrobel, K., Wrobel, K (Kazimierz) and Caruso, J.A. Sample introduction in ICP-MS: Electrothermal vaporization. *Mass spectrometry encyclopedia*, Volume 5, Eds. Beauchemin, D and Matthews, D.E. Elsevier, **2010**, 35-46.

110- Retrieved July 2014, from http://wwwp.cord.edu/dept/chemistry/analyticallabmanual/experiments/icpaes/intro.html.

111- Retrieved July 2014, from http://www.shimadzu.com/an/elemental/oes/oes.html.

112- Schäffer, U and Krivan, V. A Graphite Furnace Electrothermal Vaporization System for Inductively Coupled Plasma Atomic Emission Spectrometry. *Analytical Chemistry*, **1998**, 70, 482-490.

113- Perzl, P. R. Manual of Electrothermal Vaporisation. *Spectral systems*, Germany, **2009**.

114- Hassler, J., Detcheva, A and Forster, O. Working with a modern ETV-device and an ICP-CID spectrometer. *Annali di Chimica*, **1999**, 89, 827-836.

115- Fuge, R., Andrews, M. J and Johnson, C. C. Chlorine and iodine, potential pathfinder elements in exploration geochemistry. *Applied Geochemistry*, **1986**, 1, 111-116.

116- Chaffee, M. A. The zonal distribution of selected elements above the Kalamazoo porphyry copper deposit, San Manuel district, Pinal County, Arizona. *Journal of Geochemical Exploration*, **1976**, 5, 145-165.

117- Aramendía, M., Resano, M and Vanhaecke, F. Electrothermal vaporization–inductively coupled plasma-mass spectrometry: A versatile tool for tackling challenging samples: A critical review. *Analytica Chimica Acta*, **2009**, 648, 23-44.

118- Wang, J., Carey, J. M and Caruso, J. A. Direct analysis of solid samples by electrothermal vaporization inductively coupled plasma mass spectrometry. *Spectrochimica Acta Part B: Atomic Spectroscopy*, **1994**, 49, 193-203.

119- Vanhaecke, F., Gelaude, I., Moens, L and Dams, R. Solid sampling electrothermal vaporization inductively coupled plasma mass spectrometry for the direct determination of Hg in sludge samples. *Analytica Chimica Acta*, **1999**, 383, 253-261.

120- Detcheva, A., Barth, P and Hassler, J. Calibration possibilities and modifier use in ETV ICP OES determination of trace and minor elements in plant materials. *Analytical and Bioanalytical Chemistry*, **2009**, 394, 1485-1495.

121- Vanhaecke, F., Galbacs, G., Boonen, S., Moens, L and Dams, R. Use of the Ar^{2+} signal as a diagnostic tool in solid sampling electrothermal vaporization inductively

coupled plasma mass spectrometry. *Journal of Analytical Atomic Spectrometry*, **1995**, 10, 1047-1052.

122- Martin-Esteban, A., Slowikowski, B and Grobecker, K. H. Correcting sensitivity drift during long-term multi-element signal measurements by solid sampling-ETV-ICP-MS. *Talanta*, **2004**, 63, 667-673.

123- Martín-Esteban, A and Slowikowski, B. Electrothermal Vaporization - Inductively Coupled Plasma–Mass Spectrometry (ETV-ICP-MS): A Valuable Tool for Direct Multielement Determination in Solid Samples. *Critical Reviews in Analytical Chemistry*, **2003**, 33, 43-55.

124- Moens, L., Verrept, P., Boonen, S., Vanhaecke, F and Dams, R. Solid sampling electrothermal vaporization for sample introduction in inductively coupled plasma atomic emission spectrometry and inductively coupled plasma mass spectrometry. *Spectrochimica Acta Part B: Atomic Spectroscopy*, **1995**, 50, 463-475.

125- Kira, C. S and Maihara, V. A. Determination of major and minor elements in dairy products through inductively coupled plasma optical emission spectrometry after wet partial digestion and neutron activation analysis. *Food Chemistry*, **2007**, 100, 390-395.

126- Carey, J. M and Caruso, J. A. Electrothermal Vaporization for Sample Introduction in Plasma Source Spectrometry. *Critical Reviews in Analytical Chemistry*, **1992**, 23, 397-439.

127- Záray, G., Leis, F., Kántor, T., Hassler, J and Tölg, G. Analysis of silicon carbide powder by ETV-ICP-AES. *Fresenius' Journal of Analytical Chemistry*, **1993**, 346, 1042-1046.

128- May, W. E and Rumble, J. Certificate of Analysis: Standard Reference Material 2710. National Institute of Standards & Technology. **2003**.

129- May, W. E and Rumble, J. Certificate of Analysis: Standard Reference Material 2711. National Institute of Standards & Technology. **2003**.

130- Anderson, T. W. An Introduction to Multivariate Statistical Analysis. 2nd Edition, Wiley & Sons, New York, USA. 1984.

131- Pohl, P and Sturgeon, R. E. Simultaneous determination of hydride- and non-hydride-forming elements by inductively coupled plasma optical emission spectrometry. *Trends in Analytical Chemistry*, **2010**, 29, 1376-1389.

132- Nardi, E. P., Evangelista, F. S., Tormen, L., Saint´Pierre, T. D., Curtius, A. J., Souza, S. S. d and Barbosa, J.F. The use of inductively coupled plasma mass spectrometry (ICP-MS) for the determination of toxic and essential elements in different types of food samples. *Food Chemistry*, **2009**, 112, 727-732.

133- Pohl, P., Vorapalawut, N., Bouyssiere, B., Carrier, H and Lobinski, R. Direct multi-element analysis of crude oils and gas condensates by double-focusing sector field inductively coupled plasma mass spectrometry (ICP MS). *Journal of Analytical Atomic Spectrometry*, **2010**, 25, 704-709.

134- Mermet, J. M. Is it still possible, necessary and beneficial to perform research in ICP-atomic emission spectrometry? *Journal of Analytical Atomic Spectrometry*, **2005**, 20, 11-16.

135- Mora, J., Maestre, S., Hernandis, V and Todolí, J. L. Liquid-sample introduction in plasma spectrometry. *Trends in Analytical Chemistry* , **2003**, 22, 123-132.

136- Li, L., Hu, B., Xia, L and Jiang, Z. Determination of trace Cd and Pb in environmental and biological samples by ETV-ICP-MS after single-drop microextraction. *Talanta*, **2006**, 70, 468-473.

137- Resano, M., Verstraete, M., Vanhaecke, F., Moens, L., Van Alphen, A and Denoyer, E. R. Simultaneous determination of Co, Mn, P and Ti in PET samples by solid sampling electrothermal vaporization ICP-MS. *Journal of Analytical Atomic Spectrometry*, **2000**, 15, 389-395.

138- Masquelin, A.S., Kaveh, F., Asfaw, A.,Oates, C. J and Beauchemin, D. Solid sampling ETV-ICP-OES to study the distribution of elements in clay and soil samples for mineral exploration. *Geochemistry: Exploration, Environment, Analysis*, **2013**, 13, 11-20.

139- Prohaska, T., Hann, S., Latkoczy, C and Stingeder, G. Determination of rare earth elements U and Th in environmental samples by inductively coupled plasma double focusing sectorfield mass spectrometry (ICP-SMS). *Journal of Analytical Atomic Spectrometry*, **1999**, 14, 1-8.

140- Ren, J. M and Salin, E. D. Direct solid sample analysis using furnace vaporization with Freon modification and inductively coupled plasma atomic emission spectrometry. Vaporization of oxides and carbides. *Spectrochimica Acta Part B: Atomic Spectroscopy*, **1994**, 49, 555-566.

141- Goltz, D. M., Grégoire, D. C and Chakrabarti, C. L. Mechanism of vaporization of yttrium and rare earth elements in electrothermal vaporization inductively coupled plasma mass spectrometry. *Spectrochimica Acta Part B: Atomic Spectroscopy*, **1995**, 50, 1365-1382.

142- Capar, S., Mindak, W and Cheng, J. Analysis of food for toxic elements. *Analytical and Bioanalytical Chemistry*, **2007**, 389, 159-169.

143- Beauchemin, D. Interferences: Non-Spectroscopic interferences. *ICP-MS encyclopedia*, **2010**, 150 -158.

144- Vanhaecke, F., Boonen, S., Moens, L. U. C and Dams, R. Isotope Dilution as a Calibration Method for Solid Sampling Electrothermal Vaporization Inductively Coupled Plasma Mass Spectrometry. *Journal of Analytical Atomic Spectrometry*, **1997**, 12, 125-130.

145- Horn, I., Rudnick, R. L and McDonough, W. F. Precise elemental and isotope ratio determination by simultaneous solution nebulization and laser ablation-ICP-MS: application to U–Pb geochronology. *Chemical Geology*, **2000**, 164, 281-301.

146- Pickhardt, C., Becker, J. S and Dietze, H.-J. A new strategy of solution calibration in laser ablation inductively coupled plasma mass spectrometry for multielement trace analysis of geological samples. *Fresenius' Journal of Analytical Chemistry*, **2000**, 368, 173-181.

Appendix

Concentrations of Ag, Al, Ba, Cu, Hg, P, Pb, S and Zn in the soil fraction at 50-cm depth across the Talbot line measured by SS-ETV-ICP-OES (mean ± standard deviation, *n*=4).

Sample	East (m)	Depth (cm)	Ag (ppb)	Al (%)	Ba (ppm)
45017-1	0	-10	36.7 ± 16.2	2.7 ± 2.1	58.3 ± 19.8
45016-1	100	-10	36.6 ± 9.4	4.4 ± 3.2	57 ± 17.3
45015-1	200	-10	65.8 ± 17.5	3.6 ± 1.6	44.4 ± 22.5
45014-1	300	-10	93.8 ± 25.7	7.4 ± 0.5	89.9 ± 10.5
45013-1	400	-10	299.9 ± 14.3	6.4 ± 1.8	98.6 ± 14.6
45012-1	450	-10	63.8 ± 10.5	8.6 ± 2	77.7 ± 7.7
45011-1	500	-10	149.8 ± 36.7	17.4 ± 6.3	297 ± 115.9
45010-1	550	-10	164 ± 106.6	20.1 ± 1.8	308.6 ± 50.7
45009-1	600	-10	32 ± 17.8	5.2 ± 0.6	63.4 ± 3.2
45008-1	650	-10	55.7 ± 17.9	5.2 ± 1.1	78.6 ± 20.2
45007-1	700	-10	56.9 ± 22.4	5.5 ± 2.7	72.2 ± 34.8
45006-1	750	-10	69.1 ± 26.6	4.4 ± 1.7	51.1 ± 32.8
45005-1	800	-10	59.5 ± 13.5	5.8 ± 2.2	65.3 ± 14.5
45004-1	900	-10	22.3 ± 7	3 ± 1.6	58.9 ± 14.3
45003-1	1000	-10	8.8 ± 1.9	4.1 ± 1	64.3 ± 10.1
45017-2	0	-20	186 ± 32.4	5.4 ± 1	117.4 ± 8
45016-2	100	-20	96.4 ± 28.7	5.4 ± 0.8	95.1 ± 14.6
45015-2	200	-20	37 ± 13.6	4.5 ± 4.1	67 ± 54.7
45014-2	300	-20	82.4 ± 40.5	7 ± 0.6	82.3 ± 21.5
45013-2	400	-20	73.2 ± 11.8	5.1 ± 1.6	53.8 ± 14.3
45012-2	450	-20	64.5 ± 14.2	7 ± 1.2	68.5 ± 7
45011-2	500	-20	102.9 ± 32.2	14.6 ± 0.9	244.5 ± 25.1
45010-2	550	-20	48.2 ± 8.4	12.7 ± 3.2	226.7 ± 31.7
45009-2	600	-20	29.7 ± 7.7	3.8 ± 1.1	60.1 ± 10.2
45008-2	650	-20	56.7 ± 14	5.6 ± 0.3	71.9 ± 13.4
45007-2	700	-20	54 ± 9.8	6.5 ± 1.7	83.5 ± 12.1
45006-2	750	-20	79.8 ± 26.7	6 ± 3.1	80.8 ± 31.7
45005-2	800	-20	61.6 ± 19	6.8 ± 1.5	82.5 ± 15
45004-2	900	-20	86 ± 47.7	3.2 ± 0.5	70.7 ± 10.3
45003-2	1000	-20	11.6 ± 6	2.1 ± 0.8	42.6 ± 20.3
45017-3	0	-30	78.7 ± 7.6	1.6 ± 0.4	59.8 ± 10.2

45015-3	200	-30	189.9 ± 71.9	5.4 ± 1.8	108.8 ± 26.7
45014-3	300	-30	93.2 ± 35.4	5.3 ± 0.1	88.4 ± 10.6
45013-3	400	-30	279.5 ± 74.2	4.8 ± 1.7	67.2 ± 18.9
45012-3	450	-30	186.2 ± 97.4	11 ± 1.7	143.2 ± 7.3
45011-3	500	-30	112.6 ± 46.2	14.2 ± 7.9	240.7 ± 35.7
45010-3	550	-30	64.1 ± 16.5	10.6 ± 0.6	230.1 ± 3
45009-3	600	-30	21.1 ± 14.8	3.9 ± 2.4	51.7 ± 19.3
45008-3	650	-30	65.9 ± 31.9	5.7 ± 0.6	58.4 ± 35.9
45007-3	700	-30	83.5 ± 21	7.2 ± 0.9	101.2 ± 12.9
45006-3	750	-30	55.9 ± 29.9	5.4 ± 0.7	89.4 ± 14.9
45005-3	800	-30	86.1 ± 45.3	6.5 ± 0.5	73.6 ± 12.8
45004-3	900	-30	30.1 ± 10.6	3.2 ± 1.4	60.3 ± 22.8
45003-3	1000	-30	31.2 ± 9.7	3.7 ± 1.5	64.9 ± 18.3
45014-4	300	-40	85.1 ± 57.1	5.6 ± 1.7	85.9 ± 27.2
45013-4	400	-40	297.4 ± 122.3	5.3 ± 1	92 ± 15.1
45012-4	450	-40	69 ± 22.4	5.7 ± 1.8	83.6 ± 24.5
45011-4	500	-40	20.6 ± 4.7	7.8 ± 2.2	209.1 ± 9.9
45010-4	550	-40	263.6 ± 160.1	21.6 ± 3.7	334.6 ± 47.1
45009-4	600	-40	9.9 ± 6.4	3.4 ± 0.8	65.3 ± 6.1
45008-4	650	-40	70.8 ± 13.4	3.8 ± 1.7	71.5 ± 18.7
45007-4	700	-40	87.5 ± 16	6.3 ± 0.9	104.4 ± 2.7
45006-4	750	-40	45.6 ± 15.1	3.2 ± 2	75.2 ± 16
45005-4	800	-40	76.1 ± 28.1	6.5 ± 0.5	72.8 ± 6.1
45004-4	900	-40	31.6 ± 16	3.2 ± 0.1	73.5 ± 7
45003-4	1000	-40	25 ± 9.2	3.4 ± 1.9	63.7 ± 22.2
45014-5	300	-50	206.9 ± 129	8.5 ± 4.1	136.7 ± 54.7
45013-5	400	-50	357 ± 15.5	5.2 ± 0.1	106.9 ± 2.6
45012-5	450	-50	9.4 ± 26.6	4.5 ± 1.1	72.5 ± 11.5
45011-5	500	-50	59.7 ± 23.3	13.4 ± 5.8	291.3 ± 86
45010-5	550	-50	87.5 ± 22.6	10.7 ± 1.8	244.2 ± 16.8
45009-5	600	-50	7.1 ± 1.4	2.9 ± 0	60.3 ± 0.7
45008-5	650	-50	50.5 ± 23.1	3.8 ± 3.1	80.3 ± 40.8
45007-5	700	-50	56.2 ± 17.9	5.2 ± 1.1	91.5 ± 11.9
45006-5	750	-50	40.3 ± 33.8	5.4 ± 0.2	86.3 ± 11.7
45005-5	800	-50	46.1 ± 5.1	5.6 ± 0.9	90.9 ± 25
45004-5	900	-50	38.6 ± 18.9	3.4 ± 0.9	80 ± 21.6
45003-5	1000	-50	24.6 ± 9.2	3 ± 1.7	78.4 ± 18.4

Sample	East (m)	Depth (cm)	Cu (ppm)	Hg (ppb)	P (%)
45017-1	0	-10	17.2 ± 6.8	21.7 ± 9.1	0.01 ± 0.003
45016-1	100	-10	18.3 ± 6.2	23.2 ± 9.6	0.02 ± 0.004
45015-1	200	-10	17.3 ± 7.3	18.4 ± 5.9	0.01 ± 0.004
45014-1	300	-10	34.6 ± 7.7	50.6 ± 16.1	0.02 ± 0.003
45013-1	400	-10	41.8 ± 4.8	64.5 ± 2.2	0.07 ± 0.003
45012-1	450	-10	23.4 ± 0.4	41.3 ± 2.5	0.03 ± 0.001
45011-1	500	-10	92.5 ± 66.3	91.3 ± 37.2	0.03 ± 0.003
45010-1	550	-10	96.5 ± 45.7	184.8 ± 91.8	0.04 ± 0.004
45009-1	600	-10	19 ± 5.5	30.7 ± 10.7	0.02 ± 0.003
45008-1	650	-10	25.2 ± 3.5	37.8 ± 7.2	0.02 ± 0.003
45007-1	700	-10	26.7 ± 11.2	45.5 ± 16.7	0.02 ± 0.003
45006-1	750	-10	27.8 ± 7.9	43.2 ± 15.4	0.05 ± 0.01
45005-1	800	-10	23.2 ± 2.9	49.7 ± 18	0.02 ± 0.003
45004-1	900	-10	17.2 ± 11.5	28.7 ± 15	0.05 ± 0.012
45003-1	1000	-10	15.1 ± 3	37 ± 1.8	0.02 ± 0.006
45017-2	0	-20	61.5 ± 15.4	88.8 ± 12.2	0.19 ± 0.04
45016-2	100	-20	39.1 ± 10.6	61.4 ± 20.6	0.06 ± 0.025
45015-2	200	-20	24.1 ± 17.9	38.8 ± 33.5	0.03 ± 0.006
45014-2	300	-20	26.1 ± 9.8	36.1 ± 17.2	0.02 ± 0.005
45013-2	400	-20	29.2 ± 3	57 ± 4.8	0.08 ± 0.007
45012-2	450	-20	24.2 ± 4.7	43.4 ± 9.3	0.04 ± 0.005
45011-2	500	-20	61.8 ± 1.4	81.3 ± 23.1	0.03 ± 0.002
45010-2	550	-20	40.6 ± 2.5	62.8 ± 21.2	0.02 ± 0.003
45009-2	600	-20	13.8 ± 4.4	18.8 ± 4.7	0.02 ± 0.003
45008-2	650	-20	24.2 ± 6.2	37.9 ± 9.8	0.02 ± 0.002
45007-2	700	-20	25.9 ± 4.3	40.9 ± 5.9	0.02 ± 0.004
45006-2	750	-20	32 ± 10.2	47.4 ± 27.8	0.03 ± 0.003
45005-2	800	-20	26.1 ± 7.6	48.6 ± 20.8	0.02 ± 0.001
45004-2	900	-20	36.6 ± 11.8	60 ± 25.7	0.13 ± 0.048
45003-2	1000	-20	10.6 ± 4.2	18 ± 5.2	0.01 ± 0.001
45017-3	0	-30	31.5 ± 7.3	23 ± 6.7	0.05 ± 0.017
45015-3	200	-30	58.7 ± 18.3	72.8 ± 30.6	0.07 ± 0.02
45014-3	300	-30	29.8 ± 7.2	38.7 ± 1.8	0.02 ± 0.002
45013-3	400	-30	36.5 ± 9.5	65.8 ± 20.2	0.24 ± 0.057
45012-3	450	-30	68.6 ± 20.4	136.6 ± 50.7	0.09 ± 0.024
45011-3	500	-30	55.7 ± 18.6	68.4 ± 22.6	0.03 ± 0.007
45010-3	550	-30	38.6 ± 6.3	48.8 ± 0.2	0.03 ± 0.002
45009-3	600	-30	12.1 ± 1.7	15.1 ± 1.5	0.03 ± 0.005
45008-3	650	-30	21.5 ± 13.7	31.7 ± 17.9	0.02 ± 0.008

45007-3	700	-30	34.3 ± 12.4	47.7 ± 16	0.03 ± 0.008
45006-3	750	-30	32.5 ± 13.8	44.7 ± 18.6	0.05 ± 0.006
45005-3	800	-30	33.2 ± 11.4	68.9 ± 6	0.03 ± 0.006
45004-3	900	-30	25.8 ± 13.9	28 ± 9.3	0.04 ± 0.004
45003-3	1000	-30	19.9 ± 18	46.7 ± 33	0.02 ± 0.009
45014-4	300	-40	29.6 ± 13.7	30 ± 6	0.04 ± 0.006
45013-4	400	-40	47.6 ± 9.5	90.1 ± 15.2	0.41 ± 0.064
45012-4	450	-40	27.6 ± 15	39.1 ± 19.6	0.05 ± 0.006
45011-4	500	-40	37 ± 11.4	40.6 ± 13	0.03 ± 0.002
45010-4	550	-40	105.2 ± 40	198.7 ± 108.9	0.06 ± 0.022
45009-4	600	-40	13.1 ± 4.6	17.1 ± 2.9	0.04 ± 0.002
45008-4	650	-40	25.9 ± 9.6	38 ± 16.9	0.04 ± 0.005
45007-4	700	-40	34.7 ± 6.9	46.4 ± 6.4	0.03 ± 0.003
45006-4	750	-40	28.1 ± 16	32.4 ± 24.4	0.04 ± 0.009
45005-4	800	-40	27.7 ± 9.1	45 ± 20.5	0.03 ± 0.01
45004-4	900	-40	33.3 ± 10	34 ± 0.6	0.03 ± 0.002
45003-4	1000	-40	20 ± 10	31.1 ± 20.4	0.02 ± 0.003
45014-5	300	-50	65.2 ± 39.3	100.5 ± 40.1	0.09 ± 0.053
45013-5	400	-50	54.8 ± 2.6	93.4 ± 1.7	0.36 ± 0.007
45012-5	450	-50	19 ± 5.5	22.8 ± 2	0.05 ± 0.004
45011-5	500	-50	55.3 ± 13.5	64.1 ± 30	0.05 ± 0.027
45010-5	550	-50	50 ± 8.6	53.6 ± 12	0.04 ± 0.007
45009-5	600	-50	13.6 ± 1.2	15.3 ± 0.8	0.03 ± 0.007
45008-5	650	-50	22.6 ± 11.4	25 ± 10.8	0.05 ± 0.008
45007-5	700	-50	22.8 ± 1	24.9 ± 0.5	0.04 ± 0.003
45006-5	750	-50	34.4 ± 17	39.4 ± 21.8	0.04 ± 0.005
45005-5	800	-50	32.1 ± 19.4	39.6 ± 20.8	0.05 ± 0.016
45004-5	900	-50	39 ± 13.1	48.5 ± 22.9	0.04 ± 0.01
45003-5	1000	-50	34.5 ± 0.9	40.1 ± 22.4	0.04 ± 0.001

Sample	**East (m)**	**Depth (cm)**	**Pb (ppm)**	**S (%)**	**Zn (ppm)**
45017-1	0	-10	4.8 ± 1.8	0.004 ± 0.002	28.6 ± 6.4
45016-1	100	-10	5.3 ± 2	0.011 ± 0.003	32 ± 8.1
45015-1	200	-10	4.9 ± 1.8	0.007 ± 0.001	27.8 ± 4.5
45014-1	300	-10	9.6 ± 2.2	0.014 ± 0.004	57 ± 10.3
45013-1	400	-10	13 ± 1.3	0.304 ± 0.002	76.5 ± 2.4
45012-1	450	-10	7.3 ± 0.2	0.016 ± 0.004	52.7 ± 4.6
45011-1	500	-10	23.5 ± 16.4	0.016 ± 0.004	69.8 ± 8.8
45010-1	550	-10	25.6 ± 12.1	0.034 ± 0.015	108.8 ± 34
45009-1	600	-10	6 ± 1.7	0.021 ± 0.022	41.3 ± 9

45008-1	650	-10	8.2 ± 1.4	0.007 ± 0.003	56 ± 10.2
45007-1	700	-10	10.4 ± 0.6	0.012 ± 0.005	55.4 ± 7.3
45006-1	750	-10	8.7 ± 2.3	0.027 ± 0.005	52.4 ± 9.8
45005-1	800	-10	9 ± 3	0.014 ± 0.003	48.4 ± 9.8
45004-1	900	-10	6 ± 3	0.013 ± 0.005	50.7 ± 6
45003-1	1000	-10	5.2 ± 0.7	0.017 ± 0.007	43.8 ± 3.7
45017-2	0	-20	18.7 ± 3.4	0.065 ± 0.008	76.3 ± 7.7
45016-2	100	-20	11.7 ± 3.1	0.029 ± 0.008	60.6 ± 15.1
45015-2	200	-20	7.1 ± 5.6	0.02 ± 0.011	48.1 ± 23.1
45014-2	300	-20	7.4 ± 2.6	0.01 ± 0.004	45.1 ± 11.7
45013-2	400	-20	8.9 ± 0.8	0.038 ± 0.002	57.4 ± 4.3
45012-2	450	-20	8.4 ± 0.3	0.011 ± 0.002	58.2 ± 4
45011-2	500	-20	15.8 ± 0.3	0.016 ± 0.004	64.9 ± 11.1
45010-2	550	-20	10.1 ± 0.5	0.012 ± 0.003	52.9 ± 1.1
45009-2	600	-20	4.3 ± 1.3	0.004 ± 0.002	35.2 ± 4.3
45008-2	650	-20	8.1 ± 1.9	0.007 ± 0.004	51.8 ± 5.6
45007-2	700	-20	9.1 ± 1	0.008 ± 0.004	50.5 ± 9.7
45006-2	750	-20	9.7 ± 3.1	0.009 ± 0.002	51.7 ± 16.2
45005-2	800	-20	8.5 ± 2.3	0.007 ± 0.003	46 ± 2.1
45004-2	900	-20	10.8 ± 3.1	0.074 ± 0.021	70 ± 13.7
45003-2	1000	-20	4 ± 1	0.002 ± 0.002	37.9 ± 4.6
45017-3	0	-30	9 ± 1.8	0.023 ± 0.006	32.5 ± 6.3
45015-3	200	-30	16.6 ± 5.6	0.04 ± 0.015	70 ± 16
45014-3	300	-30	8.4 ± 2.1	0.01 ± 0.001	53.6 ± 4.7
45013-3	400	-30	11.7 ± 2.9	0.173 ± 0.02	77.5 ± 16.7
45012-3	450	-30	21.4 ± 5.9	0.048 ± 0.017	95.2 ± 24
45011-3	500	-30	13.7 ± 4.8	0.014 ± 0.004	51.1 ± 10.4
45010-3	550	-30	10 ± 2.1	0.015 ± 0.002	51.9 ± 2.8
45009-3	600	-30	3.8 ± 0.3	0.003 ± 0.001	38.5 ± 9.6
45008-3	650	-30	7.2 ± 4.2	0.01 ± 0.004	48.1 ± 9.9
45007-3	700	-30	11.3 ± 3.4	0.008 ± 0.002	53.7 ± 11.8
45006-3	750	-30	9.9 ± 3	0.015 ± 0.008	51 ± 11.2
45005-3	800	-30	9.9 ± 3.7	0.015 ± 0.002	53.3 ± 10.3
45004-3	900	-30	8.1 ± 4.7	0.018 ± 0.013	48.2 ± 25
45003-3	1000	-30	6.9 ± 5.2	0.012 ± 0.01	47.7 ± 15.3
45014-4	300	-40	6.5 ± 1.2	0.009 ± 0.002	41.4 ± 3.7
45013-4	400	-40	15 ± 2.4	0.314 ± 0.046	94.5 ± 8.4
45012-4	450	-40	8.5 ± 4.4	0.012 ± 0.007	54.7 ± 9.3
45011-4	500	-40	9.2 ± 3.2	0.009 ± 0.004	50.8 ± 11
45010-4	550	-40	28.9 ± 12.4	0.037 ± 0.019	104.8 ± 46.6
45009-4	600	-40	4.2 ± 0.7	0.006 ± 0.004	31.9 ± 1.3

45008-4	650	-40	9 ± 3.5	0.011 ± 0.006	52.2 ± 15
45007-4	700	-40	10.7 ± 1.7	0.012 ± 0.002	52.5 ± 2.5
45006-4	750	-40	8.5 ± 5	0.01 ± 0.008	48.8 ± 6.1
45005-4	800	-40	8 ± 2.4	0.012 ± 0.007	43.1 ± 2.9
45004-4	900	-40	9.5 ± 2.6	0.005 ± 0.002	43.7 ± 6.5
45003-4	1000	-40	6.1 ± 2.7	0.007 ± 0.003	42.7 ± 11
45014-5	300	-50	19.3 ± 11.4	0.032 ± 0.023	84.6 ± 46.4
45013-5	400	-50	17.3 ± 0.6	0.252 ± 0.012	82.8 ± 0.8
45012-5	450	-50	6.1 ± 1.8	0.008 ± 0.006	52.8 ± 5
45011-5	500	-50	14.6 ± 3.2	0.013 ± 0.006	59.2 ± 8.7
45010-5	550	-50	13 ± 2.9	0.012 ± 0.002	54.5 ± 2.4
45009-5	600	-50	4.3 ± 0.5	0.002 ± 0.001	29.9 ± 0.2
45008-5	650	-50	7.5 ± 3.4	0.008 ± 0.005	47.2 ± 14
45007-5	700	-50	7.8 ± 0.5	0.005 ± 0.001	42.9 ± 7.5
45006-5	750	-50	10.1 ± 4.5	0.011 ± 0.008	39.8 ± 8.9
45005-5	800	-50	9.6 ± 5.6	0.017 ± 0.01	42.4 ± 10.8
45004-5	900	-50	11.8 ± 4.6	0.012 ± 0.007	46.8 ± 7.3
45003-5	1000	-50	8.4 ± 3.3	0.016 ± 0.012	37.8 ± 8.8